# SECOND-GENERATION ORDERED POLYMERS

3

March 1989

Final Report

By: Steven P. Bitler, Andrea W. Chow, and James F. Wolfe

AD-A216 126

Prepared for:

AIR FORCE OFFICE OF SCIENTIFIC RESEARCH
Directorate of Chemical and Atmospheric Sciences
Building 410
Bolling Air Force Base
Washington, DC 20332-6448

Attention: Major Larry P. Davis

DTIC
ELECTE
NOV 17 1989
S   D
C&E

SRI International
333 Ravenswood Avenue
Menlo Park, California 94025-3493
(415) 326-6200
TWX: 910-373-2046
Telex: 334486

89 11 17 024

SRI International

TITLE:   Second Generation Ordered Polymers    **AFOSR·TR· 89 - 0 397**

PRINCIPAL INVESTIGATOR:

| | |
|---|---|
| 1 Nov 87 - 12 Aug 88 | 12 Aug 88 - 28 Oct 88 |
| Dr. James F. Wolfe | Dr. Steven P. Bitler |
| SRI International | SRI International |
| 333 Ravenswood Ave. | 333 Ravenswood Ave. |
| Menlo Park, CA  94025 | Menlo Park, CA  94025 |

INCLUSIVE DATES:   1 Nov 87 - 31 Oct 88

CONTRACT NUMBER:   F49620-88-K-0001

COSTS AND FY SOURCE:   $199,971, FY88

SENIOR RESEARCH PERSONNEL:

Dr. Steven P. Bitler                     Dr. Andrea W. Chow

JUNIOR RESEARCH PERSONNEL:

Richard Hamlin
Bock Loo
Robert Sanderson

PUBLICATIONS:

"Reaction Kinetics and Chemo-rheology of Poly($\underline{p}$-phenylenebenzo-
bisthiazole) Polymerization in the Ordered Phase," A. W. Chow, J. F.
Sandell, and J. F. Wolfe, Polymer 29 (1988) 1307.

"Chemo-rheology of PBT Polymerization in the Liquid Crystalline Phase,"
A. W. Chow and J. F. Wolfe, Proceedings of Xth International Congress on
Rheology, Sydney Australia, August 14-19 (1988), 1, 266.

"Synthesis Approaches for Improving the Nonlinear Optical Properties of
PBZ Polymers," J. F. Wolfe, B. H. Loo, R. A. Sanderson, and S. P.
Bitler, in Nonlinear Optical Properties of Polymers, eds. A. J. Heeger,
J. Orenstein, and D. R. Ulrich, Materials Research Society Symposium
Proceedings, 109 (1988) 291.

"Synthesis and Solution Properties of Extended Chain Poly(2,6-
Benzothiazole) and Poly(2,5-Benzoxazole)," A. W. Chow, S. P. Bitler, P.
E. Penwell, D. J. Osborne, and J. F. Wolfe, accepted for publication,
Macromolecules.

"Mesophase-Enhanced Polymerization and Chemo-rheology of Poly(p-phenylenebenzobisthiazole)," A. W. Chow, R. D. Hamlin, J. F. Sandell, and J. F. Wolfe, Materials Research Society Meeting Proceedings, November 1988.

"Synthesis and Dilute Solution Characterization of Extended-Chain Poly(benzazoles)," A. W. Chow, S. P. Bitler, P. E. Penwell, and J. F. Wolfe, Material Research Society Meeting Proceedings, November 1988.

"Synthesis and Characterization of Benzazole Containing Donor-Acceptor Compounds," S. P. Bitler, B. H. Loo, and J. F. Wolfe, in preparation.

ABSTRACT OF OBJECTIVES AND ACCOMPLISHMENTS:

The objectives of this program include (1) understanding the molecular structural features that result in high nonlinear optical (NLO) figures of merit for organic materials, (2) investigating the effects of temperature and shear on polymerization kinetics of liquid crystalline polymers, (3) studying the dilute and concentrated solution properties of rigid rod and extended chain polymers and (4) synthesizing high strength polymers with improved compressive strength. The first three areas of research have been explored. The final area was scheduled to be investigated in later years of the contract.

The synthesis of pi-conjugated benzazole-containing compounds terminated with electron-donating (donor) and electron-accepting (acceptor) functional groups was studied to determine which structural features result in enhanced NLO figures of merit. Specific compounds have been identified that should have high figures of merit while also increasing the processing options available to this class of thermally stable materials. The synthetic methodologies developed allow specific control of molecular length, functional group, substitution site for the functional group, and solubility.

The reaction kinetics and solution properties of lyotropic poly(benzazoles) have been investigated. In poly(p-phenylenebenzo-bisthiazole) (PBT) polymerizations, we observe an increase in reaction rate and final molecular weight when the reaction goes through a phase transition from isotropic to liquid crystalline. We call this phenomenon "mesophase-enhanced polymerization." The study of the dilute and concentrated solutions of poly(2,6-benzothiazole) (ABPBT) and poly(2,5-benzoxazole) (ABPBO) was initiated. In dilute solution, these polymers were found to have persistence lengths of 130 and 90 angstroms, respectively. The Mark-Houwink-Sakurada constants were also determined.

AFOSR Program Manager: Major Larry P. Davis

# REPORT DOCUMENTATION PAGE

| 1a REPORT SECURITY CLASSIFICATION | | | 1b RESTRICTIVE MARKINGS | | |
|---|---|---|---|---|---|
| Unclassified | | | N/A | | |

| 2a SECURITY CLASSIFICATION AUTHORITY | | 3 DISTRIBUTION/AVAILABILITY OF REPORT |
|---|---|---|
| N/A | | Approved for public release; |
| 2b DECLASSIFICATION/DOWNGRADING SCHEDULE | | distribution unlimited. |
| N/A | | |

| 4 PERFORMING ORGANIZATION REPORT NUMBER(S) | 5 MONITORING ORGANIZATION REPORT NUMBER(S) |
|---|---|
| PYU-4621 | AS |

| 6a NAME OF PERFORMING ORGANIZATION | 6b OFFICE SYMBOL (If applicable) | 7a NAME OF MONITORING ORGANIZATION |
|---|---|---|
| SRI International | | |

| 6c ADDRESS (City, State, and ZIP Code) | 7b ADDRESS (City, State, and ZIP Code) |
|---|---|
| 333 Ravenswood Avenue<br>Menlo Park, CA 94025-3493 | |

| 8a NAME OF FUNDING/SPONSORING ORGANIZATION | 8b OFFICE SYMBOL (If applicable) | 9 PROCUREMENT INSTRUMENT IDENTIFICATION NUMBER |
|---|---|---|
| AFOSR | | F49620-88-K-0001 |

| 8c ADDRESS (City, State, and ZIP Code) | 10 SOURCE OF FUNDING NUMBERS | | | |
|---|---|---|---|---|
| Building 410 | PROGRAM ELEMENT NO | PROJECT NO | TASK NO | WORK UNIT ACCESSION NO |
| Bolling Air Force Base<br>D.C. 20332-6448 | | | | |

11 TITLE (Include Security Classification)

SECOND-GENERATION ORDERED POLYMERS

12 PERSONAL AUTHOR(S)

Bitler, Steven P., Chow, Andrea W., and Wolfe, James F.

| 13a TYPE OF REPORT | 13b TIME COVERED | 14 DATE OF REPORT (Year, Month, Day) | 15 PAGE COUNT |
|---|---|---|---|
| Final | FROM 11/1/87 TO 10/31/88 | 1989 March | 70 |

16 SUPPLEMENTARY NOTATION

| 17 COSATI CODES | | | 18 SUBJECT TERMS (Continue on reverse if necessary and identify by block number) |
|---|---|---|---|
| FIELD | GROUP | SUB-GROUP | second-generation ordered polymers |
| 07 | 06 | | chemo-rheology |
| | | | poly(p-phenylenebenzobisthiazole) |

PBT
Nonlinear optics
polybenzazoles

19 ABSTRACT (Continue on reverse if necessary and identify by block number)

The goals of this research were (1) to understand the structure-property relationships that lead to organic materials with high figures of merit for nonlinear optical (NLO) applications and to develop the processibility and optical utility of such materials, (2) to investigate the effects of temperature and shear on the polymerization kinetics of lyotropic polymers, and (3) to examine the dilute and concentrated solution properties of rigid rod and extended chain polybenzazoles).

During this contract, we synthesized a homologous series of benzazole-containing donor-acceptor compounds that should exhibit high figures of merit in NLO applications. These compounds, called ALHD compounds, are composed of an electron-accepting group, an unsaturated linking group, a conjugated heterocyclic segment, and an electron-donating group [e.g., 2-(4-N,N-dimethylaminophenyl)-6-(N-nitrophenylmine) benzoxazole)].

| 20 DISTRIBUTION/AVAILABILITY OF ABSTRACT | 21 ABSTRACT SECURITY CLASSIFICATION |
|---|---|
| ☒ UNCLASSIFIED/UNLIMITED ☐ SAME AS RPT ☐ DTIC USERS | Unclassified |
| 22a NAME OF RESPONSIBLE INDIVIDUAL | 22b TELEPHONE (Include Area Code) | 22c OFFICE SYMBOL |
| | | |

DD FORM 1473, 84 MAR
83 APR edition may be used until exhausted
All other editions are obsolete

SECURITY CLASSIFICATION OF THIS PAGE

Various research groups around the United States have been supplied with samples of these compounds for investigation of their second-order NLO parameters, processibility, crystal packing arrangement, and suitability for use in optical devices.

Compounds based on the benzazole structure were synthesized because poly(p-phenylenebenzobisthiazole), or PBT, prepared at SRI has been processed into optical quality thin films with good optical response. PBT exhibits thermal stability at temperatures above 600°C in air and environmental stability. Successful device fabrication requires materials that have high second- or third-order macroscopic NLO susceptibilities as well as good environmental stability, good processibility and fabricability (i.e., the ability to form optical quality thin films or crystals), good thermal stability (stability at 1 GW/cm$^2$), and fast (subpicosecond) switching times.

The reaction kinetics and solution properties of lyotropic poly(benzazoles) have also been investigated. In PBT polymerizations, the reaction rate was observed to increase when the reaction mixture made the transition from the isotropic to the liquid crystalline phase. This phenomenon has been named mesophase-enhanced polymerization.

The study of dilute and concentrated solutions of poly(2,6-benzothiazole), or ABPBT, and poly(2,5-benzoxazole), or ABPBO, involved the use of viscometry and low angle light scattering. These polymers can be classified as intrinsically semirigid, with persistence lengths of 130 Å for ABPBT and 90 Å for ABPBO.

Accession For

| | |
|---|---|
| NTIS GRA&I | ☑ |
| DTIC TAB | ☐ |
| Unannounced | ☐ |
| Justification | |

By
Distribution/

Availability Codes

Dist | Avail and/or Special

A-1

CONTENTS

# FIGURES

TABLES

iv

# INTRODUCTION

The goal of our research was to achieve a better understanding of the molecular structures and polymerization behavior of the polybenzazole (PBZ) family of ordered polymers and the modifications that are required to extend use of these materials to second-generation applications, such as electrically conducting and nonlinear optical (NLO) devices.

Our work comprised the following tasks:

o  Study various molecular structural features within the PBZ family of polymers that give the highest figures of merit for NLO materials.

o  Determine the effect of shear on the polymerization kinetics of rigid rod polymers that can be enhanced by the "template effect" in the liquid crystalline phase.

o  Study the dependence of dilute and concentrated solution properties of extended-chain polymers on molecular weight and chain flexibility.

This report describes our progress on these tasks and the approaches we would recommend for maximizing the processibility and optical response of the PBZ materials.

We had planned for Year 2 to synthesize higher molecular weight PBZ polymers that are chain terminated with functional end groups that would improve the compressive strength of the materials, but funding was not available for the second year.

1

# SYNTHESIS AND CHARACTERIZATION OF BENZAZOLES
## FOR USE IN NLO APPLICATIONS

### Objective

The primary objective of this task was to develop new PBZ materials with improved NLO responses and the processibility that would allow them to be readily produced in a variety of useful devices.

### Approach

Our first approach was aimed at second-order materials. We synthesized a homologous series of -conjugated materials in which the variations in molecular structure and substituents were designed to affect not only the microscopic NLO response parameters and the absorption characteristics but also the processibility, stability, and macroscopic orderability. Our generic name for this series is ALHD, because the NLO-active portion of the system is composed of an electron-accepting portion, an unsaturated linking group, a conjugated heterocyclic segment, and an electron-donating segment, in that order. The ALHD methodology is summarized in Table 1. In this report we describe the synthesis of six ALHD compounds and their precursor compounds. As shown in Table 1, the ALHD compounds have four different types of A segments, one type of L group, three types of H segments, and two types of D segments. The second-order NLO parameters of these materials are being studied by Professor Anthony Garito at the University of Pennsylvania. We have modified these structures to increase their solubility, because increased solubility will allow more accurate measurement of their NLO responses and provide improved processing options.

Our second approach was aimed at structures either with centrosymmetry or without high permanent dipoles and thus provided materials that are applicable to third-order rather than second-order

# Table 1

## ALHD METHODOLOGY: SUMMARY OF BENZAZOLE-CONTAINING ACCEPTOR / DONOR COMPOUNDS

| Electron-Accepting Portion | Unsaturated Linking Group | Heterocyclic Segment | Electron-Donating Group |
|---|---|---|---|
| A | L | H | D |
| N | Im | $B^nO$  D | |
| C | Az | T | $D_{18}$ |
| $N_2$ | | TBO | |
| NH | | | |

N = 4-Nitrophenyl
C = 4-Cyanophenyl
$N_2$ = 2,4-Dinitrophenyl
NH = 3-Hydroxy-4-nitrophenyl
Im = Imino
Az = Azo
$B^nO$ = Benzoxazol-2,n-diyl
T = Benzothiazol-2,n-diyl
TBO = Thiazolyl-benzoxazolyl
D = 4-(Dimethylamino)-phenyl
$D_{18}$ = 4-(N-Octadecylamino)-phenyl

processes. We attempted to prepare random copolymers in which the phenoxazine structure replaces a portion of the p-phenylenebenzo-bisoxazole structure of poly (p-phenylenebenzobisoxazole) (PBO). We also investigated the synthesis of rigid heterocyclic units with diamine functionality for incorporation into polyamides, polyurethanes, and polyimides. The processing options of these compounds could be investigated through host/guest systems and attachment to various polymer backbones, both rigid and flexible.

Our synthetic approaches and results are discussed in detail in Appendix C, a technical paper resulting from this work, and in the Experimental Methods section, below.

## Results and Discussion

### A. Synthesis of ALHD Compounds

### 1. Precursor Synthesis

Aminobenzoxazoles (amino-BODs) are versatile precursors that allow systematic variation of terminal groups to provide model materials useful for generating a structural data base. A generalized amino-BOD structure is shown below. The various amino-BODs differ in heteroatom (oxazole or thiazole), amino site substitution, molecular length, and length of alkyl chain on the donor end.
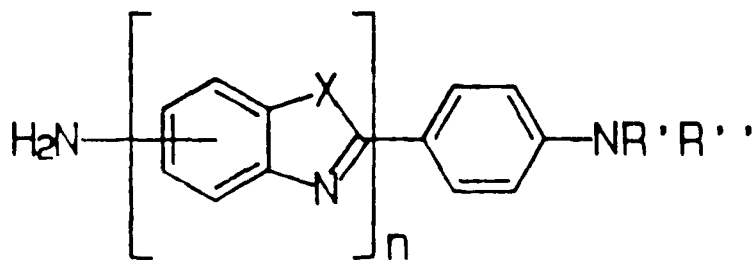


RA-4621-7

Generalized structure of amino-BODs.

4

Condensation of p-N,N-dialkylaminobenzoic acid with 2,5-diamino-
phenol in poly(phosphoric acid) (PPA) yielded 2-(p-N,N-dialkylamino-
phenyl)-6-aminobenzoxazole (amino-B$^6$OD) in 67% yield after
recrystallization. The condensation reaction allows addition of various
quantities of monomer (e.g., 4-amino-3-hydroxybenzoic acid) to produce
oligomeric species. Figure 1 shows the amino-BODs we have prepared.
These precursors have been prepared as pure compounds (except for amino-
B$^6$OT$_3$D, which is a distribution of oligomers) and analyzed by mass
spectrometry (MS), nuclear magnetic resonance (NMR) spectroscopy,
infrared spectrometry (IR), ultraviolet-visible light (UV-VIS)
spectrometry, and elemental analysis, as shown in Tables 2 and 3.

Detailed synthetic procedures and results are reported in the
Experimental Methods section, below.

To form the imino group as the linking portion, functionalized
aldehydes are required. The following aldehydes are available from
commercial suppliers: 4-nitrobenzaldehyde, 2,4-dinitrobenzaldehyde,
4-cyanobenzaldehyde, and 3-hydroxy-4-nitrobenzaldehyde.

## 2. Condensation of the Precursors

Condensation of amino-B$^6$OD with p-nitrobenzaldehyde in toluene
or toluene/dimethylsulfoxide (DMSO) yielded 2-(p-N,N-
dimethylaminophenyl)-6-(p-nitro-phenylimine)benzoxazole (NImB$^6$OD), as
shown in Figure 2, in 90% yield. Analogous compounds were prepared by
condensing various amino-BODs of different oligomeric lengths with
benzaldehydes terminated with cyano and nitro groups. Figure 3 shows
the compounds of this series that we prepared. The purity of these
donor-acceptor compounds as determined by MS, NMR, IR, and UV-VIS
spectroscopy and elemental analysis is listed in Tables 2 and 3.

## 3. Structure-Property Relationships of ALHD Compounds

Full proton NMR assignments of ALHD compounds are detailed in
Figures 4 through 9. Comparing the $^1$H-NMR spectra of amino-B$^6$OD and
NImB$^6$OD, we see the expected downfield shift of the aromatic benzazole

BOD

Amino·B$^5$OD

Amino·B$^6$OD

Amino·B$^6$OTD

Amino-B$^6$OT$_3$D

RA-M-4621-1A
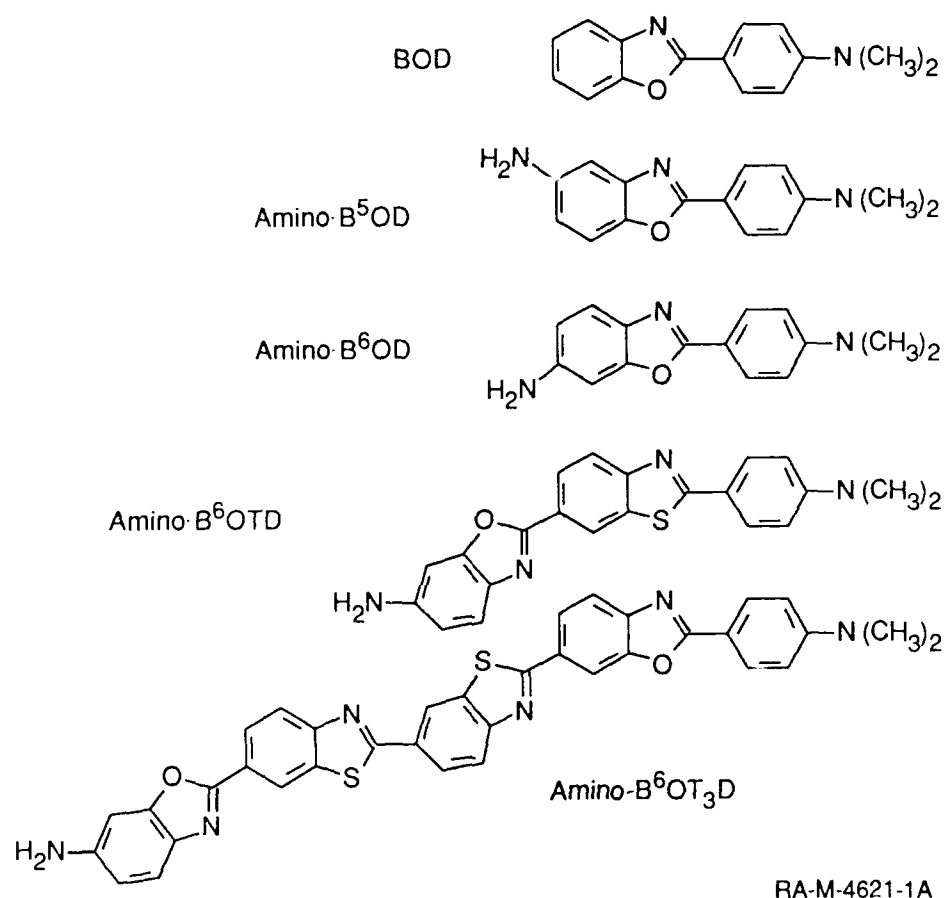
Figure 1.  ALHD precursors prepared.

6
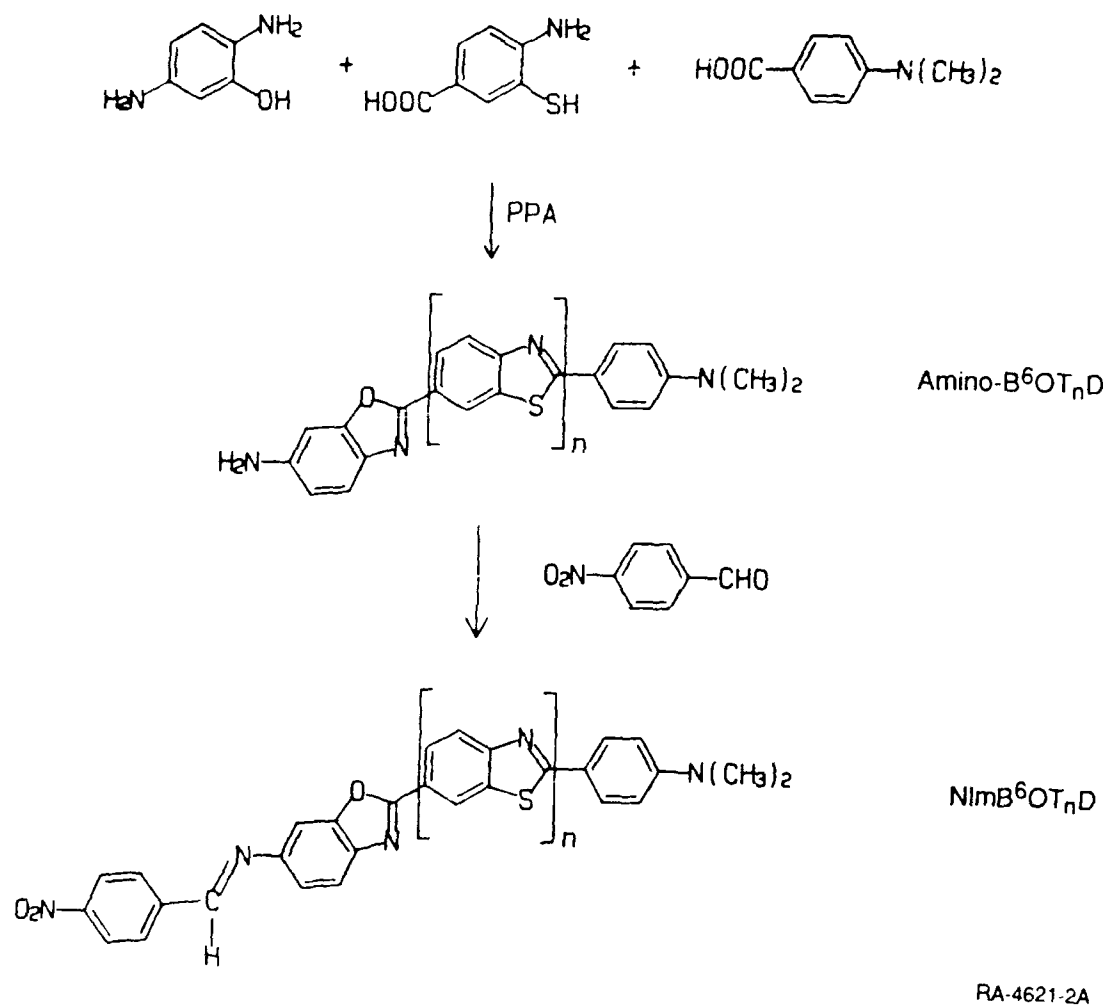
Figure 2. Synthesis of NIm-HD compounds.

RA-4621-2A

7

NImB⁵OD

NImB⁶OD

ClmB⁶OD

NImB⁶OTD

N₂ImB⁶OD

N₂ImB⁶OD₁₈

RA-M-4621-29

Figure 3.   ALHD compounds prepared.

8

NImB$^6$OD$_{18}$

NHImB$^6$OD$_{18}$

Bis(NImB$^6$OD)

R', R" = - H, - CH$_3$, - (CH$_2$)$_{17}$CH$_3$
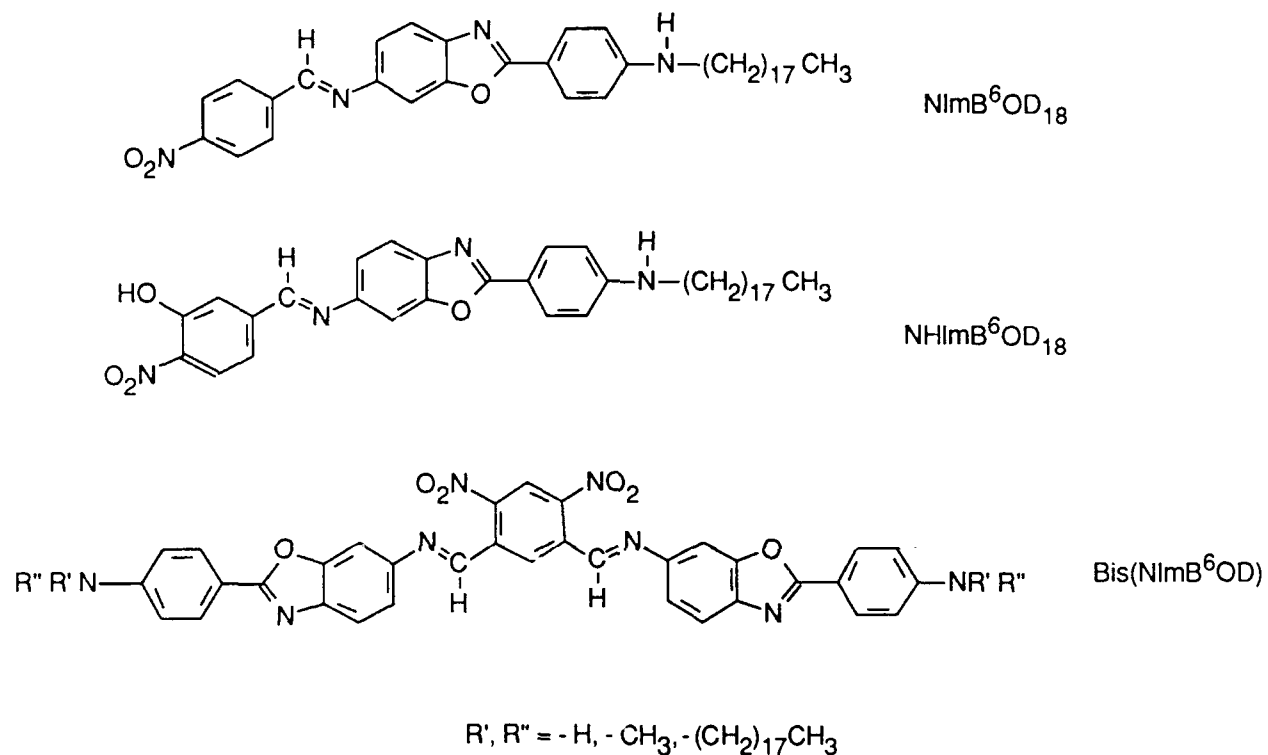
RA-M-4621-30

Figure 3. ALHD compounds prepared. (Concluded)

# Table 2

## SYNTHESIS OF BENZAZOLE-CONTAINING ALHD COMPOUNDS AND THEIR PRECURSORS

| | Yield [a] (%) | mp [b] (°C) | UV-VIS [c] ($\lambda_{max}$) | Color |
|---|---|---|---|---|
| BOD | (34) | 187 | 339 | Lt. yellow |
| Amino-$B^5OD$ | 41 (25) | 207 | 351 | Lt. yellow |
| Amino-$B^6OD$ | 98 (67) | 228 | 350 | Pink |
| Amino-$B^6OTD$ | 62 (22) | 279 | 393 (396) | Yellow |
| Amino-$B^6OT_3D$ | 88 | > 440 | 399 | Orange-red |
| Amino-$B^6OD_{18}$ | 64 (29) | 127 | 347 (353) | White |
| NImB$^5$OD | 90 | 276 | 348, 390sh (348) | Orange |
| NImB$^6$OD | 89 | 272 | 344, 418 (346, 402) | Red |
| N$_2$ImB$^6$OD | 90 | 248 | 345, 462 (350, 436) | Dark red |
| ClmB$^6$OD | 76 | 276 | 348, 399 (346sh, 387) | Yellow |
| NImB$^6$OTD | 84 | 307 | 408 | Orange |
| NImB$^6$OD$_{18}$ | 81 | 181[d] | 339, 416 (340, 406) | Yellow |
| N$_2$ImB$^6$OD$_{18}$ | 88 | 149[d] | 344, 454 (346, 428) | Red |
| NHImB$^6$OD$_{18}$ | 90 | 161[d] | 339, 426 (349) | Orange |
| Bis(NImB$^6$OD$_{18}$) | 81 | 159 | 351, 474 (352, 442) | Orange |

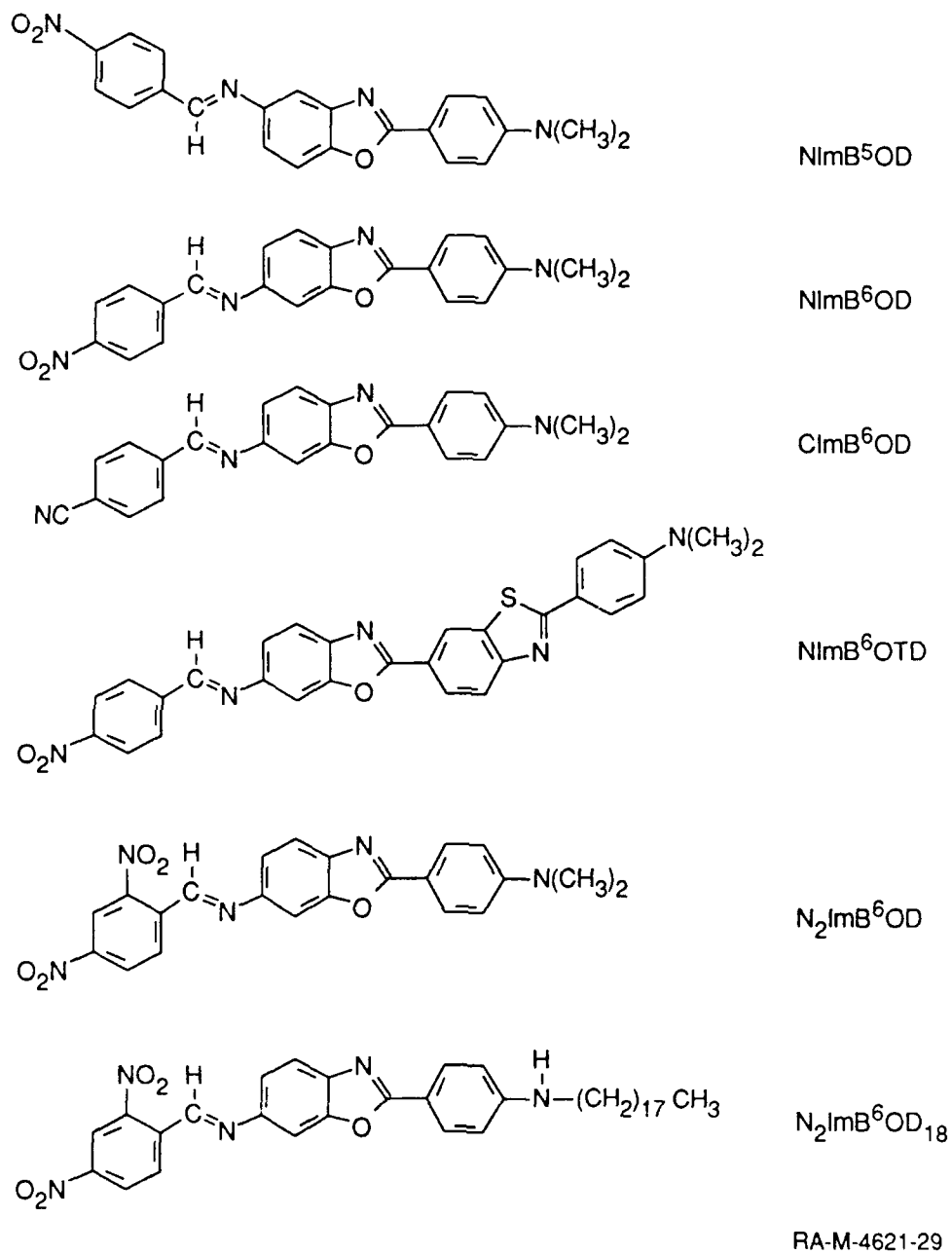[a] Crude isolated yield (yield after recrystallization).
[b] By differential scanning calorimetry, 10°C/min.
[c] Solvents: Toluene (acetonitrile).
[d] Smectic to isotropic transition.
sh = shoulder.

# Table 3

## ELEMENTAL ANALYSES
## OF ALHD COMPOUNDS AND THEIR PRECURSORS*

| | C | H | N | O |
|---|---|---|---|---|
| BOD | 75.80 | 5.81 | 11.53 | |
| | **75.61** | **5.92** | **11.76** | |
| Amino-B$^5$OD | 71.13 | 5.97 | 16.59 | |
| | **71.99** | **5.86** | **16.60** | |
| Amino-B$^6$OD | 71.13 | 5.97 | 16.59 | |
| | **71.72** | **5.95** | **16.15** | |
| Amino-B$^6$OD$_{18}$ | 77.94 | 9.92 | 8.80 | 3.35 |
| | **76.29** | **9.61** | **8.66** | **4.29** |
| Amino-B$^6$OTD | 68.37 | 4.69 | 14.50 | |
| | **68.57** | **4.81** | **14.87** | |
| NImB$^5$OD | 68.38 | 4.70 | 14.50 | |
| | **68.88** | **4.63** | **14.56** | |
| NImB$^6$OD | 68.38 | 4.70 | 14.50 | |
| | **68.70** | **4.67** | **14.65** | |
| CImB$^6$OD | 75.39 | 4.95 | 15.29 | |
| | **74.50** | **5.00** | **15.03** | |
| NImB$^6$OTD | 67.03 | 4.07 | 13.48 | |
| | **66.88** | **4.09** | **13.69** | |
| N$_2$ImB$^6$OD | 61.25 | 3.97 | 16.23 | 18.54 |
| | **61.19** | **3.95** | **16.17** | **18.56** |
| NImB$^6$OD$_{18}$ | 74.72 | 8.25 | 9.17 | 7.86 |
| | **73.57** | **8.18** | **8.98** | **8.48** |
| N$_2$ImB$^6$OD$_{18}$ | 69.59 | 7.53 | 10.68 | 12.19 |
| | **68.17** | **7.53** | **10.63** | **12.23** |
| NHImB$^6$OD$_{18}$ | 72.81 | 8.04 | 8.94 | 10.21 |
| | **71.94** | **8.38** | **8.73** | **10.67** |
| Bis(NImB$^6$OD$_{18}$) | 73.52 | 8.29 | 9.80 | 8.40 |
| | **72.25** | **8.64** | **9.61** | **9.31** |

* Top number in each pair = calculated, bottom number = found.

11
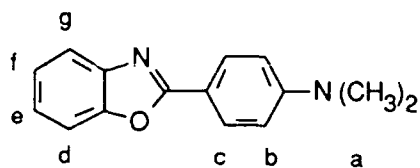
BOD $^1$H NMR DATA (ppm) in DMSO-$d_6$:

| | | |
|---|---|---|
| a | 3.03 | s |
| b | 6.85 | AB quartet |
| c | 7.98 | $J_{bc}$ = 9.21 Hz |
| d | 7.68 | m |
| e | 7.32 | m |
| f | 7.32 | m |
| g | 7.68 | m |
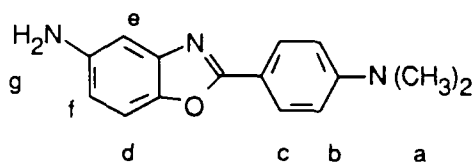


amino-B$^5$OD $^1$H NMR DATA (ppm) in DMSO-$d_6$:

| | | |
|---|---|---|
| a | 3.01 | s |
| b | 6.82 | AB quartet |
| c | 7.91 | $J_{bc}$ = 9.15 Hz |
| d | 7.30 | dd, $J_{df}$ = 8.56, $J_{de}$ = 0.46 Hz |
| e | 6.77 | dd, $J_{ef}$ = 2.22, $J_{ed}$ = 0.48 Hz |
| f | 6.55 | dd, $J_{fd}$ = 8.58, $J_{fe}$ = 2.21 Hz |
| g | 4.99 | s |
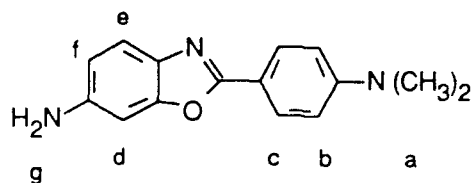


amino-B$^6$OD $^1$H NMR DATA (ppm) in DMSO-$d_6$:

| | | |
|---|---|---|
| a | 2.99 | s |
| b | 6.81 | AB quartet |
| c | 7.87 | $J_{bc}$ = 9.15 |
| d | 6.76 | d, $J_{df}$ = 2.02 Hz |
| e | 7.29 | d, $J_{ef}$ = 8.42 Hz |
| f | 6.57 | dd, $J_{fe}$ = 8.44, $J_{fd}$ = 2.06 Hz |
| g | 5.27 | s |

RA-m-4621-19

Figure 4. NMR data for BOD, amino-B$^5$ OD, and amino-B$^6$ OD.

amino-B⁶OTD ¹H NMR DATA (ppm) in DMSO-d₆:
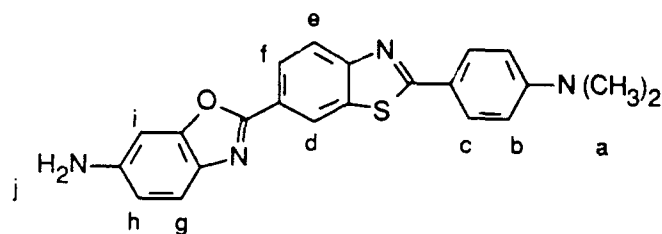
amino-B$^6$OTD $^1$H NMR DATA (ppm) in DMSO-$d_6$:

| | | |
|---|---|---|
| a | 3.04 | s |
| b | 6.83 | AB quartet |
| c | 7.92 | $J_{bc}$ = 9.09 Hz |
| d | 8.75 | dd, $J_{df}$ = 1.75, $J_{de}$ = 0.53 Hz |
| e | 8.02 | dd, $J_{ef}$ = 8.61, $J_{ed}$ = 0.53 Hz |
| f | 8.15 | dd, $J_{fe}$ = 8.56, $J_{fd}$ = 1.77 Hz |
| g | 7.41 | d, $J_{gh}$ = 8.61 Hz |
| h | 6.65 | dd, $J_{hg}$ = 8.47, $J_{hl}$ = 2.01 Hz |
| i | 6.83 | d, $J_{ih}$ = 1.97 |
| j | 5.34 | broad |



NImB⁶OTD ¹H NMR DATA (ppm) in DMSO-d₆:
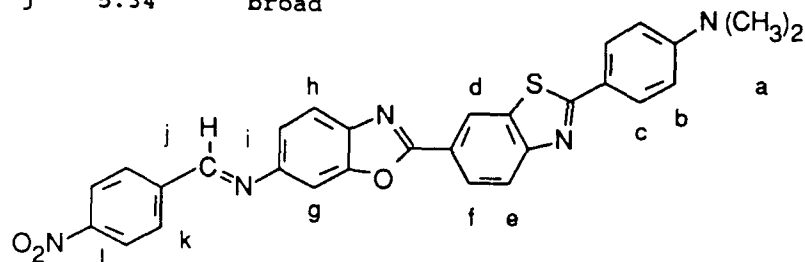
NImB$^6$OTD $^1$H NMR DATA (ppm) in DMSO-$d_6$:

| | | |
|---|---|---|
| a | 3.15 | s |
| b | 6.86 | AB quartet |
| c | 7.95 | $J_{bc}$ = 8.62 Hz |
| d | 7.84 | d, $J_{df}$ = 1.69 Hz |
| e | 7.86 | d, $J_{ef}$ = 8.46 Hz |
| f | 7.48 | dd, $J_{fe}$ = 8.23, $J_{fd}$ = 1.89 Hz |
| g | 8.90 | d, $J_{gi}$ = 1.46 Hz |
| h | 8.09 | d, $J_{hi}$ = 8.42 Hz |
| i | 8.29 | dd, $J_{ih}$ = 8.50, $J_{ig}$ = 1.30 Hz |
| j | 8.96 | s |
| k | 8.24 | AB quartet |
| l | 8.38 | $J_{kl}$ = 8.49 Hz |

RA-m-4621-20

Figure 5.   NMR data for amino-B⁶ OTD and NImB⁶ OTD.

13
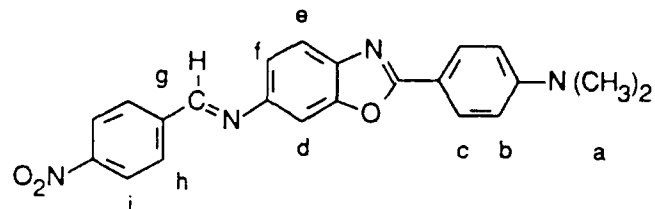
NImB<sup>6</sup>OD <sup>1</sup>H NMR DATA (ppm) in DMSO-d$_6$:

| | | |
|---|---|---|
| a | 3.05 | s |
| b | 6.87 | AB quartet |
| c | 8.00 | $J_{bc}$ = 9.20 Hz |
| d | 7.75 | dd, $J_{df}$ = 1.97, $J_{de}$ = 0.5 Hz |
| e | 7.55 | dd, $J_{ef}$ = 8.38, $J_{ed}$ = 0.5 Hz |
| f | 7.41 | dd, $J_{fe}$ = 8.40, $J_{fd}$ = 1.97 Hz |
| g | 8.93 | s |
| h | 8.21 | AB quartet |
| i | 8.36 | $J_{hi}$ = 9 Hz |
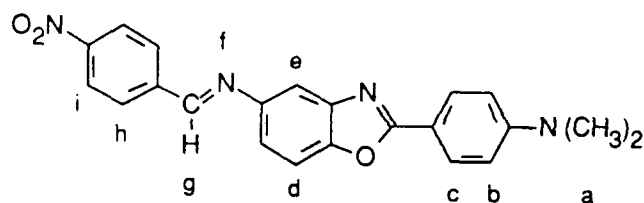


NImB<sup>5</sup>OD <sup>1</sup>H NMR DATA (ppm) in DMSO-d$_6$:

| | | |
|---|---|---|
| a | 3.05 | s |
| b | 6.87 | AB quartet |
| c | 8.01 | $J_{bc}$ = 9.2 Hz |
| d | 7.73 | d, $J_{df}$ = 8.5 Hz |
| e | 7.68 | d, $J_{ef}$ = 2.1 Hz |
| f | 7.36 | dd, $J_{fd}$ = 8.5, $J_{fe}$ = 2.1 Hz |
| g | 8.91 | s |
| h | 8.22 | AB quartet |
| i | 8.37 | $J_{hi}$ = 8.9 Hz |

RA-m-4621-21

Figure 6.   NMR data for NImB<sup>6</sup> OD and NImB<sup>5</sup> OD.

14
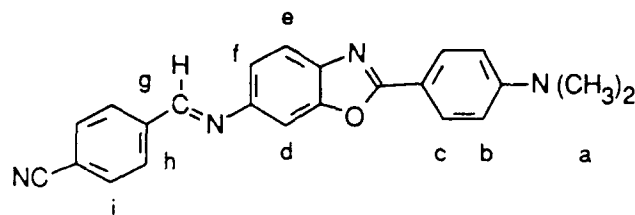
CImB$^6$OD $^1$H NMR DATA (ppm) in DMSO-d$_6$:

| | | |
|---|---|---|
| a | 3.04 | s |
| b | 6.87 | AB quartet |
| c | 8.00 | J$_{bc}$ = 9.1 Hz |
| d | 7.71 | d, J$_{df}$ = 1.95 Hz |
| e | 7.70 | d, J$_{ef}$ = 8.37 Hz |
| f | 7.37 | dd, J$_{fe}$ = 8.36, J$_{fd}$ = 1.97 |
| g | 8.85 | s |
| h | 7.97 | AB quartet |
| i | 8.13 | J$_{hi}$ = 8.42 Hz |
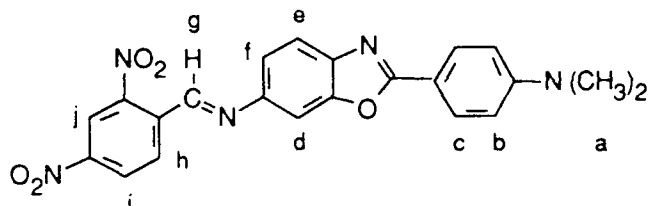


N$_2$ImB$^6$OD $^1$H NMR DATA (ppm) in DMSO-d$_6$:

| | | |
|---|---|---|
| a | 3.05 | s |
| b | 6.87 | AB quartet |
| c | 8.00 | J$_{bc}$ = 8.98 Hz |
| d | 7.73 | d, (overlaps 7.74 ppm resonance) |
| e | 7.74 | d, J$_{ef}$ = 8.46 Hz |
| f | 7.40 | dd, J$_{fe}$ = 8.42, J$_{fd}$ = 2.01 Hz |
| g | 9.40 | s |
| h | 8.47 | d, J$_{hi}$ = 8.47 Hz |
| i | 8.65 | dd, J$_{ih}$ = 8.57, J$_{ij}$ = 2.38 Hz |
| j | 8.83 | d, J$_{ji}$ = 2.24 |

RA-m-4621-22

Figure 7.  NMR data for CImB$^6$ OD and N$_2$ImB$^6$ OD.

15
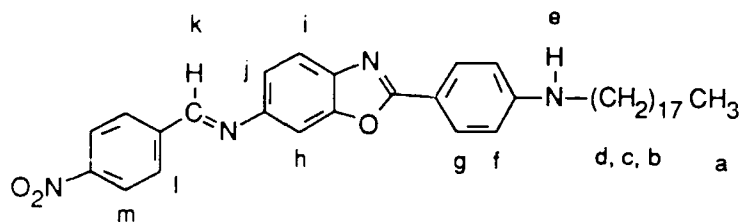
NImB$^6$OD$_{18}$ $^1$H NMR DATA (ppm) in CDCl$_3$:

| | | |
|---|---|---|
| a | 0.85 | t |
| b | 1.24 | m |
| c | 1.58 | m |
| d | 3.10 | broad |
| e | 6.32 | broad |
| f | 6.72 | AB quartet |
| g | 7.90 | $J_{fg}$ = 8.79 Hz |
| h | 7.70 | d, $J_{hi}$ = 1.87 Hz |
| i | 7.67 | d, $J_{ij}$ = 8.38 Hz |
| j | 7.38 | dd, $J_{ji}$ = 8.42, $J_{jh}$ = 1.83 Hz |
| k | 8.91 | s |
| l | 8.22 | AB quartet |
| m | 8.35 | $J_{lm}$ = 8.80 Hz |
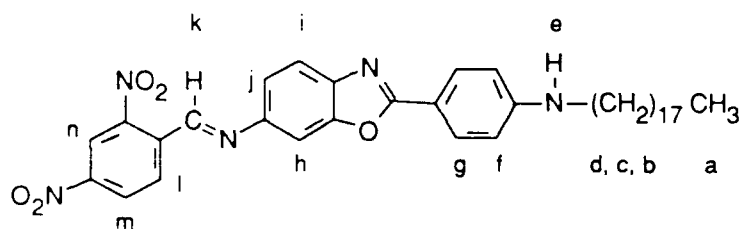


N$_2$ImB$^6$OD$_{18}$ $^1$H NMR DATA (ppm) in CDCl$_3$:

| | | |
|---|---|---|
| a | 0.86 | t, $J_{ab}$ = 6.73 Hz |
| b | 1.24 | m |
| c | 1.64 | m |
| d | 3.18 | t, $J_{dc}$ = 7.14 Hz |
| e | 4.1 | broad |
| f | 6.63 | AB quartet |
| g | 8.02 | $J_{fg}$ = 8.89 Hz |
| h | 7.50 | d, $J_{hi}$ = 1.55 Hz |
| i | 7.68 | d, $J_{ij}$ = 8.40 Hz |
| j | 7.34 | dd, $J_{ji}$ = 8.38, $J_{jh}$ = 1.98 Hz |
| k | 9.07 | s |
| l | 8.61 | d, $J_{lm}$ = 8.68 Hz |
| m | 8.51 | ddd, $J_{ml}$ = 8.66, $J_{mn}$ = 2.25 Hz |
| n | 8.90 | d, $J_{nm}$ = 2.22 Hz |

RA-m-4621-23

Figure 8. NMR data for NImB$^6$ OD$_{18}$ and N$_2$ImB$^6$ OD$_{18}$.

16
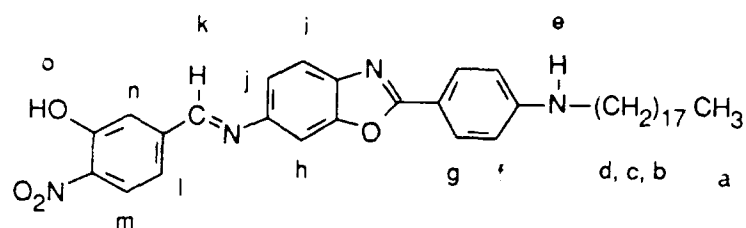
NHImB^6OD_{18} $^1$H NMR DATA (ppm) in CDCl$_3$:

| | | |
|---|---|---|
| a | 0.84 | t |
| b | 1.23 | m |
| c | 1.58 | m |
| d | 3.11 | t |
| e | 6.4 | broad |
| f | 6.71 | AB quartet |
| g | 7.89 | $J_{fg}$ = 8.79 Hz |
| h | 7.64 | s, broad |
| i | 7.47 | d, $J_{ij}$ = 8.64 Hz |
| j | 7.35 | dd, $J_{ji}$ = 8.24, $J_{jh}$ = 1.83 Hz |
| k | 8.75 | s |
| l | 7.66 | d, $J_{lm}$ = 8.57 Hz |
| m | 7.98 | d, $J_{ml}$ = 8.46 Hz |
| n | 7.68 | d, $J_{nl}$ = 1.79 Hz |
| o | 6.4 | broad |
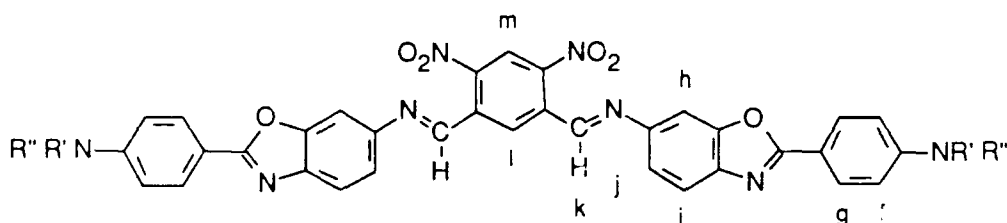


R', R" = - H, - CH$_3$, -(CH$_2$)$_{17}$CH$_3$

e          d,c,b          a

bis(NImB^6OD_{18}) $^1$H NMR DATA (ppm) in CDCl$_3$:

| | | |
|---|---|---|
| a | 0.86 | t, $J_{ab}$ = 6.61 Hz |
| b | 1.24 | m |
| c | 1.54 | m |
| d | 3.19 | t, $J_{dc}$ = 7.24 Hz |
| e | 3.5 | broad |
| f | 6.66 | AB quartet |
| g | 8.05 | $J_{fg}$ = 8.89 Hz |
| h | 7.58 | d, $J_{hi}$ = 1.46 Hz |
| i | 7.72 | d, $J_{ij}$ = 8.01 Hz |
| j | 7.42 | dd, $J_{ji}$ = 8.40, $J_{jh}$ = 1.97 Hz |
| k | 9.14 | s |
| l | 8.83 | s |
| m | 9.33 | s |

RA-m-4621-24

Figure 9. NMR data for NHImB^6 OD$_{18}$ and bis (NImB^6 OD$_{18}$).

17

protons when the electron-withdrawing group nitrophenylimine is substituted for the electron-donating amino group. If we compare the UV-VIS spectra of AImD compounds with constant conjugation length but various A groups in a single solvent, we find that the $\pi-\pi^*$ transition remains nearly constant (344-343 nm), while the $n-\pi^*$ transition varies (from 390 to 462 nm) with type, number, and site of the A group. $NImB^6OD$ and $CImB^6OD$ differ only in the presence of a nitro or a cyano group. If we compare the UV-VIS spectra of these compounds in toluene, the $n-\pi^*$ transition in $NImB^6OD$ occurs at a longer wavelength: 418 nm for the $NImB^6OD$ compared to 399 nm for $CImB^6OD$. In the spectrum of $N_2ImB^6OD$, a shift of the $n-\pi^*$ transition to 462 nm (lower energy) shows the effect of an additional nitro group. The $\pi-\pi^*$ transition is shifted to 408 nm by extending the conjugation length in $NImB^6OTD$. The electronic dipole is affected by acceptor substitution in the following way: $(NO_2)_2 > NO_2 > CN$. The absorption maximum of $NImB^5OD$ is shifted to a shorter wavelength (390 nm) than that of $NImB^6OD$ (418 nm) in toluene. We attribute this difference to a resonance structure of $NImB^5OD$ that does not allow participation of the nitrophenylimine $\pi$-orbitals. UV-VIS spectra of $NImB^6OD$ in solvents of differing polarity show a blue shift (to higher energy) in the $n-\pi^*$ transition and a red shift (to lower energy) in the $\pi-\pi^*$ transition when the solvent is changed from toluene to acetonitrile.

The DSC thermograph of $NImB^6OTD$ exhibits melting with decomposition at 307°C as seen in Figure 10. In sharp contrast, $N_2ImB^6OD_{18}$ (Figure 11) and $NImB^6OD_{18}$ (Figure 12), which have attached octadecyl alkyl segments, exhibit multiple endotherms prior to melting at 149°C and 181°C, respectively. $NImB^6OD_{18}$ exhibits crystal to crystal phase transitions at 79°, 89°, and 99°C, then a crystal to smectic A phase transition at 135°C and a smectic A to isotropic phase transition at 181°C. $N_2ImB^6OD_{18}$ exhibits a crystal to smectic A transition at 126°C and a smectic A to isotropic phase transition at 149°C.
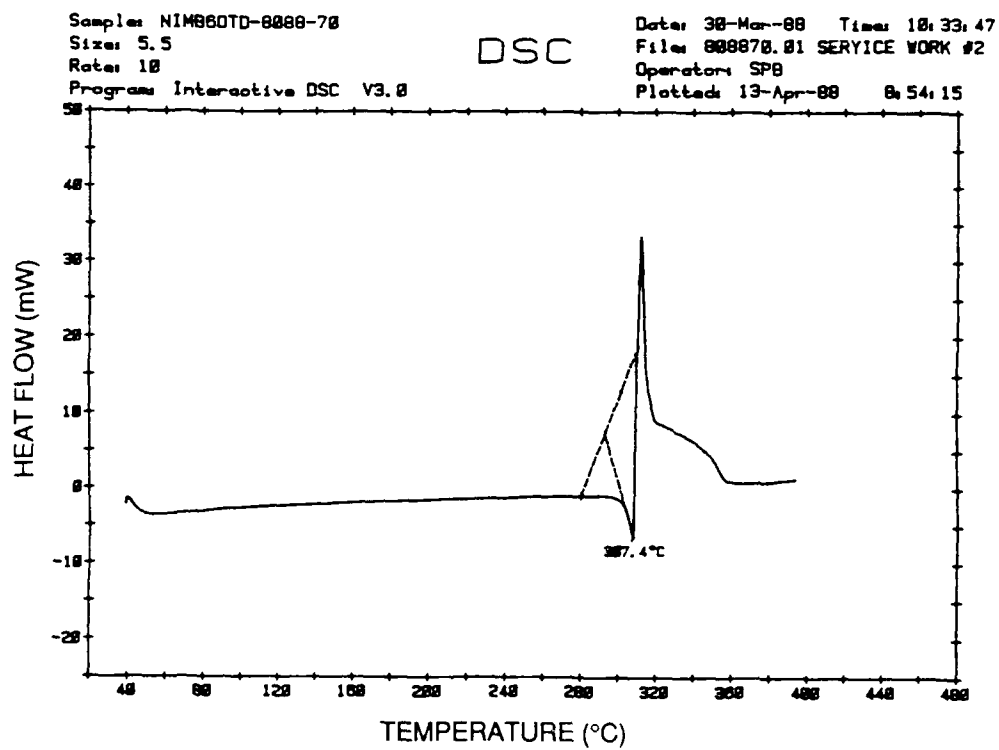
Figure 10. DSC of NImB[6] OTD.
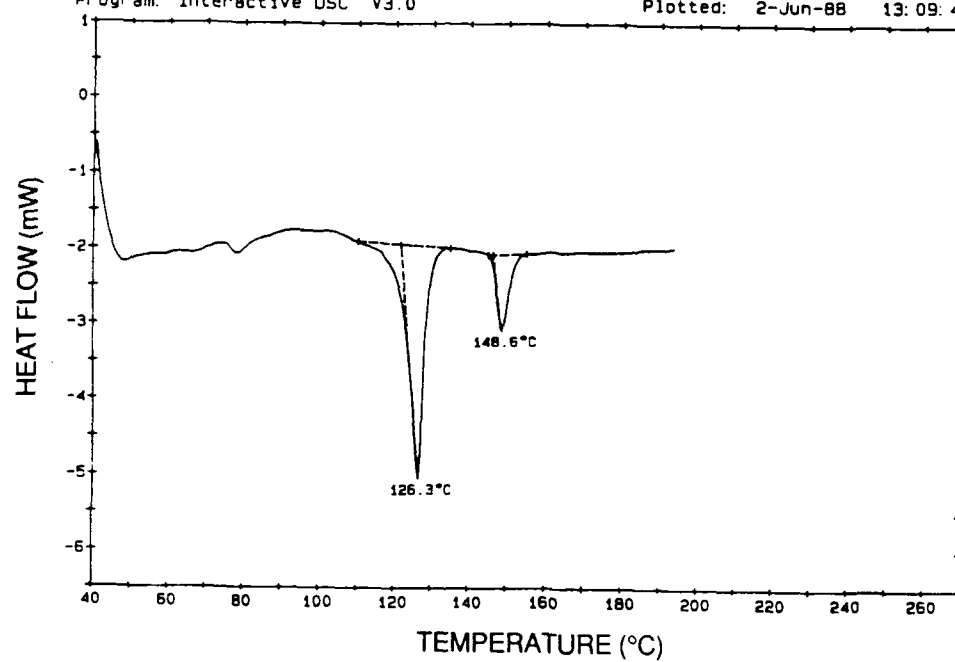
Figure 11. DSC of $N_2ImB^6$ $OD_{18}$.
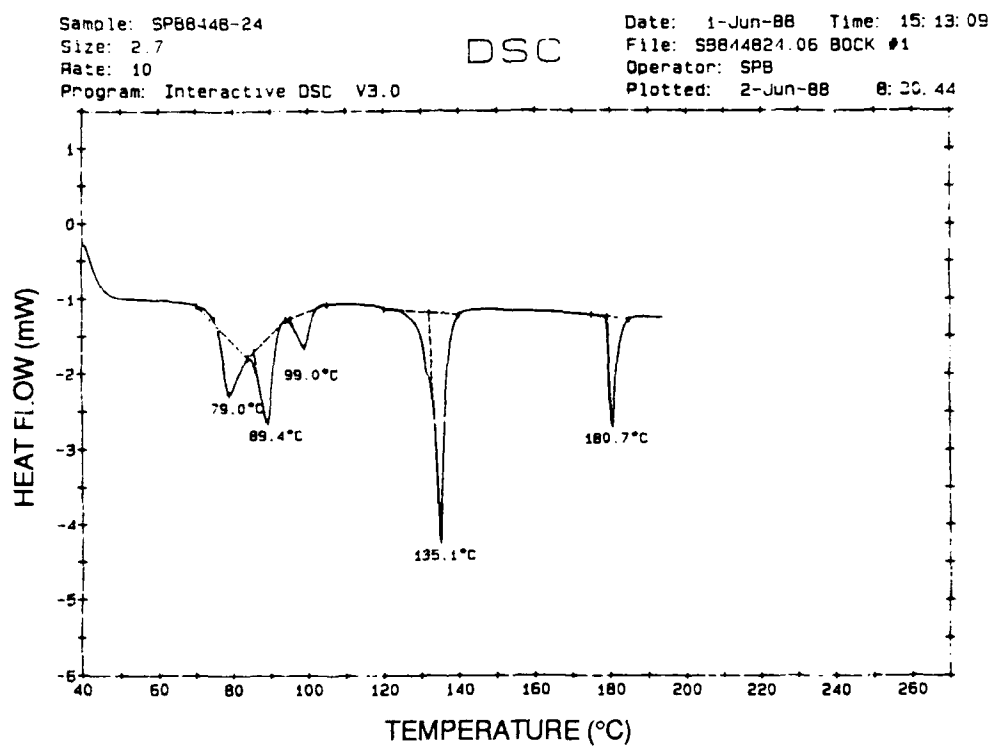
Figure 12.   DSC of NImB$^6$ OD$_{18}$.

## 4. NLO Measurement

Preliminary measurements of the hyperpolarizability of $NImB^6OD$ by Professor Anthony Garito at the University of Pennsylvania have yielded $\beta\mu = 500 \times 10^{-30}$ cm$^5$ D/esu. We made two important modifications to $NImB^6OD$ to produce $N_2ImB^6OD_{18}$, as shown in Figure 3. The latter compound has two nitro groups on the terminal phenyl ring, which we know from NMR measurements decreases the electron density of the terminal ring relative to that of $NImB^6OD$, and a $C_{18}$ alkyl chain on the donor group, which increases solubility (see below).

We have sent the following compounds to Professor Garito for NLO evaluation: $BOD$, amino-$B^6OD$, amino-$B^5OD$, $CImB^6OD$, $NImB^5OD$, $NImB^6OD$, $N_2ImB^6OD$, $NImB^6OTD$, $N_2ImB^6OD_{18}$, $NImB^6OD_{18}$, $NHImB^6OD_{18}$, and $bis(NImB^6OD_{18})$.

## 5. Synthesis of Benzazoles with Solubilizing Alkyls

When we N-alkylated 4-aminobenzoic acid with octadecyl bromide and condensed the product of this reaction with 2,5-diaminophenol in PPA, the resulting product was the N-alkyl analog of amino-$B^6OD$. Condensation of amino-$B^6OD_{18}$ with 2,4-dinitrobenzaldehyde yielded the dark red dinitro derivative, $N_2ImB^6OD_{18}$ (Figure 2).

Incorporation of the long alkyl groups results in a higher solubility for $N_2ImB^6OD_{18}$ (3.9 mg/mL) than for $N_2ImB^6OD$ (0.38 mg/mL) in toluene at 25°C. The greater solubility should allow easier incorporation into flexible polymer hosts and easier determination of NLO properties of the $N_2ImB^6OD_{18}$ at higher concentrations in organic solvents than are possible with $NImB^6OD$.

## 6. ALHD Compounds in Host/Guest Systems

We have conducted preliminary experiments to determine the stability of ALHD compounds in PPA (83.8% $P_2O_5$) and methanesulfonic acid (MSA). Isolation of $NImB^5OD$ from 100°C PPA or MSA after 1 hour yielded the starting compound $NImB^5OD$, as determined by IR analysis. We began

to incorporate ALHD compounds into solutions of poly (p-phenylenebenzo-bisthiazole) (PBT) in PPA; NImB$^5$OD was incorporated in 15% PBT/PPA by using a Brabender mixer at 90-100°C for 2 hours. The resulting solutions are expected to yield host PBT films with guest ALHD compounds.

### 7. Preparation of Bis(ALHD) Compounds

We synthesized bis(NImB$^6$OD$_{18}$) by condensing 4,6-dinitro-1,3-benzenedialdehyde with amino-B$^6$OD$_{18}$. The product, shown in Figure 3, has two nitro groups at the center of the molecule that draw electron density from both ends. This compound should preserve the $\chi^{(2)}$ contribution by inhibiting crystallization of the molecules that have dipoles oriented in opposite directions.

## B. Synthesis of Materials for $\gamma^{(3)}$

### 1. Synthesis of PBO/POL (Phenoxazine Ladder Polymer) Copolymer

We conducted four polymerizations by condensing one equivalent of 4,6-diamino-1,3-benzenediol with either 0.9 or 0.95 equivalent of terephthalic acid and either 0.1 or 0.05 equivalent of 2,5-dihydroxybenzoquinone (DHBQ) in PPA. The desired copolymer structure resulting from these condensations is shown in Figure 13 and should have 90-95% p-phenylenebenzobisoxazole units and 5-10% phenoxazine units. The intrinsic viscosities of the isolated products, measured in methanesulfonic acid (MSA), were 9.5 and 11.5 dL/g when 5% DHBQ (0.05 equivalent) was used and 6.6 and 7.8 dL/g when 10% DHBQ (0.1 equivalent) was used. The presence of phenoxazine units in the copolymer has not been confirmed, but the polymer could be analyzed by solid state NMR in an attempt to detect the presence of phenoxazine units. We believe this copolymer structure is one way of improving the third-order response of PBO while maintaining its liquid crystalline processibility.

### 2. Synthesis of Symmetrical Benzazoles

We synthesized 2,6-bis(4-aminophenyl)benzo [1,2-d:4,5-d']

bisthiazole (BAPBBT) (Figure 13) because of its potential for polymerization through the terminal amino groups. Mass spectral analysis confirmed the BAPBBT structure, but elemental analysis showed a slightly low value for carbon and thus suggested the presence of a bound impurity, possibly a phosphate. The diamino compound was originally prepared because the diol analog tenaciously held on to phosphate even with extensive heating with aqueous NaOH. Both the diol and the diamino compounds can be incorporated into flexible polymers through reaction with acid chlorides or isocyanates to form esters, amides, and urethanes. Prasad[1] has found LARC-TPI, a thermoplastic polyimide, to be an order of magnitude lower in $\chi^{(3)}$ than PBT. He attributes this difference to the more extensive π-electron conjugation in PBT. Copolymers might be synthesized that incorporate symmetrical benzazole units to take advantage of the extended π-conjugation and fast switching speed of these units.

## Experimental Methods

Infrared spectra were determined on a Perkin Elmer 281B Spectrometer. [1]H (400 MHz) and [13]C (100 MHz) spectra were determined with a Varian XL400 NMR spectrometer. UV-VIS spectra were determined with a Hewlett Packard 8450A spectrometer. Melting points and decomposition points were determined on a Dupont 1090 Differential Scanning Calorimeter. Elemental analyses were determined by Galbraith Analytical Laboratories of Knoxville, TN.

The following compounds were prepared by published procedures: 4,6-dinitro-1,3-benzenedicarboxaldehyde, 4-amino-3-mercaptobenzoic acid hydrochloride, and 4-N-octadecylaminobenzoic acid. 2,5-Diamino phenol was synthesized by reduction of 2,5-dinitrophenol using stannous chloride in HCl.

The following compounds were purchased from Aldrich Chemical

---

[1]P. N. Prasad, in "Nonlinear Optical and Electroactive Polymers," Ed. P. N. Prasad and D. R. Ulrich, Plenum Press, N.Y., 1988.
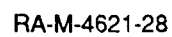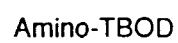
Figure 13. Structures of amino-TBOD, BAPBBT, and PBO/POL.

Company:  4-nitrobenzaldehyde, 2,4-dinitrobenzaldehyde, 3-nydroxy-4-nitrobenzaldehyde, 4-N,N-dimethylaminobenzoic acid, 4-aminobenzoic acid, and 2,4-diaminobenzoic acid.

## Synthesis of 6-Amino-2-(4-N,N-dimethylaminophenyl) Benzoxazole (Amino-B[6]OD).

The synthesis of one member of the amino-BOD class is presented; the others were similarly prepared.

Into a 100-mL, three-neck flask equipped with mechanical stirrer and reflux condenser were placed 2,5-diaminophenol dihydrochloride (3.25 g, 16.5 mmol) and 115% poly(phosphoric acid) (75 g, 83.8% $P_2O_5$). The mixture was heated to 50-100°C for 16 hours with stirring under inert atmosphere to remove HCl and then stirred under reduced pressure until clear. To the solution was added 4-N,N-dimethylaminobenzoic acid (2.85 g, 17.3 mmol); the resulting solution was heated to 180-185°C over 1 hour. The solution was maintained at 180-185°C for 20 hours and then allowed to cool. The calculated final $P_2O_5$ content of the PPA after complete reaction is 83.15%. The reaction mixture was poured into 400 mL of water. The mixture was neutralized with aqueous NaOH, then filtered to yield 4.08 g of brownish-yellow solid. Recrystallization from toluene yielded 2.78 g (67%) of a light pink crystalline solid that was dried under reduced pressure at 45-50°C:  mp 228°C (by DSC); mass spectrum m/e 253 ($M^+$, parent); $^1H$ NMR (400 MHz, in $Me_2SO-d_6$, ppm) 2.99, s, $-NMe_2$, 5.27, s, $-NH_2$, 6.81 and 7.87, AB quartet, $J_{ab}$ = 9.15 Hz, aromatic N,N-dimethylaminophenyl, 6.57, dd, J = 8.44 Hz, J = 2.06 Hz, 6.76, d, J = 2.02 Hz, 7.29, d, 8.42 Hz; UV-VIS (toluene, nm) 350. Analysis calculated for $C_{15}H_{15}N_3O$:  C, 71.13; H, 6.00; N, 16.59. Found:  C, 71.72; H, 5.95; N, 16.15.

## Synthesis of Amino-B[5]OD.

This compound was synthesized as above in 41% yield from 2,4-diaminophenol dihydrochloride and 4-N,N-dimethylaminobenzoic acid in PPA. The product was recrystallized in 25% yield from toluene to yield light yellow crystals:  mp 207°C (by DSC), mass spectrum m/e 253 ($M^+$, parent); $^1H$ NMR (400 MHz, in $Me_2SO-d_6$, ppm integration) 3.01 (6) s, $-NMe_2$, 6.82 (2) and 7.91 (2), AB quartet, $J_{ab}$ =

9.15 Hz, aromatic N,N-dimethylaminophenyl, 6.55 (1), dd, J = 8.58 Hz, J = 2.21 Hz, 6.77 (1) dd, J = 2.22 Hz, J = 0.48 Hz, 7.30 (1) dd, J = 8.56, J = 0.46, 4.99 (2) s; UV-VIS (toluene) 351 nm. Analysis calculated for $C_{15}H_{15}N_3O$: C, 71.13; H, 6.00; N, 16.59. Found: C, 71.99; H, 5.86; N, 16.60.

Synthesis of BOD. This compound was synthesized as above in 34% yield by condensing 2-aminophenol with 4-N,N-dimethylaminobenzoic acid in PPA. The product was recrystallized from toluene in 28% yield as white crystals: mp 187°C (by DSC); mass spectrum m/e 238 ($M^+$ parent); $^1$H NMR (400 MHz, ppm integration), 3.03 (6), s, 6.85 (2), and 7.98 (2), AB quartet (aromatic 4-N,N-dimethylaminophenyl), $J_{ab}$ = 9.21 Hz, $-NMe_2$, 7.32 (2), m, 7.68 (2), m; UV-VIS (toluene) 339 nm. Analysis calculated for $C_{15}H_{14}N_2O$: C, 75.80; H, 5.81; N, 11.53. Found: C, 75.61; H, 5.92; N, 11.76.

Synthesis of Amino-B[6]OTD. Into a 500-mL, three-neck flask equipped with a mechanical stirrer and reflux condenser were placed 2,5-diaminophenol dihydrochloride (9.8535 g, 50 mmol), 4-N,N-dimethylaminobenzoic acid (8.2595 g, 50 mmol), 4-amino-3-mercaptobenzoic acid (10.2835 g, 50 mmol), and 115% poly(phosphoric acid) (400 g, 83.8% $P_2O_5$). The mixture was heated under inert atmosphere at 55-60°C for 48 hours and then under reduced pressure for 6 hours to remove the HCl. The reaction mixture was then heated to 180-185°C for 16 hours. The calculated final $P_2O_5$ content of the PPA is 83.05%. The reaction mixture was then quenched in 3 L of water and filtered. The resulting solid was then neutralized with aqueous NaOH and filtered to yield 12.01 g (66%) of brownish red solid that was dried under reduced pressure at 45-50°C. Recrystallization of 5.2 g of crude product from toluene yielded 1.8 g of yellow solid (22%): mp 279°C (by DSC); mass spectrum m/e 386 ($M^+$ parent); $^1$H NMR (400 MHz, in $Me_2SO-d_6$, ppm integration); 3.04 (6), s, $-NMe_2$, 5.34 (2), s, $-NH_2$, 6.83 (2) and 7.92 (2), AB quartet, $J_{ab}$ = 9.09 Hz, 6.65 (1), dd, J = 3.47, J = 2.01, 6.83 (1), d, J = 1.97, 7.41 (1), d, J = 8.61, 8.02 (1), dd, J = 8.61, J = 0.53, 8.15 (1), dd, J = 8.56, J = 1.77, 8.75 (1), dd, J = 1.75, J = 0.53; UV-VIS

(toluene, nm) 393, (CH$_3$CN, nm) 396. Analysis calculated for C$_{22}$H$_{18}$N$_4$OS: C, 68.37; H, 4.69; N, 14.50. Found: C, 68.57; H, 4.81; N, 14.87.

Synthesis of NImB$^6$OD. The synthesis of one member of this class is presented; the others were similarly prepared.

Into a 200-mL, three-neck flask equipped with a Dean-Stark trap, reflux condenser, and magnetic stir bar were placed 6-amino-2-(4-N,N-dimethylaminophenyl) benzoxazole (amino-B$^6$OD) (1.09 g, 4.30 mmol), 4-nitrobenzaldehyde (0.65 g, 4.32 mmol), and toluene (175 mL). The reaction mixture was heated to distill off the toluene/water azeotrope. The solvent was distilled off until only 10-15 mL remained, leaving a dark red solution. On cooling of the solution, red crystals formed. The mixture was filtered to yield red crystals that were washed with diethyl ether and dried for 16 hours under reduced pressure at 120-130°C, giving 1.48 g (89%) of analytically pure product: mp 272°C (by DSC); mass spectrum m/e 386 (M$^+$, parent); $^1$H NMR (400 MHz, in Me$_2$SO-d$_6$, ppm integration); 3.05 (6), s, -NMe$_2$, 6.87 (2), J$_{ab}$ = 9.26 and 8.00 (2), J$_{ab}$ = 9.14, AB quartet, 7.41 (1), dd, J = 1.97, J = 8.40, 7.55 (1), dd, J = 8.38, J = 0.5, 7.75 (1), dd, J = 1.97, J = 0.5, 8.21 (2) J$_{ab}$ = 9.15 and 8.36 (2), J$_{ab}$ = 8.79 AB quartet, 8.93 (1), s; UV-VIS (toluene, nm) 344, 418, (CH$_3$CN, nm) 346, 402. Analysis calculated for C$_{22}$H$_{18}$N$_4$O$_3$: C, 68.38; H, 4.70; N, 14.50. Found: C, 68.70; H, 4.67; N, 14.65.

Synthesis of NImB$^6$OTD. This compound was synthesized as above in 84% yield as orange crystals by condensing amino-B$^6$OTD with 4-nitrobenzaldehyde in toluene: mp 307°C (by DSC); mass spectrum 519 (M, parent); $^1$H NMR (DMSO, ppm integration), 3.15 (6), s, 6.86 (2) and 7.95 (2), AB quartet, J$_{ab}$ = 8.62 Hz, 7.48 (1), dd, J = 8.23, J = 1.89, 7.84 (1), d, J = 1.69, 7.86, d, J = 8.46, 8.09 (1), d, J = 8.42, 8.29 (1), dd, J = 8.50, J = 1.30, 8.90 (1), s, 8.96 (1), s, 8.24 (2), J = 8.46 and 8.38 (2) J = 8.52, AB quartet, UV-VIS (toluene) 408 nm. Analysis calculated for C$_{29}$H$_{21}$N$_5$O$_3$: C, 67.03; H, 4.07; N, 13.48. Found: C, 66.88; H, 4.09; N, 13.69.

Synthesis of N$_2$ImB$^6$OD. This compound was synthesized as above as

dark red crystals in 90% yield by condensing amino-$B^6OD$ with 2,4-dinitrobenzaldehyde in toluene: mp 248°C (by DSC); mass spectrum 431 (M, parent); UV-vis (toluene) 345, 462 nm, (acetonitrile) 350, 436 nm; $^1H$ NMR ($d_6$ DMSO,ppm integration) 3.05 (6), s, 6.87 (2) and 8.00 (2), AB quartet, $J_{ab}$ = 8.97 Hz, 7.40 (1), dd, J = 8.42 Hz, J = 2.01 Hz, 7.73 (1), d, overlapping 7.74 ppm resonance, 7.74 (1), d, J = 8.46, 8.47 (1), d, J = 8.47 Hz, 8.65 (1), dd, J = 8.57, J = 2.38, 8.83 (1), d, J = 2.24, 9.40 (1), s. Analysis calculated for $C_{22}H_{17}N_5O_5$: C, 61.25; H, 3.97; N, 16.23; O, 18.54. Found: C, 61.19; H, 3.95; N, 16.17; O, 18.56.

Synthesis of $NImB^5OD$. This compound was synthesized as above as orange needles in 90% yield by condensing amino-$B^5OD$ with 4-nitrobenzaldehyde in PPA: mp 276°C (by DSC); mass spectrum 386 (M, parent); $^1H$ NMR (400 MHz, in $Me_2SO-d_6$ ppm (integration) 3.05 (6), s, 6.87 (2) and 8.01 (2), AB quartet, $J_{ab}$ = 9.2 Hz, aromatic N,N-dimethyl-aminophenyl, 7.36 (1), dd, J = 2.1, J = 8.5, 7.68 (1), d, J = 2.1, 7.73 (1), d, J = 8.5, 8.22 (2), $J_{ab}$ = 8.97 Hz and 8.37 (2), $J_{ab}$ = 8.83 Hz, AB quartet, 4-nitrophenyl, 8.91 (1), s (imine); UV-VIS (toluene) 348, 390 (shoulder) nm, (acetonitrile) 348 nm; IR (KBR $cm^{-1}$) 1610 s, 1510 s, 1370 m, 1340 s, 1180 m. Analysis calculated for $C_{22}H_{18}N_4O_3$: C, 68.38; H, 4.70; N, 14.50. Found: C, 68.88; H, 4.63; N, 14.56.

Synthesis of $CImB^6OD$. This compound was synthesized as above as yellow crystals in 76% yield by condensing amino-$B^6OD$ with 4-cyanobenzaldehyde in toluene: mp 276°C (by DSC), mass spectrum 366 (M, parent); $^1H$ NMR (400 MHz, in $Me_2SO-d_6$ ppm (integration) 3.04 (6), s, -$NMe_2$, 6.87 (2), $J_{ab}$ = 9.16 Hz and 8.00 (2), $J_{ab}$ = 9.11 Hz, AB quartet, 4-dimethyl-aminophenyl, 7.37 (1), dd, J = 1.97, J = 8.36, 7.70 (1), d, J = 8.37, 7.71 (1), d, 7.97 (2) and 8.13 (2) AB quartet, $J_{ab}$ = 8.42 Hz, 8.85 (1), s, IR (KBr) ($cm^{-1}$) 1610 s, 1510 s, 1430 m, 1370 m, 1180 m. Analysis calculated for $C_{23}H_{18}N_4O$: C, 75.39; H, 4.95; N, 15.29. Found: C, 74.50; H, 5.00; N, 15.03.

Synthesis of $N_2ImB^6OD_{18}$. This compound was prepared as above in 88% yield as red crystals by condensing amino-$B^6OD_{18}$ with 2,4-dinitrobenzaldehyde in toluene: mp by DSC (second heating cycle) 126°C

29

(crystalline to smectic A), 149°C (smectic A to isotropic melt); mass
spectrum 655 (M + H$^+$, parent); UV-VIS (toluene) 344, 454 nm
(acetonitrile) 346, 428 nm; $^1$H NMR (CDCl$_3$) 0.86 (3), t, J = 6.73 Hz,
-CH$_3$, 1.24, m, 1.64, m, 3.18 (2), t, J = 7.14 Hz, -NH-CH$_2$-, 4.1 (1),
broad, -NH-, 6.63 (2), J$_{ab}$ = 8.93 and 8.02 (2), J$_{ab}$ = 8.85, AB quartet,
7.34 (1), dd, J = 8.38, J = 1.98, 7.50 (1), d, J = 1.55, 7.68 (1), d, J
= 8.40, 8.51 (1), ddd, J = 8.66 Hz, J = 2.25 Hz, J = 0.5 Hz, 8.61 (1),
d, J = 8.68, 8.90 (1), d, J = 2.22, 9.07 (1), s. $^{13}$C NMR (100 MHz, ppm)
14.33, 22.89, 27.30, 29.55, 29.60, 29.79, 29.85, 29.89, 32.12, 43.65,
103.36, 112.21, 119.24, 120.35, 127.34, 129.51, 131.25, 135.91, 143.11,
146.22, 148.38, 151.09, 151.37, 151.70, 151.73, 165.46.  Analysis
calculated for C$_{38}$H$_{49}$N$_5$O$_5$:  C, 72.81; H, 8.04; N, 8.94; O, 10.21.
Found:  C, 71.94; H, 8.38; N, 8.73; O, 10.67.

Synthesis of NHImB$^6$OD$_{18}$.  This compound was prepared as above in
90% yield as orange crystals by condensing amino-B$^6$OD$_{18}$ with 3-hydroxy-
4-nitrobenzaldehyde in toluene:  mp by DSC (second heating cycle) 99°C
and 130°C (crystal to crystal phase), 140°C (crystal to smectic A
phase), 161°C (smectic A to isotropic melt); mass spectrum 626 (M + H$^+$,
parent), UV-VIS (toluene) 339, 426 nm, (acetonitrile) 349 nm;
$^1$H NMR (CDCl$_3$, ppm integration) 0.84 (3), t, -CH$_3$, 1.23, m, 1.58, m,
3.11 (2), t, 6.71 and 7.89, AB quartet, J$_{ab}$ = 8.79, 7.35 (1), dd, J =
8.24, J = 1.83, 7.47 (1), d, J = 8.64, 7.64 (1), broad s, 7.66 (1), d, J
= 8.57, 7.68 (1), d, J = 1.79, 7.98 (1), d, J = 8.46, 6.40 (1), broad,
OH or NH.  Analysis calculated for C$_{38}$H$_{50}$N$_4$O$_4$:  C, 72.81; H, 8.04; N,
8.94; O, 10.21.  Found:  C, 71.94; H, 8.38; N, 8.73; O, 10.67.

Synthesis of NImB$^6$OD$_{18}$.  This compound was synthesized as above in
81% yield as yellow crystals by condensing amino-B$^6$OD$_{18}$ with 4-
nitrobenzaldehyde in toluene:  mp by DSC (second heating cycle) 79°,
89°, 99°C (crystal to crystal phases), 135°C (crystal to smectic A),
181°C (smectic A to isotropic melt); mass spectrum 610 (M + H$^+$, parent);
UV-VIS (toluene) 339, 416 nm (acetonitrile) 340, 406 nm; $^1$H NMR (ppm
integration) 0.85 (3), t, 1.24, m, 1.58, m, 3.10 (3), broad, 6.32 (1),
br, 6.72 (2) and 7.90 (2), AB quartet, J$_{ab}$ = 8.79, 4-N-alkylaminophenyl,

7.38 (1), dd, J = 8.42, J = 1.83, 7.67 (1), d, J = 8.38, 7.70 (1), d,
J = 1.87, 8.22 (2) and 8.35 (2), AB quartet, $J_{ab}$ = 8.80 Hz. $^{13}C$ NMR
(100 MHz, ppm) 14.25, 22.80, 27.20, 29.46, 29.49, 29.69, 29.79, 32.02,
43.54, 102.88, 112.08, 114.79, 118.28, 119.07, 123.91, 129.22, 141.47,
142.04, 147.10, 149.06, 151.1, 156.25, 164.88. Analysis calculated for
$C_{38}H_{50}N_4O_3$: C, 74.72; H, 8.25; N, 9.17; O, 7.86. Found: C, 73.57; H,
8.18; N, 8.98; O, 8.48.

Synthesis of Bis($NImB^6OD_{18}$). This compound was synthesized as
above in 81% yield as orange crystals by condensing amino-$B^6OD_{18}$ with
1,3-diamino-4,6-dinitrobenzene in toluene: mp by DSC (second heating
cycle) 159°C (crystal to isotropic phase); mass spectrum 1143 ($M + H^+$,
parent); UV-VIS (toluene) 351, 474 nm, (acetonitrile) 352, 442 nm; $^1H$
NMR (ppm, integration) 0.86 (6), t, J = 6.61, 1.24, m, 1.54, m, 3.19
(4), t, J = 7.24, 3.5, broad, 6.66 (4) and 8.05 (4), AB quartet, $J_{ab}$ =
8.89, 7.42 (2), dd, J = 8.40, J = 1.97, 7.72 (2), d, J = 8.01, 7.58 (2),
d, J = 1.46, 8.83 (1), s, 9.14 (2), s, 9.33 (1), s. Analysis calculated
for $C_{70}H_{94}N_8O_6$: C, 73.52; H, 8.29; N, 9.80; O, 8.40. Found: C, 72.25;
H, 8.64; N, 9.61; O, 9.31.


## Collaborations Under Way

The following individuals are performing AFOSR-supported research
in collaboration with this project.

1. Professor Anthony Garito of the University of Pennsylvania will
measure the NLO properties of the polymers, oligomers, and model
compounds synthesized by our research group. We have sent the following
compounds to Professor Garito for evaluation: BOD, amino-$B^6OD$, amino-
$B^5OD$, $ClImB^6OD$, $NImB^5OD$, $NImB^6OD$, $N_2ImB^6OD$, $NImB^6OTD$, $N_2ImB^6OD_{18}$,
$NImB^6OD_{18}$, $NHImB^6OD_{18}$, and bis($NImB^6OD_{18}$).

2. Dr. Al Fratini of AFWAL/MLBP will determine the crystal
structure of the ALHD series of compounds. We have sent the following
compounds to Dr. Fratini for evaluation: BOD, amino-$B^6OD$, amino-$B^5OD$,
$ClImB^6OD$, $NImB^5OD$, $NImB^6OD$, $N_2ImB^6OD$, amino-$B^6OTD$, amino-$B^6OD_{18}$,
$NImB^6OTD$, $NImB^6OD_{13}$, $NHImB^6OD_{18}$, $N_2ImB^6OD_{18}$, and bis($NImB^6OD_{18}$).

3. Professor Anselm Griffin of the University of Southern Mississippi will investigate the synthesis of polyimines using dialdehydes prepared in his laboratory and diamines prepared in our laboratory, for example, 2,6-diaminobenzo [1,2-d:4,5-d ] bisthiazole (DABBT) or 2,6-bis(4-aminophenyl)benzo [1,2-d:4,5-d'] bisthiazole (BAPBBT). We have sent DABBT to Professor Griffin. We have also sent Professor Griffin $NImB^6OD_{18}$, $NHImB^6OD_{18}$, $N_2ImB^6OD_{18}$, and bis($NImB^6OD_{18}$) for investigation of their liquid crystalline nature.

4. Dr. James F. Wolfe of Lockheed Missiles and Space Co., Palo Alto, CA, will investigate the optical properties, processing options, and structure-property relationships of the ALHD compounds. We have sent Dr. Wolfe amino-$B^5OD$, amino-$B^6OD$, amino-$B^6OTD$, amino-$B^6OD_{18}$, BOD, $CImB^6OD$, $NImB^5OD$, $NImB^6OD$, $N_2ImB^6OD$, $NImB^6OTD$, $NImB^6OD_{18}$, $NHImB^6OD_{18}$, $N_2ImB^6OD_{18}$, and bis($NImB^6OD_{18}$).


Recommendations for Future Research

We suggest the following methods to optimize the optical response and processibility of the ALHD compounds.

A. Flexible and Rigid Polymers with ALHD Pendants

We suggest synthesizing aldehyde precursors that would allow the ALHD active unit to be incorporated into polymer chains as side chain pendants. For example, we would synthesize $NImB^6OD$ with an alkyl substituent terminated by a diester and then condense this diester functional group with diols or diamines. The backbone can be flexible or rigid depending on the choice of diamine or diol. For example, long chain alkyl diols would result in a flexible polymer, whereas condensation with 4,6-diamino-1,3-benzenediol dihydrochloride (DABDO) would yield a much more rigid polymer. This scheme is shown in Figure 14.


B. $\chi^{(2)}$ Materials with Optimized Properties

Compounds based on the ALHD systems but with more electron-
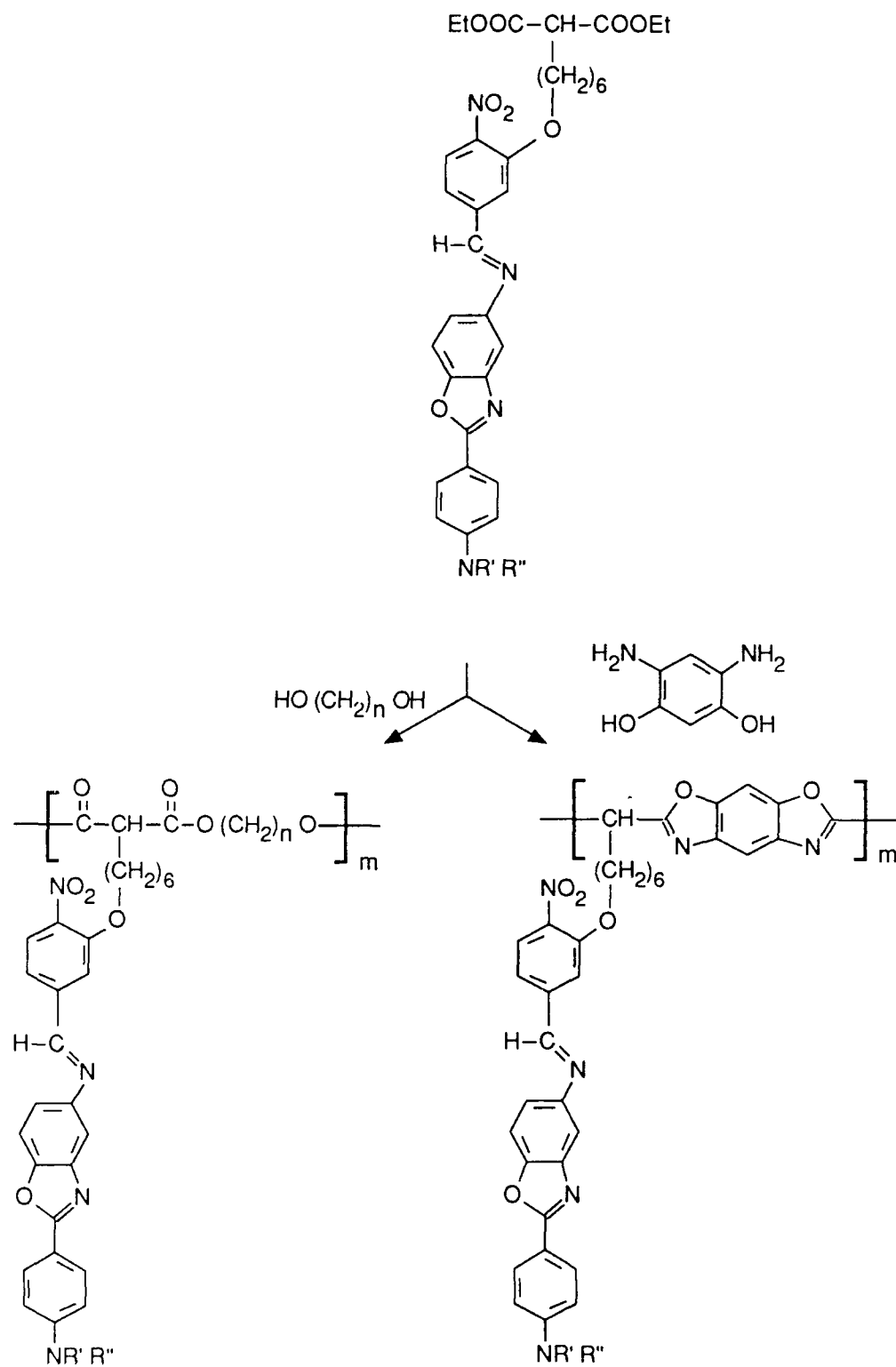
RA-M-4621-5

Figure 14. Synthesis of ALHD side chain pendant polymer.

33

donating or -withdrawing power should be synthesized. For example, condensation of amino-$B^6OD$ with 2,4-dinitrobenzaldehyde yielded the dinitro product $N_2ImB^6OD$ (Figure 3). We suggest synthesizing the analogous dinitro compound with two dialkylamino groups at the opposite end of the molecule. The resulting product should have a high dipole moment and a high -value, or $^{(2)}$ due to the extra electrons available for polarization.

We also suggest synthesizing a linear analog of the ALHD compounds we have prepared. This compound, 2-amino-6-(4-N,N-dimethylaminophenyl)benzo [4,5-d] thiazole [1,2-d] oxazole (amino-TBOD) (Figure 13), may provide new information concerning orbital overlap in linear chains compared with that in bent chains and how that overlap results in higher NLO response in benzazole materials.

The azo analog of our current imine materials should be synthesized so that the relative stability of various connecting groups can be evaluated under anticipated conditions in optical devices.

Additional suggestions include (1) extension of the NImBOD system to include $NImB^6OT_3D$; (2) extension of the $N_2ImBODs$ to include the oligomeric series, as with the NImBODs; and (3) synthesis of more oligomers with attached long chain alkyl groups for improved solubility and miscibility with flexible polymers.

## C. Materials for $^{(3)}$

The copolymer synthesis of PBO/POL should be optimized so that processible active polymers can be obtained. We had begun to synthesize bis-amino terminated benzazoles for incorporation into polymeric species. These difunctional compounds would form the basis for a polymer with NLO-active units in the flexible main chain.

## Objective

The objective of this task was to increase the understanding of factors that affect the polymerization kinetics of lyotropic ordered polymers. We hypothesized that the rate and conversion of the polymerization can be enhanced by formation of the liquid crystalline phase. By studying polymerizations of various concentrations, we can observe the isotropic-nematic transition that occurs at different stages of conversion and determine the resulting polymerization kinetics and molecular weight profile. We have investigated the effect of an externally applied shear field, one important force that may alter the degree of order in the liquid crystalline phase.

## Approach

Initially, we studied the polymerization of 15 wt% PBT in PPA. The reaction kinetics of the polycondensation were monitored by measuring the intrinsic viscosity of aliquots removed periodically from the reacting medium. The effects of shear and temperature on the reaction were studied by polymerizing the monomer mixtures in a sealed cone and plate cell in a rheometer at different shear rates with different temperature profiles. Our approach and results are discussed in detail in Appendices A, B, and E, technical papers resulting from this work.

## Results and Discussion

The kinetic study quantitatively confirms a phenomenon that has been observed for some time during the synthesis of PBT and related rodlike polymers. We call this phenomenon mesophase-enhanced polymerization (MEP). During the course of the reaction, the 15 wt% PBT mixture goes through a phase transition from isotropic to liquid crystalline. The intrinsic viscosity measurements, shown in Figure 15, indicate that the rate of reaction is greatly enhanced when the reaction mixture becomes anisotropic.

35
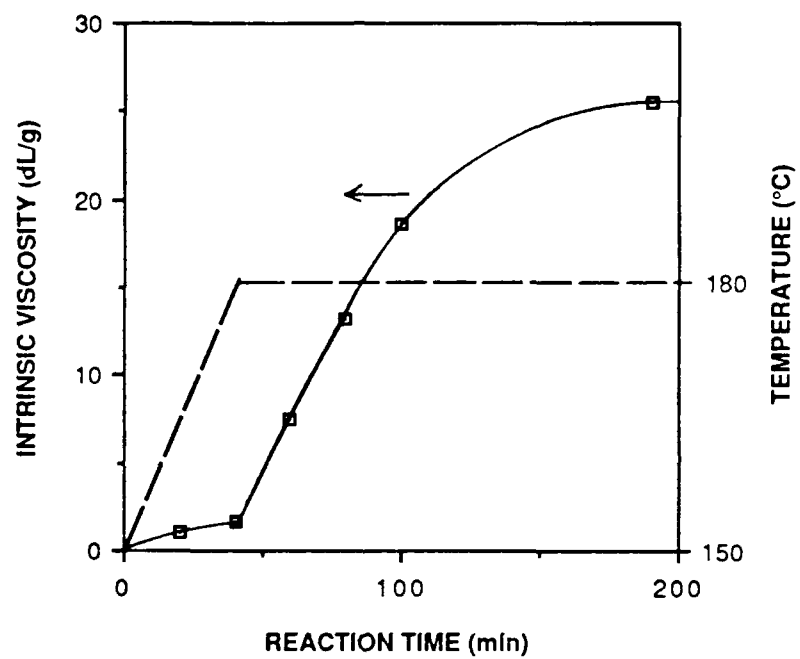
JA-8970-31

Figure 15. Increase in polymer intrinsic viscosity during
polycondensation of 15 wt% PBT in PPA.

36

Chemo-rheological measurements at low shear rates throughout the polymerization are quite insensitive to the phase change of the reacting media, especially at low shear rates (Figure 16). At higher shear rates, the phase transition is more obvious in the viscosity data. In addition, we observed an anomaly in the rheology data that appears to be due to flow instability in the ordered phase.

Shear and temperature greatly affect the polymerization of PBT. We found that successful polymerization was achieved only when the applied shear rate was $0.1$ s$^{-1}$ or higher. When the applied shear rate was less than $0.1$ s$^{-1}$, the reaction products contained only low molecular weight species. Moreover, the shear effects are most influential in the premixing stage (at temperatures below 150°C) and much less influential in the polymerizing stage (at temperatures above 150°C). Such results suggest that once the monomer mixture is well dispersed, the polymerization can be performed satisfactorily under a wide range of reaction conditions. In the range of shear rate investigated, up to 50 s$^{-1}$, the final achievable molecular weight of the reaction products tends to increase with shear rate. Similarly, the temperature profile during the mixing period below 150°C has a significant influence on the polymerization, whereas the temperature profile above 150°C has less effect. The results of the temperature and shear rate studies can be explained by a rapid polymerization for which an intimate mixture is critical and by the decreased sensitivity of oligomeric species to thermal decomposition.

We have also studied the polymerization kinetics of PBT at lower concentrations quantitatively. As the polymer concentration decreases, it reaches a critical concentration below which the reacting mixture remains isotropic throughout the polymerization. Direct observation and intrinsic viscosity measurements of aliquots removed from the reacting medium indicate that this critical concentration is about 5 wt%.
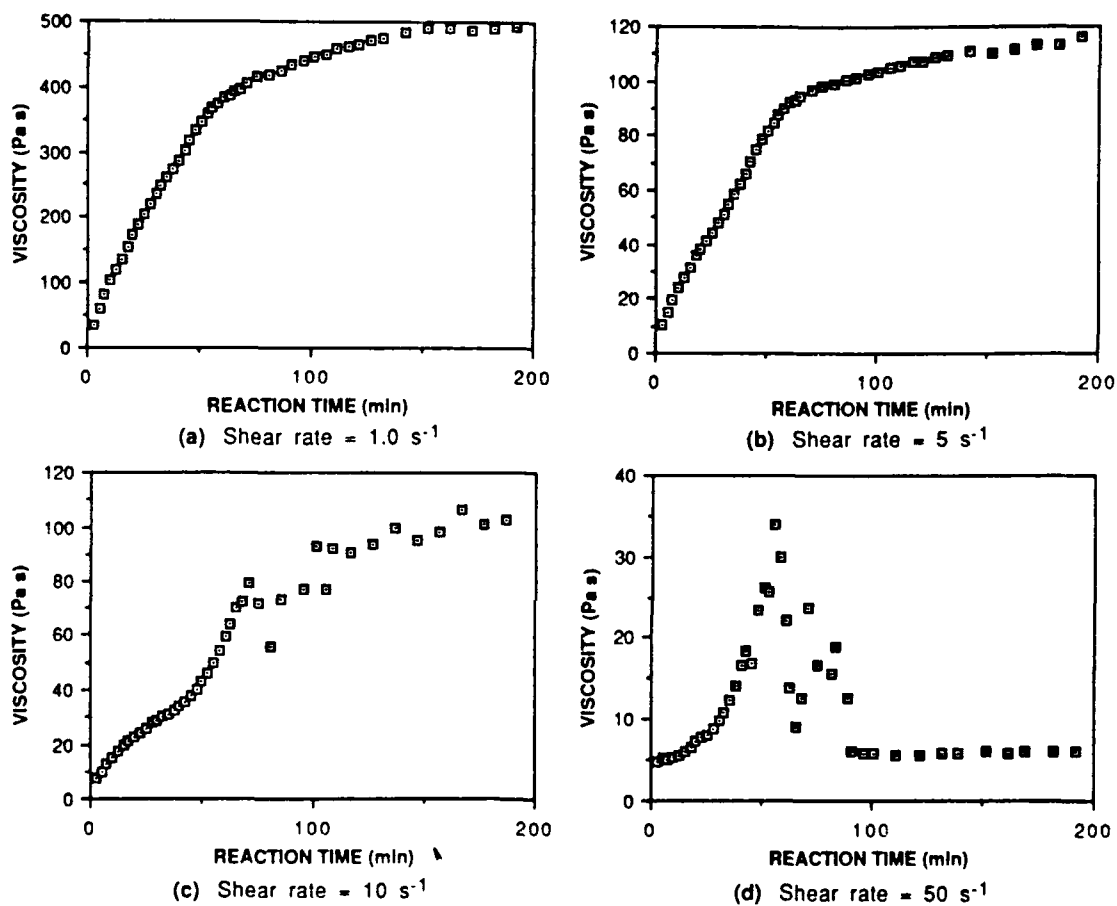
Figure 16. Shear viscosity versus reaction time during polymerization of 15 wt% PBT in PPA at shear rates of 1.0 s$^{-1}$, 5.0 s$^{-1}$, 10 s$^{-1}$, and 50 s$^{-1}$.

## Recommendations for Future Research

The effects of shear on the polymerization of PBT near 5 wt% should be explored.  This study is important for elucidating the ordering mechanism of rodlike polymers during the isotropic-nematic phase transition.  The study should be extended to include semiflexible polymers, such as ABPBT and ABPBO, that exhibit a transition to the ordered phase during polymerization at much higher polymer concentrations, such as 15 wt%.  The experimental techniques used in our research should be applied to investigate the reaction kinetics and chemo-rheological properties of these extended chain poly(benzazole) polymers.

DILUTE AND CONCENTRATED SOLUTION PROPERTIES

## Objective

The objective of this task was to elucidate the dependence of
dilute and concentrated solution properties of extended-chain polymers
on molecular weight and chain flexibility.

## Approach

Our approach to this task and our results are discussed in detail
in Appendices D and F, technical papers resulting from this work.

## Results and Discussion

We studied the dilute solution properties of the semirigid polymers
poly(2,6-benzothiazole) (ABPBT) and poly(2,5-benzoxazole) (ABPBO) by
using viscometry and low angle light scattering techniques. The Mark-
Houwink-Sakurada (MHS) constants relating intrinsic viscosity to
molecular weight have been experimentally determined for the molecular
weight range of 2000 to 200,000 daltons. The MHS exponents, about unity
for both polymers, indicate that this class of poly(benzazoles) is
characterized by an intrinsically semirigid structure. Their behavior
in dilute solutions is in good agreement with the Yamakawa-Fujii
wormlike cylinder model (Figure 17). By comparing the model with the
experimental data, we deduced persistence lengths of 130 $\mathring{A}$ and 90 $\mathring{A}$ for
ABPBT and ABPBO, respectively.

We began to characterize the concentrated solution properties of
the rigid rodlike poly(benzazoles) by rheological measurements. The
rheology of liquid crystalline polymers is a developing, active research
area. In the attempt to measure the steady state shear viscosity of
PBT, we found an anomalous behavior: in the ordered phase at high shear
rates, the lyotrope does not seem to achieve steady state viscosity
values. Instead, the bulk viscosity fluctuates for a long time after
the inception of the shear flow. This phenomenon may be associated with
the flow instability observed during the polymerization of PBT.
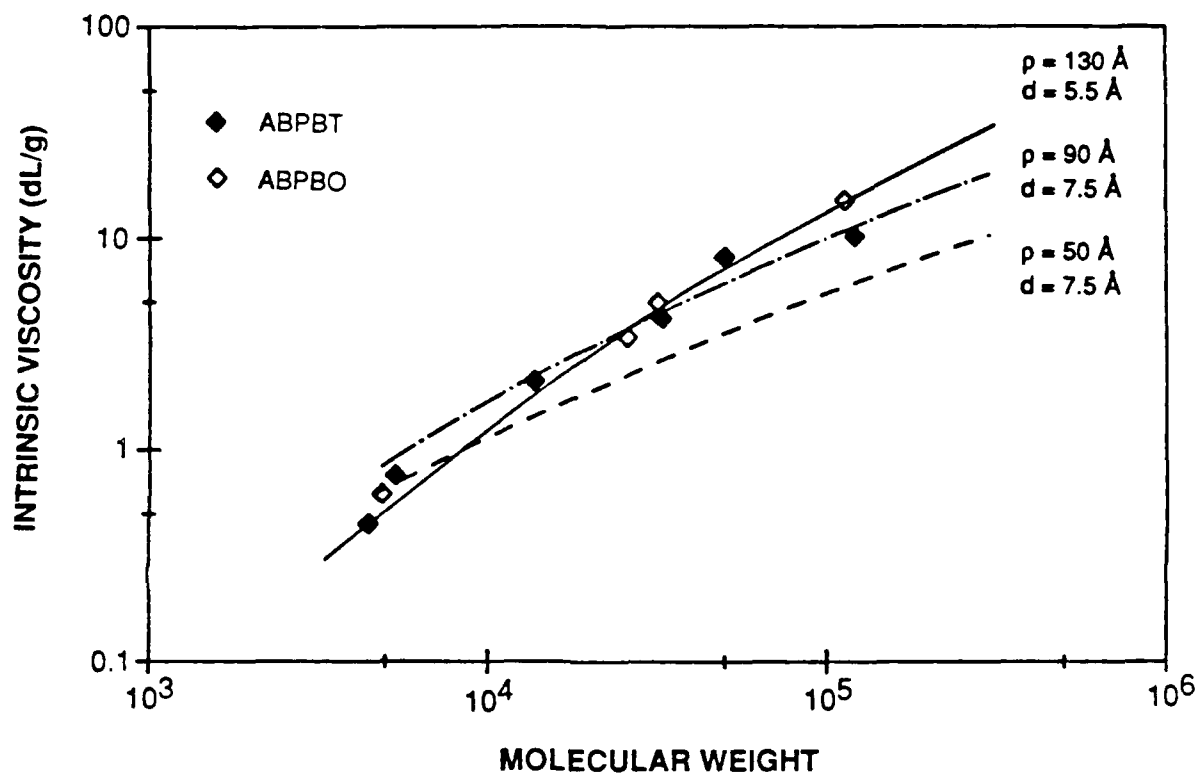
RA-4621-13

Figure 17. Intrinsic viscosity of ABPBZ polymers as a function of molecular weight. ————— = Model preduction for ABPBT, — — — and —·— = model predictions for ABPBO based on values listed, ◆ and ◇ = experimental results.

41

## Recommendations for Future Research

The research on the rheological properties of concentrated PBT solutions should be continued. The time-dependent behavior of both isotropic and liquid crystalline systems in relation to the inception of shear is of particular interest, and the anomalous shear flow behavior observed previously with this class of materials should be studied in more detail. The rheological properties of the semirigid poly(benzazoles) should also be characterized and the effects of molecular weight and chain flexibility of these extended-chain polymers on their flow properties should be studied.

# COLLABORATIONS, INVENTIONS, PUBLICATIONS, AND PRESENTATIONS

## Collaborations

Several collaborative efforts are under way with other research projects sponsored by AFOSR. These are described in the section on Task 2, above.

## Inventions

The following invention was funded under this contract:

Invention Disclosure

"Synthesis and Applications of Benzazole-Containing Acceptor/Donor Compounds," J. F. Wolfe and S. P. Bitler, April 1988.

## Publications

1.  A. W. Chow, J. F. Sandell, and J. F. Wolfe, "Reaction Kinetics and Chemo-rheology of Poly(p-phenylenebenzobisthiazole) Polymerization in the Ordered Phase," Polymer 29, 1307 (1988). (Appendix A).

2.  A. W. Chow and J. F. Wolfe, "Chemo-rheology of PBT Polymerization in the Liquid Crystalline Phase," to appear in Proceedings of the Xth International Congress on Rheology, August 1988. (Appendix B).

3.  J. F. Wolfe, B. H. Loo, R. A. Sanderson, and S. P. Bitler, "Synthesis Approaches for Improving the Nonlinear Optical Properties of PBZ Polymers," in Nonlinear Optical Properties of Polymers, Materials Research Society 109, A. J. Heeger, J. Orenstein, and D. R. Ulrich, eds. (Materials Research Society, Pittsburgh, PA, 1988), p. 291. (Appendix C).

4.  A. W. Chow, S. P. Bitler, P. E. Penwell, D. J. Osborne, and J. F. Wolfe, "Synthesis and Solution Properties of Extended Chain Poly (2,6-Benzothiazole) and Poly(2,5-Benzoxazole), to be published in Macromolecules, 1989. (Appendix D).

5.  A. W. Chow, R. D. Hamlin, J. F. Sandell, and J. F. Wolfe, "Mesophase-Enhanced Polymerization and Chemo-Rheology of Poly (p-phenylenebenzobisthiazole)," in Materials Society Meeting Proceedings, November 1988. (Appendix E).

6.  A. W. Chow, S. P. Bitler, P. E. Penwell, and J. F. Wolfe, "Synthesis and Dilute Solution Characterization of Extended-Chain Poly (benzazoles)," in Materials Society Meeting Proceedings, November 1988. (Appendix F).

## Presentations

1.  J. F. Wolfe, B. H. Loo, R. A. Sanderson, and S. P. Bitler, "Synthesis Approaches for Improving the Nonlinear Optical Properties of PBZ Polymers," Materials Research Society, Boston, MA, December 1-3, 1987.

2.  J. F. Wolfe and S. P. Bitler, "Synthesis and Characterization of Benzazole-Containing NLO Materials," Nonlinear Optical Polymers Contractors Conference, Washington, DC, April 20-21, 1988.

3.  A. W. Chow and J. F. Wolfe, "Chemo-rheology of PBT Polymerization in the Liquid Crystalline Phase," Xth International Congress on Rheology, Sydney, Australia, August 1988.

4.  J. F. Wolfe, "Rigid-Rod Polymer Synthesis: Development of Mesophase Polymerization in Strong Acid Solutions," Materials Research Society, Boston, MA, November 28-December 2, 1988.

5.  A. W. Chow, J. F. Sandell, and J. F. Wolfe, "Reaction Kinetics and Chemo-Rheology of Poly(p-Phenylenebenzobisthiazole): Polymerization in the Liquid Crystalline Phase," Materials Research Society, Boston, MA, November 28-December 2, 1988.

6.  A. W. Chow, S. P. Bitler, P. E. Penwell, and J. F. Wolfe, "Synthesis and Solution Properties of Extended-Chain Poly(2,6-Benzothiazole) and Poly(2,5-Benzoxazole)," Materials Research Society, Boston, MA, November 28-December 2, 1988.

Appendix A

REACTION KINETICS AND CHEMO-RHEOLOGY OF POLY(p-PHENYLENE-
BENZOBISTHIAZOLE) POLYMERIZATION IN THE ORDERED PHASE

# Reaction kinetics and chemo-rheology of poly(p-phenylenebenzobisthiazole) polymerization in the ordered phase

Andrea W. Chow, Janet F. Sandell and James F. Wolfe

*Polymer Sciences, Chemistry Laboratory, SRI International, 333 Ravenswood Avenue, Menlo Park, CA 94025, USA*
*(Received 27 October 1987; accepted 4 December 1987)*

The phenomenon of mesophase-enhanced polymerization of the rodlike polymer poly(p-phenylenebenzobisthiazole) at 15%, by weight in polyphosphoric acid has been investigated. The reacting mixture becomes anisotropic at an early stage of the polymerization. The reaction rate increases significantly at the isotropic–nematic phase transition as the rods are aligned in positions more favourable for the condensation reaction to occur. The chemo-rheological properties at high shear rates ( > 10 s⁻¹), but not at low shear rates ( < 5 s⁻¹), also indicate the occurrence of the phase change. A systematic study of the effects of shear rate and temperature suggests that initial mixing of the monomer mixture below the polymerization temperature greatly influences the final achievable molecular weight of the polycondensation reaction.

(Keywords: poly(p-phenylenebenzobisthiazole); rodlike polymer; mesophase-enhanced polymerization; reaction kinetics; ordered phase; chemo-rheology)

## INTRODUCTION

Polybenzazoles (PBZ), a class of aromatic, heterocyclic rigid rod polymers, have received increasing interest as advanced materials for applications requiring high thermal, oxidative and structural stability. Because of the rigidity of the backbone, these polymers can form ordered phases in solutions at high chain concentrations. Such orderability has been known to provide great advantages to the polymer processibility and the physical properties of the fabricated products. Exceptional mechanical properties can be obtained in fibres and films fabricated from these lyotropic polymers. A tensile strength of 4.2 GPa (607 000 psi) and a tensile modulus of 330 GPa (48 million psi) have been reported for heat-treated fibres spun from poly(p-phenylenebenzobisthiazole) (PBT)[1], one of the most rigid polymers in the PBZ family.

Benefits can also be realized when polymer synthesis is performed in the ordered phase. Initial research on the synthesis of PBT was conducted in polyphosphoric acid (PPA) at concentrations below 3 wt% of polymers to avoid the extremely high shear viscosity of the reacting media. Such polymerization mixtures remained isotropic throughout the polymerization, but the maximum attainable molecular weight was low, and the polymer had to be isolated and redissolved at higher concentration for fibre processing. The practical need for higher efficiency motivated attempts to polymerize at higher concentrations. At greater than 5 wt%, liquid crystalline domains were formed during the polymerization of PBT, and the reacting mixture remained tractable. The reaction kinetics and final attainable molecular weight were greatly enhanced. Moreover, the processibility of the dope was improved significantly.

A study on the polymerization kinetics of another rodlike polybenzazole, poly(p-phenylenebenzobisoxazole) (PBO), at concentrations below the liquid crystalline phase transition indicates that the rate of increase in molecular weight with reaction time decreases with the molecular weight of the rodlike chains[2]. This result suggests that the polymerization rate is diffusion limited because the rotational diffusivity depends strongly on the molecular length. In the ordered phase, however, the molecules are already aligned in positions favourable for condensation, and the polymerization rate is therefore expected to increase. We call this phenomenon mesophase-enhanced polymerization (MEP).

Because of the scientific as well as technological importance of polycondensation of rodlike polymers in the ordered phase, we investigated MEP in more detail. We describe a quantitative study on the reaction kinetics and chemo-rheological properties of PBT polycondensation at high concentration under conditions that cause liquid crystalline phase transition to occur during polymerization. The effects of phase change, shear and temperature are discussed.

## EXPERIMENTAL

*Material preparation*

The synthesis of PBT, reported in detail previously[3], is typically performed by the condensation of 2,5-diamino-1,4-benzenedithiol dihydrochloride (DABDT) and terephthalic acid (TA) in PPA following the removal of hydrogen chloride

DABDT          TA          PBT

A-1
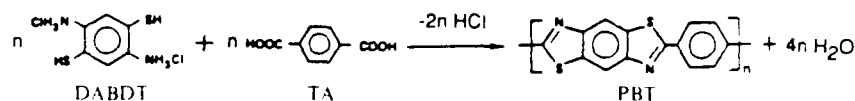
Preparation of DABDT monomers follows the rigorous purifying procedures described in the literature[3]. In all experiments, the monomer concentration is chosen to yield a final polymer concentration of 15 %, by weight. In this reaction. PPA serves as a solvent, catalyst and dehydrating agent. Hydrogen chloride is first completely removed from the reaction mixture of DABDT in PPA before the addition of 10 μm TA particles. Solid $P_2O_5$ is then added according to the $P_2O_5$ adjustment method[4] to ensure adequate reaction conditions for a high degree of polymerization. Benzoic acid of 0.50 mol %, based on DABDT is used as endcapping agent to control the final molecular weight of the polymer. After the original mixture of DABDT and PPA at 90 C is stirred for sufficient time to remove the hydrogen chloride, the mixture of monomers, benzoic acid, PPA and $P_2O_5$ is ready for polymerization at temperatures above 150 C.

*Polymerization kinetics*

Most of the polymerization runs in this study follow a temperature profile known to produce satisfactory conditions for the polymerization. The monomer mixture is first heated from 90 to 180 C at a rate of 0.75 C min$^{-1}$. When the mixture reaches 180 C, the temperature is maintained at 180 C throughout the polymerization. In a few cases, different temperature profiles are used to investigate their effects on the reaction.

All monomer mixtures are prepared in 500 ml glass reactors with three attached ground glass joints. This reactor design allows constant mechanical stirring of the reaction mixture and continuous argon purge. During polymerization, small aliquots of the reaction mixture are removed periodically from the glass reactor. The reactor also allows removal of samples for analysis without exposing the reacting mixture to air or introducing other contaminants. A heated oil bath is used to control the reactor temperature.

A portion of the removed aliquot is placed on a microscope slide for direct observation under an optical microscope. The remaining portion is precipitated in deionized water, and the residual PPA is thoroughly removed by extraction with water in a Soxhlet apparatus. The polymer is completely dried under reduced pressure at >130 C overnight.

The weight-average molecular weight, $M_w$, of PBT can be determined by measuring the intrinsic viscosity of the polymer in dilute concentrations and using the following Mark Houwink relationship[5]:

$$[\eta] = 4.86 \times 10^{20} (d_H^2 M_1)(M_w M_1)^{1.8} \quad (1)$$

$$M_n = M_w (M_z / M_w)^{4.8} \quad (2)$$

The intrinsic viscosity $[\eta]$ is in dl g$^{-1}$; $d_H$ is the hydrodynamic diameter of a chain element taken to be $7 \times 10^{-7}$ cm for PBT; $M_1$ is the mass per unit length, which is $2.15 \times 10^9$ cm$^{-1}$, $M_z$ is the z-average molecular weight, and $M_z / M_w$ is 1.3 for PBT.

Experimentally, the intrinsic viscosity of PBT solutions is measured at 30.0 C using an automated Cannon Ubbelohde microdilution viscometer. The solutions are prepared by dissolving dried PBT in freshly distilled methane sulphonic acid (MSA), and the intrinsic viscosity is measured within 48 h after the solutions are prepared. Four successive dilutions are used to extrapolate the measurements of specific and inherent viscosities to

infinite dilution. The solution efflux times are chosen to fall within 1.1 to 1.5 times the solvent efflux time. No kinetic correction is necessary because the efflux times are longer than 100 s.

*Rheology*

Rheological measurements on the polymerizing mixtures are performed using a Rheometrics RMS-605 mechanical spectrometer. Because of the high sensitivity of the reaction mixtures to oxygen and moisture, a modified cone-and-plate fixture is used to prevent exposure of the reacting mixture to moisture over a long period (at least several hours). The fixture, made of Hastelloy C to resist acid corrosion at elevated temperature, consists of additional outer, concentric rings on both the cone and the plate such that dried, high-temperature-grade silicone oil can be introduced to form a barrier to moisture and oxygen as shown in *Figure 1*. The diameter of the plate is 25 cm and the cone angle is 0.1 radian.

About 1 ml of the prepared monomer mixture at 90 C is removed from the bulk sample under nitrogen purge and loaded onto the cone-and-plate fixture carefully to minimize contaminant introduction. The flow cell is preheated to 90 C to avoid reprecipitation of the dissolved components. The sample is kept under a nitrogen blanket until the flow cell is closed and sealed with silicone oil. The temperature of the sample is then increased according to a predetermined temperature profile to initiate the polymerization. Different temperature profiles have been followed to investigate the effect of temperature on the polymerization.

The effect of shear is studied by subjecting the polymerizing media to continuous steady shear throughout the reaction (including the initial temperature ramp) at shear rates from 0.01 to 50 s$^{-1}$. The rheometer is programmed to record the torque reading and calculate the shear viscosity at about two-minute intervals. At the end of each run, the dope is removed from the flow cell for molecular weight determination using intrinsic viscosity measurements.

After a series of polymerization runs, the remaining bulk monomer mixture is polymerized in the glass reactor using a similar temperature profile for comparison purposes.

## RESULTS AND DISCUSSION

*Polymerization kinetics*

*Figure 2* shows the change in the intrinsic viscosity as a function of reaction time of 15 wt %, PBT in PPA. The broken line shows the temperature profile throughout the reaction starting from 150 C. The intrinsic viscosity can
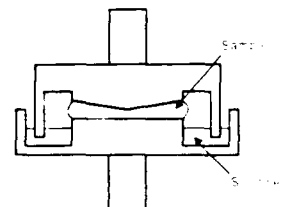


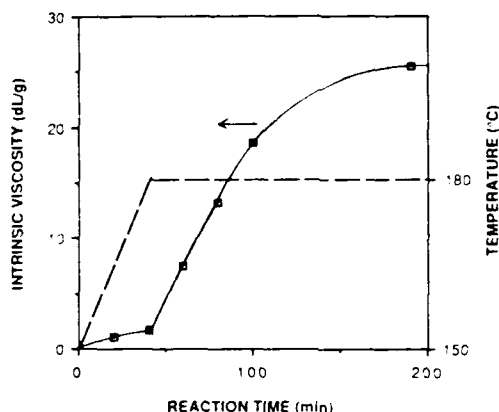**Figure 1** Modified cone-and-plate with moisture seal

**Figure 2** Increase in polymer intrinsic viscosity during polycondensation of 15 wt% PBT in PPA

kinetics is too dramatic to be due to the gradual increase in temperature as performed in our experiments

The polymer molecular weight at which the phase transition occurs can be compared with theoretical predictions using Flory's statistical mechanical model for athermal systems. The model predicts that $\phi_c$, the critical volume fraction of rodlike solute at which phase separation first occurs, is related to the axial ratio (x) of monodisperse rods by

$$\phi_c = (8/x)(1 - 2/x) \qquad (4)$$

In our polymerization of PBT, the specific gravity of PBT is about 1.5 and that of PPA is 2.0, $\phi$ is therefore 0.19 and x is 40 according to equation (4). Experimentally we observed a phase change when the number-average molecular weight of PBT is less than 6016 dalton. If we assume 0.7 nm to be the molecular diameter of PBT, and 1.25 nm to be the length of a repeat phenylenebenzobis-

be converted to the weight-average molecular weight $(M_w)$ using equation (1). The number-average degree of polymerization $(x_n)$ can then be determined by the molecular weight of the repeat unit $(M_0)$ and $M_w$:

$$x_n = 2(M_w/1.3M_0) \qquad (3)$$

The factor of 2 is needed because two condensing species form each repeat unit. The constant 1.3 within the parentheses is used to convert weight-average to number-average molecular weight by assuming a polydispersity of 1.3 (refs 2 and 6). *Figure 3* plots $x_n$ as a function of reaction time.

The salient feature of *Figures 2* and *3* is the sharp increase in the intrinsic viscosity and $x_n$ at about 40 min $(t_1)$ after time $t = 0$ at 150°C. The slope of the curve immediately following $t_1$ is increased significantly. *Figure 4* shows the rate of polymerization, $dx_n/dt$, which is calculated from the slope of the curve in *Figure 3* at the midpoint between data points. More than a five-fold increase in the polymerization rate is observed at the transition. In contrast, polycondensation of PBO at low concentrations (below 2 wt%) exhibits only a decreasing rate of polymerization with increasing molecular weight throughout the entire reaction.[5]

Direct observation indicates that, at the same time that the kinetic rate increases abruptly, the reacting dope becomes stir-opalescent, indicating the onset of a liquid crystalline phase in the dope. Analysis of thin samples under a polarized optical microscope shows that the dope is birefringent at $t \geq t_1$ but isotropic at $t < t_1$. The abrupt increase in the reaction rate is therefore interpreted as a quantitative description of the mesophase-enhanced polymerization by which the enhancement in kinetics is due to the alignment of rigid rods in the ordered phase.

It is coincidental that $t_1$ appears very close to the point at which the temperature reaches 180°C. We suspect that the abrupt increase in the kinetic rate is a result of the temperature profile and not due to the phase transition. However, previous study on polycondensation of PBO in the isotropic phase does not indicate any discontinuous change in the polymerization rate with temperature from 150 to 185°C. Therefore, the observed change in the
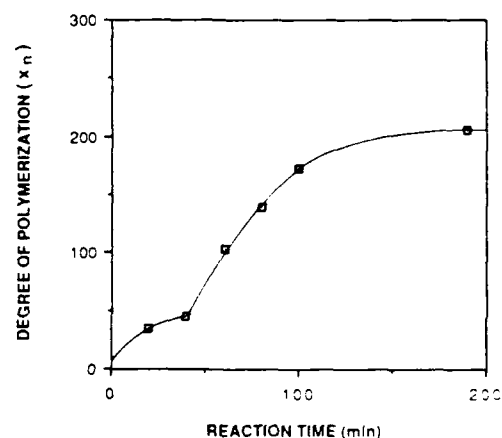


**Figure 3** Degree of polymerization as a function of reaction time in polycondensation of 15 wt% PBT in PPA
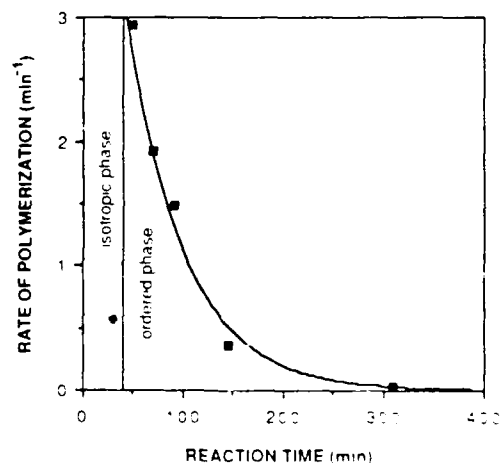


**Figure 4** Rate of polymerization as a function of reaction time in polycondensation of 15 wt% of PBT in PPA

A-3

thiazole unit based on crystallographic results on model compounds[5], the critical number-average axial ratio of PBT is calculated to be about 40 ($x_p = 45$) when the phase transition was first detected. Our experimental result compares favourably with the theoretical value.

Flory's theory also predicts a wholly anisotropic phase to occur when $x \sim 12.5 \phi$ for a monodisperse system. Calculations based on this model indicate a narrow biphasic region, when a complete nematic phase at $x = 66$ ($x_p = 73$) for PBT. Although a broader biphasic region is expected for polydisperse systems[9], the rapid polymerization rate at 180 C makes it difficult to determine accurately the breadth of the biphasic region.

*Figure 4* suggests that, in the liquid crystalline phase, the polymerization rate versus reaction time can be empirically described by an exponentially decaying function, and the degree of correlation of such curve fitting is 0.99. The decrease in the rate of polymerization is a function of the amount and reactivity of endcapping agent, the reactivities of side reactions, and possibly the molecular weight of the polymers. More research is needed to understand better the physical significance of such exponential dependence.

*Chemo-rheological properties*

The rheological behaviour of lyotropic, rigid rod macromolecules near the isotropic nematic phase transition has been a subject for numerous theoretical as well as experimental investigations[10]. In most experimental studies, the shear viscosity is measured as a function of concentration at a fixed molecular weight and temperature. Characteristically, the viscosity first

increases with concentration, reaches a maximum near the phase transition, then decreases in the nematic phase region at high concentrations.

In the PBT polymerization, the volume fraction of rods stays constant while the molecular weight and the temperature vary with time. The shear viscosity of the reacting media, monitored by the rheometer in cone-and-plate geometry, is shown in *Figure 5* for shear rates of 1, 5, 10 and $50 s^{-1}$. The temperature profile in these experiments follows that in the kinetic study described in the last section: an increase of 0.75 C min$^{-1}$ from 90 to 180 C, followed by a hold at 180 C throughout the remaining time of the reaction.

In all the experiments shown in *Figure 5* the specified shear was applied starting from 90 C. Previous experience indicates that no appreciable reaction can be detected until the temperature reaches at least 150 C. data acquisition therefore begins at 150 C. At shear rates of $1 s^{-1}$ and higher, the resulting dopes at the end of all runs appear green and stir-opalescent, and it is easy to draw long fibres from the dope. These are indications of moderately high molecular weight polymers in the ordered phase.

To our surprise, the rheological data at low shear rates (1 and $5 s^{-1}$) provide little indication of the isotropic nematic phase transition. The viscosity increases monotonically and quite smoothly with reaction time. At higher shear rates (10 and $50 s^{-1}$), a slight break in slope in the viscosity function near 40 to 50 min is observed. This break is very close to, and therefore suspected to be related to, the phase transition observed in the kinetic study.
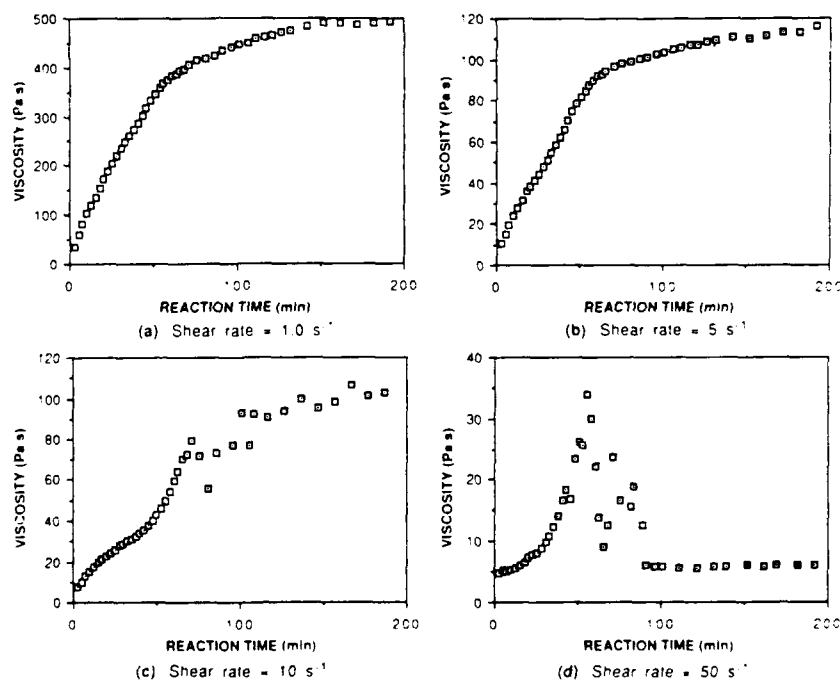


(a) Shear rate = 1.0 s⁻¹

(b) Shear rate = 5 s⁻¹

(c) Shear rate = 10 s⁻¹

(d) Shear rate = 50 s⁻¹

**Figure 5** Shear viscosity versus reaction time during polymerization of 15 wt %, PBT in PPA at shear rates of 1.0, 5.0, 10 and 50 s

A-4

In *Figures 5a* and *5b*, the viscosity increases very slowly or levels off at long reaction time. *Figures 5c* and *5d*, however, exhibit more unusual features beyond the phase transition. *Figure 5c* shows a dip in viscosity at 81 min. *Figure 5d* shows a dip at 66 min, followed by a dramatic drop in viscosity after 90 min. The origins of these sudden reductions in viscosity are unclear. Some may be due to changes in the degree of order in the nematic phase, and some may be artefacts resulting from secondary flows, sample slippage or sample being spun out of the flow cell due to the high rotational rate of the cell. Without further experimental evidence, we believe that the decrease is unlikely to be a manifestation of the biphasic nematic phase transition.

Polymerizations performed at shear rates below $1.0\,s^{-1}$ were less successful than those at higher shear rates. At $0.1\,s^{-1}$, the final greenish dope shows poor fibre-forming properties. Below $0.1\,s^{-1}$, the final material appears brownish-orange with black streaks, and no fibre can be drawn. Such appearance suggests low molecular weight materials. *Figure 6* illustrates the intrinsic viscosity of the final dope versus the shear rate at which the polymer is polymerized. This figure suggests that the shear rate has significant effects on the final molecular weight.

We also observe that the degree of polymerization of PBT polymerized in the cone-and-plate cell is significantly less than those polymerized in the glass reactor. The same batch of monomer mixture polymerized in the glass reactor after the series of shear experiments were conducted yields an intrinsic viscosity of $16.7\,dl\,g^{-1}$; no higher than $13\,dl\,g^{-1}$ is obtained in the rheometer as shown in *Figure 6*. This discrepancy may be due to one or more of the following: (1) contaminants (e.g. oxygen, moisture) introduced during loading of the monomer mixture onto the rheometer; (2) contaminants on the surface of the flow cell; (3) surface effects of the flow cell; and (4) differences in monomer mixing in early stages of the polymerization. However, this problem does not invalidate our earlier observation that the phase change effect does not seem to manifest itself in the low shear
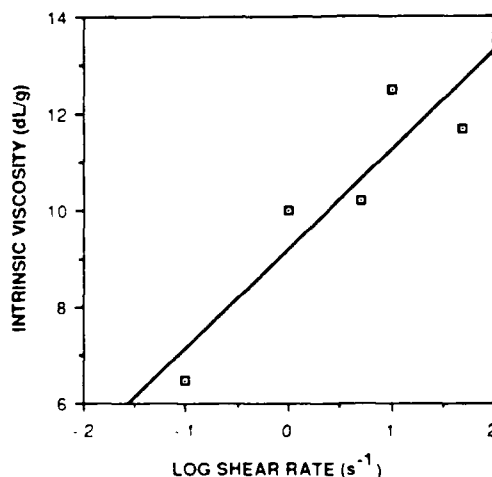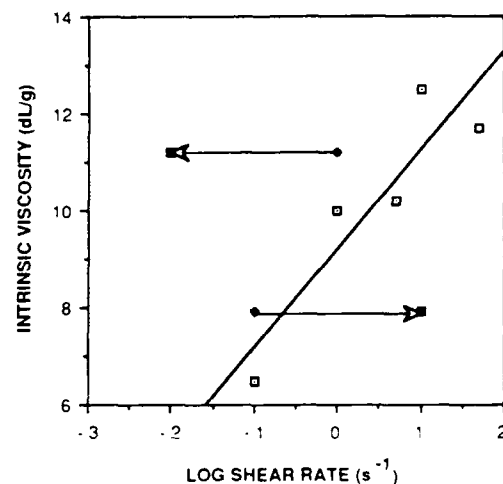


**Figure 7**   Semilogarithmic plot of the final polymer intrinsic viscosity versus the shear rates used for the polymerization. The arrows indicate direction of shear rate change at 150 C

viscosity function since the final dopes from the rheometer are indeed liquid crystalline.

The shear dependence on the final degree of polymerization could be a result of an enhancement in molecular alignment during shearing, or simply better mixing of the monomer mixture or the reacting medium. To distinguish between these two possible mechanisms, we performed two experiments in which a combination of shear rates was used. In one polymerization run, the monomer mixture was first sheared at $1\,s^{-1}$ from 90 to 150 C, and the shear rate was reduced to $0.01\,s^{-1}$ starting at 150 C throughout the polymerization. This shear profile yielded polymer with a final intrinsic viscosity of $11.2\,dl\,g^{-1}$, although the shear rate of $0.01\,s^{-1}$ alone has been found to be inadequate to achieve successful polymerization. In a second polymerization run, a shear rate of $0.1\,s^{-1}$ was applied below 150 C and $10\,s^{-1}$ above 150 C, and the resulting polymer exhibited an intrinsic viscosity of only $7.9\,dl\,g^{-1}$. These results suggest that a mixing effect, not molecular alignment, is the underlying reason for the shear dependence of the degree of polymerization.

*Figure 7* illustrates the results on final intrinsic viscosity versus shear rates used for polymerizing the monomers. The arrows indicate the direction of change in shear rate at 150 C. Good correlation with previous polymerization results can be obtained when the initial shear rates, not the final ones, are used in a plot of the intrinsic viscosity versus shear rate.

We investigated the effects of different temperature profiles on the polymerization at a constant shear rate of $1\,s^{-1}$. *Figure 8* shows three profiles. In the first one described previously, the final PBT shows an intrinsic viscosity of $10.0\,dl\,g^{-1}$. The second profile shows a sharp increase from 90 to 180 C in 20 min, and we only found a brownish-black residue, which appears to be a degradation product of the monomer at the end of the polymerization. The third profile contains an increase from 90 to 150 C in 20 min, a hold at 150 C for 100 min, and a sharp increase from 150 to 180 C. This profile
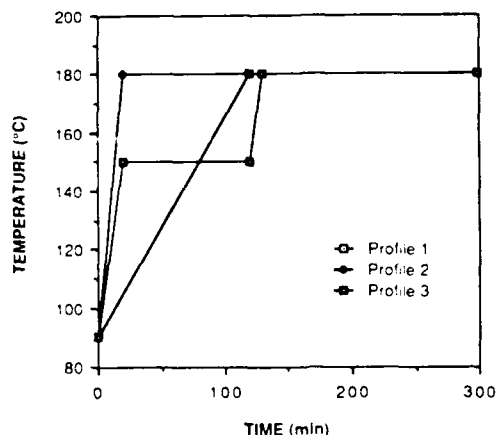


**Figure 6**   Semilogarithmic plot of the final polymer intrinsic viscosity versus the combination of shear rate used for the polymerization

A-5

produced the best results, a final polymer intrinsic viscosity of 12.6 dl g$^{-1}$, which is one of the highest obtained among all polymerization runs performed in the rheometer.

These data indicate that the temperature profile during the mixing period below 150 C has a drastic influence on the polymerization. whereas the temperature profile above 150 C has less effect on the resulting product. The results of the temperature and shear rate studies can be explained by a rapid polymerization for which an intimate mixture is critical and by the decreased sensitivity of oligomeric species to thermal decomposition.

## CONCLUSIONS

This study demonstrates quantitatively the enhancement in the polymerization kinetics of PBT when ordered domains form in the polymerizing solution. Chemorheological measurements at low shear rates throughout the polymerization, however, are a poor indication of the dramatic change in the reaction rate due to the phase change. At higher shear rates, the viscosity function exhibits features believed to result from the phase transition. Moreover, at long time and high shear, the viscosity displays characteristics that have uncertain origins. These results are difficult to simulate by model study because the shear viscosity is a complicated

function of the temperature, molecular weight, P$_2$O$_5$ content, shear rate and the degree of order in the nematic phase. Currently, there is no satisfactory unified theory on the rheology of rodlike polymers that can account for these complicated effects.

The shear rate and temperature effects on the polymerization products were not anticipated. Our data indicate that these parameters are most influential in the premixing stage (below 150 C) and much less influential in the polymerizing stage (above 150 C). Such results suggest that, once the monomer mixture is well dispersed initially, the polymerization can be performed to satisfaction under a wide range of reaction conditions. Conversely, if good mixing is not achieved in the early stage when the viscosity is low, later mixing is much less effective after PBT starts to polymerize significantly. We suspect that the dissolution of TA particles may be the limiting step to good mixing in the early stage.

Several unanswered questions have risen in this study. We have not yet been able to resolve the discrepancy in the final degree of polymerization between the glass reactor and rheometer runs. We are now investigating the possible effects of contamination and flow cell geometry.

## REFERENCES

1   Ly, W. C., Mammone, J. F. and Shambelan, C. paper presented at the 15th SAMPE Technical Conference, October 1983. Ly, W. C. and Mammone, J. F. paper presented at the Cellulose Division, Am. Chem. Soc., Miami, April 1985
2   Cotts, D. B. and Berry, G. C. *Macromolecules* 1981, **4**, 930
3   Wolfe, J. F., Loo, B. H. and Arnold, F. E. *Macromolecules* 1981, **4**, 915
4   Wolfe, J. F., Sybert, P. D. and Sybert, J. R. U.S. Patent 4 533 693 (1985)
5   Berry, G. C., Metzger, P. C., Venkatraman, S. and Cotts, D. B. *Am. Chem. Soc., Div. Polym. Chem.* 1979, **20**, 42
6   Berry, G. C. *Am. Chem. Soc., Div. Polym. Mat. Sci. Eng.* 1985, **52**, 82
7   Flory, P. J. *Proc. R. Soc. London (A)* 1956, **234**, 73
8   Wellman, M. W., Adams, W. W., Wolff, R. A., Dudis, D. S., Wiff, D. R. and Fratini, A. V. *Macromolecules* 1981, **14**, 935
9   Flory, P. J. and Frost, R. S. *Macromolecules* 1978, **11**, 1126
10  Wissbrun, K. F. *J. Rheol.* 1981, **25**, 619, and references therein

A-6

Appendix B

CHEMO-RHEOLOGY OF PBT POLYMERIZATION IN THE LIQUID
CRYSTALLINE PHASE

# CHEMO-RHEOLOGY OF PBT POLYMERIZATION IN THE LIQUID CRYSTALLINE PHASE

A. W. Chow and J. F. Wolfe
SRI International, Chemistry Laboratory
333 Ravenswood Avenue, Menlo Park, California 94025 U.S.A.

## INTRODUCTION

Poly(p-phenylenebenzobisthiazole) (PBT) is a rigid rod polymer with aromatic heterocyclic units in the backbone. This polymer forms a lyotropic liquid crystalline (LC) phase at high polymer concentrations. Such orderability provides great advantages to the polymer processibility and the physical properties of fabricated products (e.g., ultra high-strength, high-modulus fibers). Polymer synthesis in the ordered phase can also be highly beneficial. It has been reported that the polymerization rate is increased, and the final molecular weight of PBT can be enhanced significantly. [1] We call this phenomenon "mesophase-enhanced polymerization."

In this manuscript, we examine the chemo-rheology of PBT at concentrations sufficient to form the liquid crystalline phase during polymerization. This study is of fundamental interest because it may provide insight to the rheological behavior of lyotropic LC polymers during the phase transition. From the technological standpoint, knowledge of rheology is useful for processing optimization.

The rheological properties of solutions near the isotropic-nematic phase transition has been a subject for numerous theoretical as well as experimental investigations. [2] In many experimental studies on lyotropic LCs, the shear viscosity is measured as a function of concentration at a fixed molecular weight and temperature. Characteristically, the shear viscosity first increases with concentration, reaches a maximum near the phase transition, then decreases in the nematic phase region at high concentrations. The decrease in viscosity is due to the molecular alignment within the nematic phase. For thermotropic LC polymers, rheological measurements are usually performed as a function of temperature at a fixed concentration of rigid segments and molecular length. In some systems, a viscosity maximum has also been observed as the temperature is increased through the nematic-isotropic transition. [3,4] Our study on the chemo-rheology of PBT polymerization offers yet another cross-section of the rheological functions of LC polymers. During the polycondensation reaction, the volume fraction of rods stays constant while the molecular weight and temperature vary with time.

## EXPERIMENTAL
### Material Preparation

The synthesis of PBT is typically performed by the condensation of 2,5-diamino-1,4-benzenedithiol dihydrochloride (DABDT) and terephthalic acid (TA) in polyphosphoric acid (PPA) following the removal of hydrogen chloride: [5]
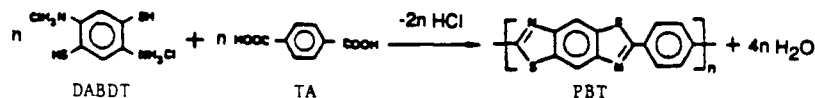


In this reaction, PPA serves as a solvent, catalyst, and dehydrating agent. Solid $P_2O_5$ is added according to the $P_2O_5$ adjustment method [6] to ensure adequate reaction conditions for a high degree of polymerization. In all experiments reported here, the final polymer concentration is 15% by weight and the final $P_2O_5$ content of the PPA is 82.9%. Benzoic acid (0.50 mole% based on DABDT) is used as endcapping agent to control the final molecular weight of the polymer. After the original mixture of DABDT and PPA is stirred at 90°C for sufficient time to remove the hydrogen chloride, TA and benzoic acid are added. The mixture of monomer, benzoic acid, and TA is then ready for polymerization at temperatures above 150°C.

### Rheological Characterization

Rheological measurements on the polymerizing mixtures are performed using a Rheometrics RMS-605 mechanical spectrometer. Because of the high sensitivity of the reaction mixtures to oxygen and moisture, a modified cone-and-plate fixture is used to prevent exposure of the reacting mixture to moisture over a long period (at least several hours). The fixture is made of Hastelloy C to resist acid corrosion at elevated temperatures. It consists of additional outer, concentric rings on both the cone and the plate such that dried, high-temperature-grade silicone oil can be introduced to form a barrier to moisture as shown in Figure 1. The diameter of the plate is 25 cm and the cone angle is 0.1 radian.

About 1 mL of the prepared monomer mixture at 90°C is removed from the bulk sample under nitrogen purge and loaded onto the cone-and-plate fixture carefully to minimize contaminant introduction. The flow cell is preheated to 90°C to avoid precipitation of the dissolved components. The sample is kept under a nitrogen blanket until the flow cell is closed and sealed with silicone oil. The temperature of the sample is then increased to initiate the polymerization. It is first heated from 90°C to 180°C at a rate of 0.75°C/min. When the mixture reaches 180°C, the temperature is maintained at 180°C until the end of the polymerization.

The effects of shear are studied by subjecting the polymerizing media to continuous steady shear throughout the reaction at shear rates from 0.01 s$^{-1}$ to 50 s$^{-1}$. The rheometer is programmed to record the torque reading and calculate the shear viscosity at about two-minute intervals.

## RESULTS AND DISCUSSION

The reaction kinetics of the polymerization of 15 wt% PBT were monitored by removing aliquots periodically from a 50 mL reacting mixture throughout the course of the reaction, and analyzing them for the molecular weight of the polymerized products. Figure 2 shows a plot of the extent of reaction ($x_n$) as a function of reaction time. Also indicated in the figure is the corresponding reactor temperature. A break in the slope of the curve coincides with the appearance of stir opalescent in the reacting medium by direct observation, and thus is identified as the isotropic-nematic phase transition.

When the monomer mixtures are polymerized in ~1 mL quantities within the Hastelloy cone-and-plate fixture under similar temperature profile, the reacting medium achieved the liquid crystalline phase during the polymerization when the applied shear rates were 0.1 s$^{-1}$ and above. When the applied shear rate was less than 0.1 s$^{-1}$, the reaction products contained only low molecular weight species.

Figure 3 shows the shear viscosity of the reacting medium as a function of reaction time at four different shear rates: 1.0, 5.0, 10, and 50 s$^{-1}$. To our surprise, the measure of the shear viscosity at low shear rates of 1.0 and 5.0 s$^{-1}$ provides very little indication of the phase transition. The viscosity increases monotonically throughout the reaction, with may be a very slight change in slope in the curve near 40 to 50 min reaction time at which the phase transition has been observed previously. At about 100 min, the viscosity starts to level off, reminiscent of the kinetics curve of Figure 2. The final products of both runs are characterized by persistent opalescence and high polymer molecular weight which are evidence of liquid crystallinity. This insensitivity of the shear viscosity to the phase change during the reaction will be analyzed later.

As the applied shear is increased to 10 s$^{-1}$, a more pronounced change in the slope of the viscosity curve can be observed at about 45 min. An even more drastic feature of the viscosity function is that it no longer changes monotonically with reaction time. The function decreases from 76 to 81 min followed by a further increase, and the signals appear to be quite "noisy" after the dip.

At 50 s$^{-1}$, the viscosity function exhibits quite unusual and unexpected behavior. The function in general increases to a maximum at 86 min, then decreases and levels off at longer times. The signals, however, become very noisy after the initial smooth increase from zero to 43 min, at which time fluctuations in the viscosity function begin to appear.

The origins of the sudden reduction and fluctuation in viscosity at high shear rates are not clearly understood. Some may be due to changes in the degree of order in the nematic phase, and some may be artifacts resulting from secondary flows or instability. The "noisiness" in the signals following the first dip in viscosity suggests that flow instability, not intrinsic material property, may be the cause.

To elucidate the high shear phenomenon of this lyotropic LC polymer, we examined the rheological behavior of a nematic PBT solution in more detail. The PBT in this sample is characterized by an extent of reaction, $x_n$, of 161 (or weight-average molecular weight of 27,800). The solution also contains 15 wt% PBT in PPA as in the previous experiments. Figure 4 shows both the steady and dynamic shear viscosity of the LC solution at 180°C. The data indicate shear thinning behavior over the entire range of shear rate measured. The two viscosity curves appear to converge at low shear and diverge significantly at high shear. On this double logarithmic plot, the slope of shear thinning under steady shear is about -0.6 to -0.7 from 0.01 to 1.0 s$^{-1}$, whereas it changes to almost -2 at higher shear. This drastic change in slope is reminiscent of the melt fracture phenomenon of flexible polymer melts, and flow instability is suspected. Although the Hastelloy cone-and-plate fixture does not allow direct observation of the flow cell during the experimental run, we noticed after the high shear experiment that a portion of the sample has been thrown out of the gap between the fixture, further indicating the occurrence of secondary flows in the flow cell at high shear rates. Such anomaly was not observed after the dynamic shear experiment. Other observations on flow instability of LC polymers has recently been reported by Denn et al. [7]

We performed another series of experiments to examine the sheared structure of the nematic PBT solutions at different shear rates. The PBT solution at 180°C was first subjected to steady shear of a chosen shear rate for 5 min, immediately followed by a dynamic shear sweep to high frequencies at 10% strain. Figure 5 shows the resulting plot of dynamic viscosity at high frequency regains the zero pre-shear value at the end of the 20 min run. For 10 and 100 s$^{-1}$ steady shear rates, however, the dynamic viscosity is drastically reduced even at high frequencies, supporting the previous observation that flow instability occurs at high shear, possibly causing changes in the sample that cannot be relaxed back to the original equilibrium state.

In retrospect, the relative insensitivity of the shear viscosity to the isotropic-nematic phase transition may not be as unusual as it originally appeared. The polydispersity in rod length tends to broaden out the isotropic-biphasic-nematic phase transition. [8] During the PBT polymerization, the longer rods will first be preferentially incorporated in the ordered phase whereas the shorter ones will be left in the isotropic phase. Because of the phenomenon of mesophase-enhanced polymerization, the rods in the ordered domains will react at a faster rate than those in the isotropic domains, causing an even greater difference in the average rod length in each phase and further broadening the biphasic transition. This broadened transition is likely to mask the local reduction in viscosity due to ordering of rods by the continuous increase in the average molecular weight of the polymer with reaction time.

## ACKNOWLEDGMENT

REFERENCES

[1] Chow, A. W., Sandell, J. F., Wolfe, J. F., "Reaction Kinetics and Chemo-Rheology of Poly(p-phenylenebenzo-bisthiazole) Polymerization in the Ordered Phase," Polymer, in press.
[2] Wissbrun, K. J.; Rheol., 25, 619 (1981), and references therein.
[3] Suto, S., White, J. L., and Fellers, J. F.; Rheologica Acta, 21, 62 (1982).
[4] Kiss, G.; J. Rheol., 30, 585 (1986).
[5] Wolfe, J. F., Loo, B. H., and Arnold, F. E.; Macromolecules, 4, 915 (1981).
[6] Wolfe, J. F., Sybert, P. D., and Sybert, J. R.; U.S. Patent 4,533,693, 1985.
[7] Kalika, D. S., Giles, D. W., and Denn, M. M.; "Anomalous Rheology of a Thermotropic Liquid Crystal Polyester," presented at the 59th Annual Meeting of the Soc. of Rheol., October 1977.
[8] Flory, P. J., and Frost, R. S.; Macromolecules, 11, 1126 (1978).
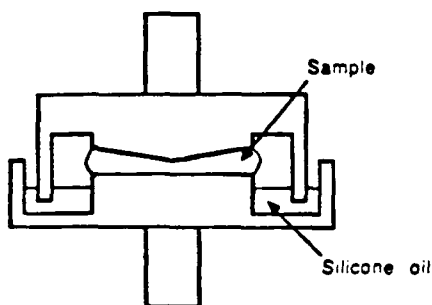
Figure 1 Modified cone-and-plate with moisture seal.
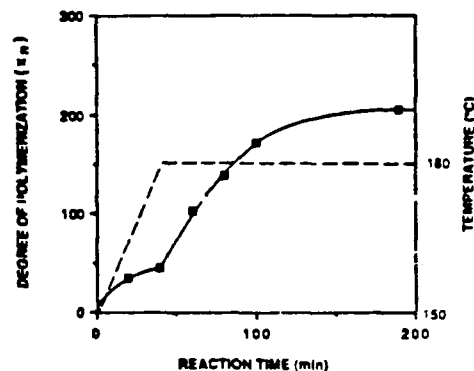


Figure 2 Degree of polymerization as a function of reaction time for polycondensation of 15 wt% PBT in PPA.



(a) Shear rate = 1.0 s⁻¹

(b) Shear rate = 5 s⁻¹

(c) Shear rate = 10 s⁻¹

(d) Shear rate = 50 s⁻¹
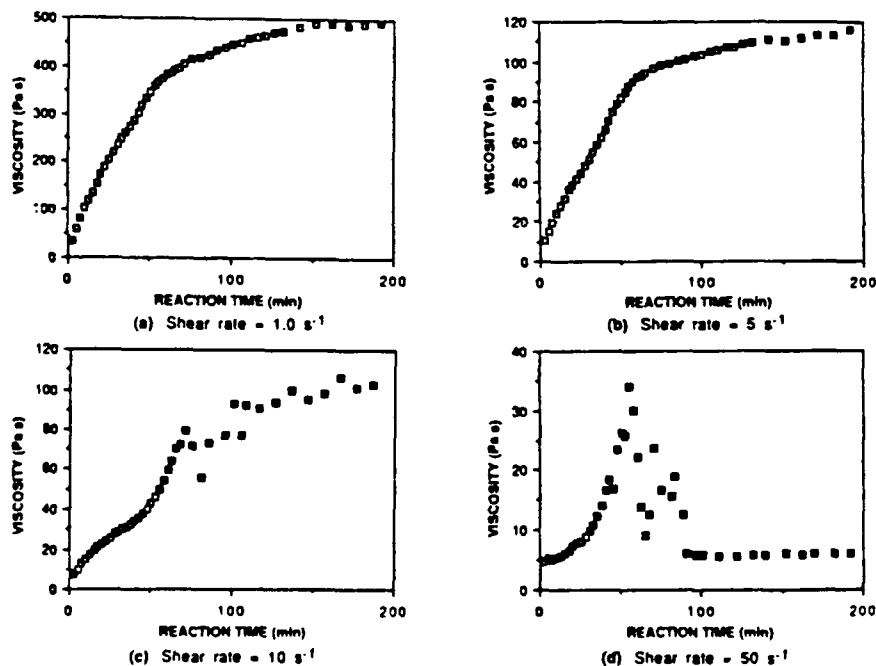
Figure 3 Shear viscosity versus reaction time during polymerization of 15 wt% PBT.
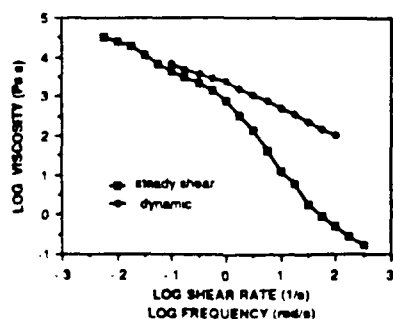


Figure 4 The steady and dynamic shear viscosity of a LC PBT solution.
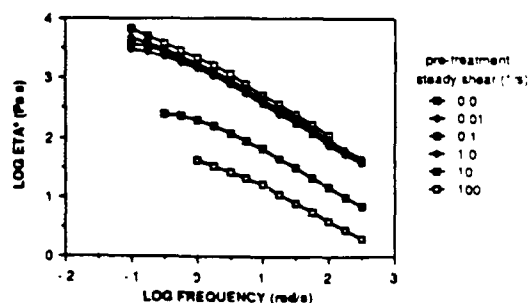
Figure 5 Dynam. shear viscosity of a LC PBT solution after steady shear of 0, 0.01, 0.1, 1.0, 10, and 100 s⁻¹.

Appendix C

SYNTHESIS APPROACHES FOR IMPROVING THE NONLINEAR OPTICAL
PROPERTIES OF PBZ POLYMERS

# SYNTHESIS APPROACHES FOR IMPROVING THE NONLINEAR OPTICAL PROPERTIES OF PBZ POLYMERS

JAMES F. WOLFE, BOCK H. LOO, ROBERT A. SANDERSON, AND STEVEN P. BITLER

   Chemistry Laboratory, SRI International, 333 Ravenswood Ave., Menlo Park, CA 94025

## ABSTRACT

   The synthesis of three types of functionalized benzazole structures is described.  A centrosymmetric dihydroxy-benzobis-thiazole has been synthesized for incorporation in flexible polymers having rigid, conjugated, third order nlo active units in the main chain.  Benzazole structures terminated with an N,N-dimethylamino group and a carboxyl group have been synthesized for use as second order nlo pendants with flexible polymers.  Benzazole structures terminated with an N,N-dimethylamino group and an amino group have been synthesized as precursors to second order nlo guest molecules.
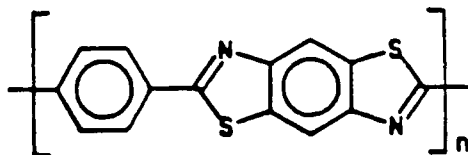
## INTRODUCTION

   Benzazoles have been identified as desirable nlo active units since the measurement of a high third order optical non-linear susceptibility, $\chi^{(3)}$, with a subpicosecond response, for poly(p-phenylenebenzo[1,2-d:4,5-d']bisthiazole (PBT) [1].



PBT

$\chi^{(3)} = 10\text{-}50 \times 10^{-12}$ esu

The macroscopic nlo activity arises from the existence of highly charge correlated virtual excitations on individual conjugated units in the backbone and the nature of the orientation of these units [1].  The size of the nlo active units of polybenzazoles (PBZ) is thought to be as small as about 22-28 atoms [2], which corresponds to the intrinsic delocalization length of these systems.  This finding suggests that structures with rigid benzazole units much shorter than found in PBT may be desirable--if they offer new processing options that would lead to improved device fabrication.

   The goal of our current synthesis effort is to incorporate rigid benzazole units, of various lengths, in new orderable polymeric systems that will provide processing options suitable for nlo applications.  The existence of macroscopic orientation of the nlo active unit is required to maximize the magnitude of the nlo response.  The particular molecular structure that causes that order is a strong determinant of the processibility, perhaps more so than it determines the nlo response.  Molecular organizations that can result in macroscopically ordered systems are depicted schematically in Figure 1.  Structure A represents a rigid rod molecule, such as PBT.  The nlo active units, shown

as the individual rectangles, are highly aligned, not only in the backbone, but also in the macroscopic array that results upon fabrication from strong acid solutions. Liquid crystalline solutions are obtained at relatively low polymer concentrations (above 5 wt %) and nematic ordering can be achieved at relatively low degrees of polymerization. Structure B represents a second class of PBZ polymers comprised of benzazole units, such as 2,5-benzoxazole or 2,6-benzothiazole. Unlike the rigid rod polymers, the conformation of these polymers in solution is concentration dependent [3]. At concentrations below 13 wt %, the conformation is that of a semiflexible coil and the overall orientation of the rigid units is random. At concentrations above 13 wt % the preferred conformation is a chain-extended, planar zig-zag and nematic phases are obtained. Block copolymers, depicted by structure C, have been prepared [4] and show liquid crystalline behavior in the concentrated polymerization medium when the rigid block has a sufficient degree of polymerization.

Although structures such as those depicted by D, E, and F have been prepared using other chemistries [5], they have not been prepared to our knowledge with benzazole units. These structures present a difficult challenge when the nlo active unit is so rigid because thermal processes are required for both synthesis and fabrication.
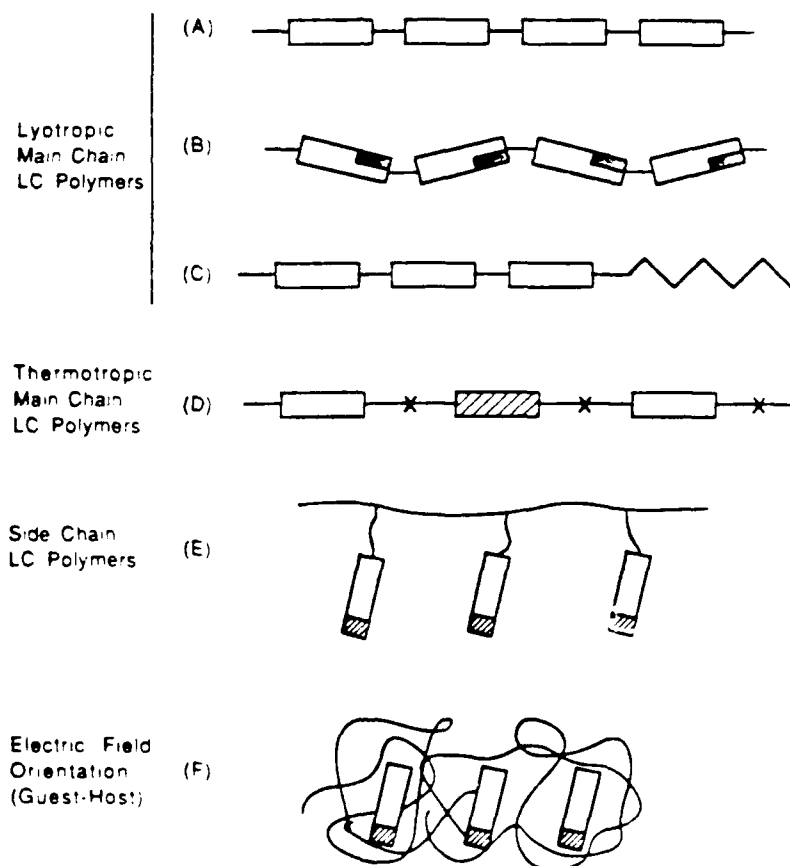


Figure 1
Schematic representations of Orderable Polymer Systems

This paper gives a preliminary report on our work, and our approaches for future research, toward the synthesis of benzazole compounds that we view as the essential components for structures of types D, E, and F.

RESULTS AND DISCUSSION

General Synthesis

Benzazoles are a family of aromatic heterocycles comprised of benzoxazoles, benzothiazoles, and benzimidazoles. They are most commonly prepared in poly(phosphoric acid) by the condensation of an ortho-amino-phenol, -thiophenol, or -aniline with either aliphatic or aromatic carboxylic acid derivatives. In PPA, the rate and the course of the reaction are influenced strongly by the electronic nature of the condensing monomers. We found that the presence of a nitro group in either condensing species resulted in decomposition of the more oxidatively sensitive compounds.

Synthesis Approaches to Benzobisazole-containing Polymers Linked by Flexible Spacers (Structure D)

Our initial approach to prepare polymers with alternating rigid and flexible units relied on preparing dihydroxybenzobisthiazoles (1). The length of the rigid benzobisazole segment could be varied by adjusting y, as outlined in Figure 2, if the basic reaction proceeded in high yield. Using a y value of one would assure an n value of one. Compound 1 could then be used to prepare polymers, such as polyesters and polyurethanes.



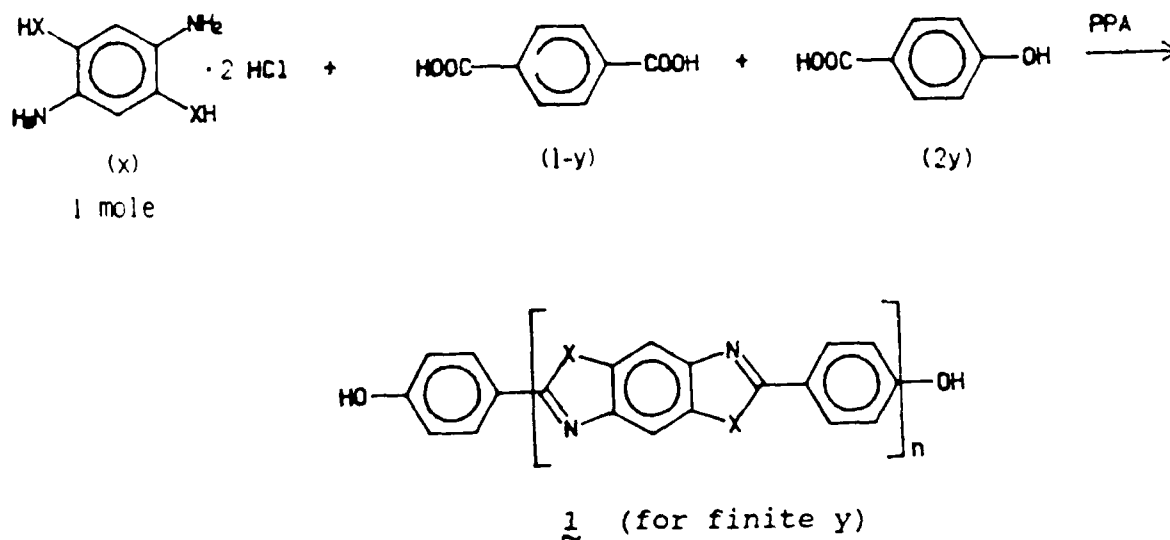(x)               (1-y)               (2y)

1 mole



1 (for finite y)

Figure 2
Synthesis of Hydroxy-terminated Benzobisazoles

2,6-Di(4-hydroxyphenyl)benzo[1,2-d:4,5-d']bisthiazole (1, X=S, n=1) was synthesized by condensing 2,5-diamino-1,4-benzenedithiol dihydrochloride (DABDT) with 4-hydroxybenzoic acid in

PPA. The electron-donating character of the hydroxyl group was expected to have two effects. The reactivity of the carboxyl group was expected to decrease because of inductive stabilization of the acyl carbonium ion, which is believed to be one of the necessary reactive moieties. In addition, the condensed phenyl ring should be activated toward acylation side reactions by another molecule of 4-hydroxybenzoic acid. We believe both of these effects can be mediated by varying the reactivity of the PPA, which is accomplished by adjusting the $P_2O_5$ content, and by varying the excess of the 4-hydroxybenzoic acid. The highest isolated yield obtained to date is only 53%. The product is a yellow solid with poor solubility in organic solvents; no suitable recrystallization solvent could be found. The mass spectral and IR analyses were consistent with the assigned structure. However, an anomalous elemental analysis is unexplained at this time. The product showed a sharp melting endotherm at $450^\circ$-$460^\circ C$ by differential scanning calorimetry (dsc).

The low yields obtained to date do not allow a systematic study of rigid-segment length. The poor solubility, which would be lower with compounds having larger n values, appears to limit synthesis procedures to strongly acidic solutions. These results have suggested an alternative route to obtaining flexible polymers with short benzobisthiazole units in the backbone. Our future research will focus on the synthesis of carboxyl-terminated benzobisazole compounds, 2, in PPA. Polymers with flexible spacers will then be prepared by condensation

Y = COOH
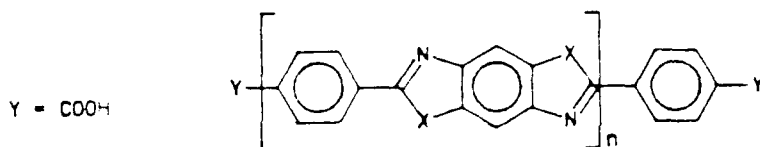


2

in PPA. The rigid segment will be prepared, for example, by adding 1 mole of DABDT to a PPA mixture of 2 moles of terephthaloyl chloride. The flexible segment will be prepared in a separate pot by condensing 1 mole of sebacoyl chloride, for example, with 2 moles of DABDT in PPA. Admixing the two PPA solutions and continuing the reaction should give a polymer that has a high percentage of alternation of flexible with rigid units.

## Synthesis Approach to Flexible Polymers with Benzazole-containing Pendants (Structure E)

Our approach to preparing polymers of type E is outlined in Figure 3. The approach relies on first forming the monoester with a triol and a pendant, and then polymerizing through the free hydroxyl groups of the triol moiety to form either a polyester or a polyurethane. The systematic synthesis of pendants of various lengths should be possible in these systems by varying the ratio of endcapping 4-(dimethylamino)benzoic acid as shown in Figure 4.
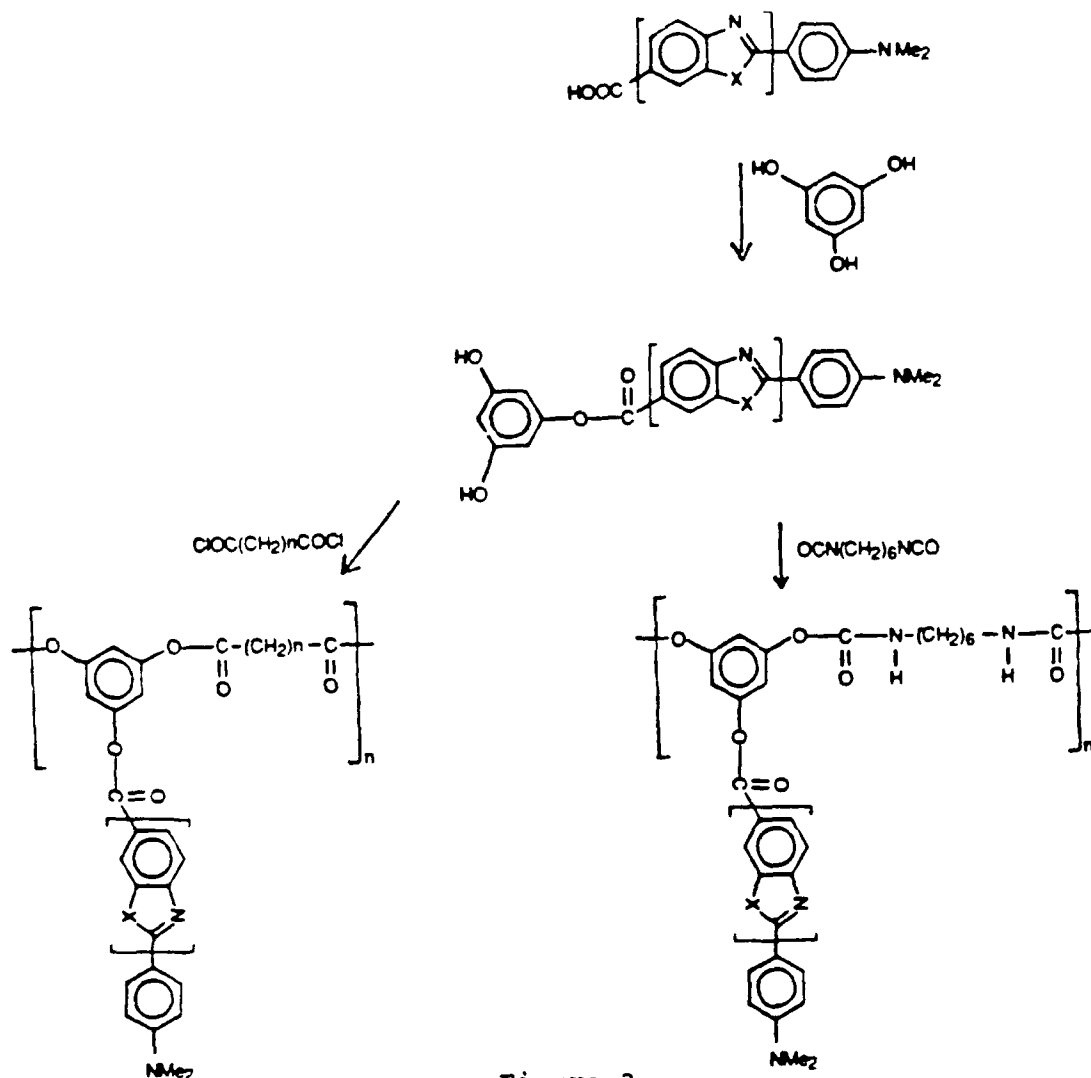
Figure 3
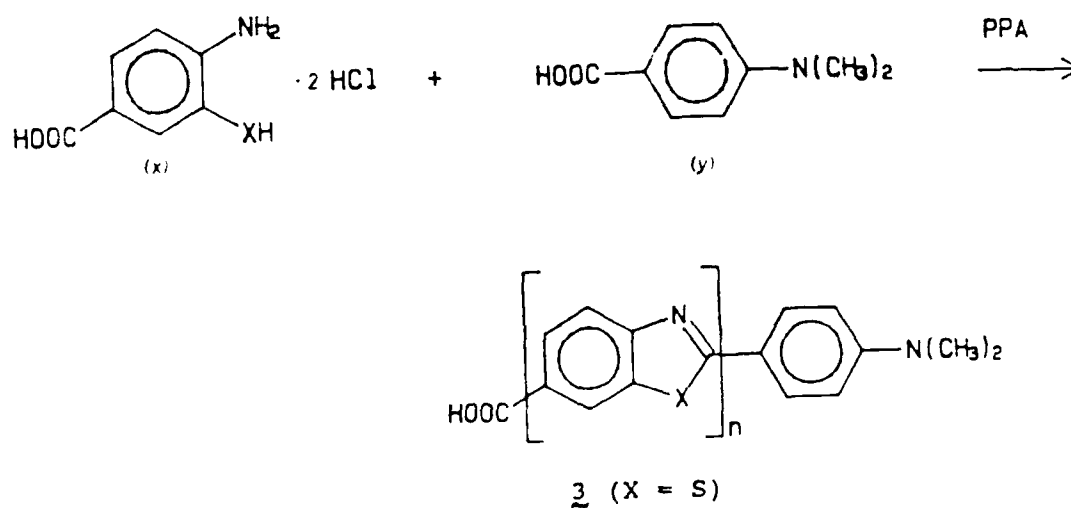Approach to the Synthesis of Flexible Polymers
with Benzazole Pendants



3 (X = S)

Figure 4
Pendant Synthesis

We have prepared 2-(4-(dimethylamino)phenyl)-6-carboxy-benzothiazole (3, X=S) and 2-(4-(dimethylamino)phenyl)-5-carboxybenzoxazole (4, X=O). Compound 3 was prepared by condensing 4-amino-3-mercaptobenzoic acid with 4-(dimethylamino)-benzoic acid in PPA. Compound 4 was similarly prepared by condensing 3-amino-4-hydroxybenzoic acid with 4-(dimethyl-amino)benzoic acid in PPA. These condensations should result in production of some dimer and trimer because the starting carboxyaminophenol can self-condense. Mass spectral analysis confirms the presence of minor quantities of both the dimer and trimer. Condensation to form the dihydroxy ester is currently in progress.

With the carboxyl group para to the benzazole nitrogen, compound 3 should have a greater dipole moment than compound 4. The contribution from a resonance structure with a positive charge on the dimethylamino nitrogen and a negative charge on the carbonyl oxygen is possible in 3, but not in 4. Compounds 3 and 4 should exhibit second order nlo activity because they are fully conjugated and lack a center of symmetry. Orientation of the pendants will be attempted by poling the polymers above their glass transition temperatures.

## Synthesis Approach to Benzazole-containing Guest Molecules (Structure F)

The target compounds for this segment of our study (Compounds 7 and 8) have a dimethylamino group at one end of the conjugated system and a nitro group at the other, as shown in Figure 5.

5,  Y = NH$_2$, X = O

7,  Y = NO$_2$, X = O



6,  Y = NH$_2$, X = O

8,  Y = NO$_2$, X = O
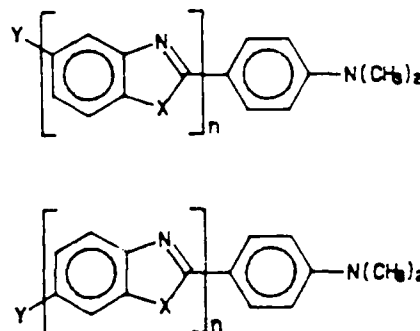


**Figure 5**
Target Compounds and Precursors for nlo Active Guest Molecules

Preparation of a series of compounds of various oligomeric lengths and isomeric structures was initiated by preparing the model compounds 2-(4-(dimethylamino)phenyl)-5-aminobenzoxazole (5) and 2-(4-(dimethylamino)phenyl)-6-aminobenzoxazole (6). These compounds were prepared by condensing 2,5- and 2,6-diaminophenol with 4-(dimethylamino)benzoic acid in PPA. The two step synthesis of the target compounds became necessary when the attempted condensation of 5-nitro-2-aminophenol with 4-(dimethylamino)benzoic acid gave extensive decomposition products. We are currently investigating methods of oxidizing the amino groups to nitro groups, thereby synthesizing compounds with high dipole moments. Attempts to oxidize 5 using either potassium permanganate or peracetic acid have given mostly

starting material, some evidence of N-oxide formation, and only minor amounts of the desired product, 2-(4-(dimethyl-amino)phenyl)-5-nitrobenzoxazole (7). Various oligomeric lengths of the precursor amino-compounds can be prepared, as a distribution of oligomers, by condensing various ratios of 2,5-diaminophenol, 4-(dimethylamino)benzoic acid, and 4-amino-3-mercaptobenzoic acid, as shown in Figure 6. Preparing the two isomeric structures will allow the comparison of the expected differences in the dipole moments and their effect on the nlo response. We will study the incorporation and orientation of these compounds into glassy polymers in a guest/host fashion.
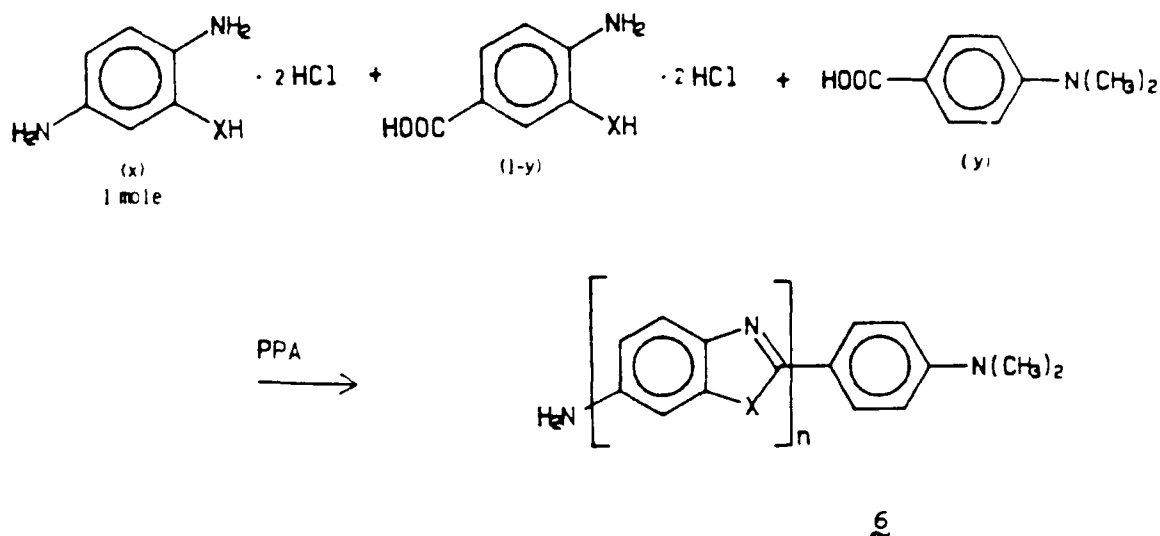


Figure 6
Synthesis of Compound 6 with Variable Chain Length

EXPERIMENTAL

Poly(phosphoric acid) (PPA)

PPAs having $P_2O_5$ contents between 84 and 62% are conveniently prepared by mixing 115% phosphoric acid (FMC, 84% $P_2O_5$) and 85% phosphoric acid (Baker Chemical Co., 62% $P_2O_5$) and heating for 2 h at 115°-120°C under reduced pressure with stirring. For in situ removal of hydrochloride protecting groups, we have found a $P_2O_5$ content of 77% to be convenient. For condensations, the $P_2O_5$ content must be raised to a calculated value, by the addition of powdered $P_2O_5$, such that the $P_2C_3$ content is above 82% after the hydrolysis of the PPA by the water of condensation.

2,6-Di(4-hydroxyphenyl)benzo[1,2-d:4,5-d']bisthiazole (1)

2,5-Diamino-1,4-benzenedithiol dihydrochloride [6] (32.43856 g, 132.3 mmol) was placed in a 300 mL resin kettle equipped with mechanical stirrer and 176.08 g of PPA was added at room temperature. The PPA (77.8% $P_2O_5$) was prepared by heating a mixture of 129.8 g of 115% phosphoric acid and 46.4 g of 85.3% phosphoric acid to 115°-120°C for 2 h under reduced pressure. The mixture was heated at 50°-60°C for 48 h to remove the gaseous hydrogen chloride. 4-Hydroxybenzoic acid (38.37944 g,

277.9 mol) was then added to the resulting yellow solution. The $P_2O_5$ content was raised to a post-condensation value of 82.9 % by adding 98.43 g of powdered $P_2O_5$. The mixture was stirred at $90^O$-$95^O$C for 16 h and then at $180^O$-$185^O$C for 27 h. The reaction mixture was poured into water, neutralized with sodium hydroxide, and the yellow solid was collected by filtration. After washing with methanol, the product was dried at $40^O$-$50^O$C under reduced pressure to give 49.80 g (53%) of 1. mp $450^O$-$460^O$C (dsc); Mass spectrum: m/e 377 (M+1)$^+$.


## 2-(4-(Dimethylamino)phenyl)-6-carboxybenzothiazole (3)

4-Amino-3-mercaptobenzoic acid hydrochloride (6.42 g, 31.22 mmol) was placed in a 100 mL resin kettle equipped with mechanical stirrer and 61.27 g of PPA (74.8% $P_2O_5$) was added. The PPA was prepared by heating a mixture of 37.19 g of 115% phosphoric acid and 24.08 g of 85.3% phosphoric acid to $115^O$-$120^O$C under reduced pressure for 2 h. The mixture was heated to $50^O$-$55^O$C under reduced pressure for 48 h to remove the hydrogen chloride. To the clear light yellow solution was added 9.79 g (59.27 mmol) of 4-(dimethylamino)benzoic acid and 35.30 g of $P_2O_5$. The mixture was then stirred at $90^O$-$95^O$C for 16 h. The mixture was then heated at $180^O$-$185^O$C for 16 h. The reaction mixture was poured into water, neutralized with sodium hydroxide, and the solid separated by centrifugation. The green solid was washed twice with methanol and then dried under reduced pressure at $70^O$-$75^O$C for 16 h. The yield of a green solid was 6.79 g (73%) that is soluble in glacial acetic acid, N,N-dimethylformamide, and dimethyl sulfoxide: mp > $280^O$C; mass spectrum m/e 298 (M+, n=1) and 431 (M$^+$, n=2); ir (cm$^{-1}$): 3150-3500 br (OH), 1680 m (CO).


## 2-(4-(Dimethylamino)phenyl)-5-carboxybenzoxazole (4)

To a 100 ml resin kettle equipped with mechanical stirrer containing 10.41068 g (67.98 mmol) of 3-amino-4-hydroxybenzoic acid and 11.79055 g (71.37 mmol) of 4-(dimethylamino)benzoic acid was added 58.15 g of PPA (77.8% $P_2O_5$). The PPA had been prepared by heating 42.839 g of 115% phosphoric acid and 15.311 g of 85.3% phosphoric acid to $115^O$-$120^O$C for 2 h under reduced pressure. Powdered $P_2O_5$ (39.2 g )was added to give a final calculated $P_2O_5$ content of 82.7%. The reaction mixture was heated to $90^O$-$95^O$C for 16 h. The reaction mixture was then heated to $160^O$-$165^O$C over 3 h and held at that temperature for 6 h. After the reaction mixture was poured into water, the light green solid was collected by filtration and washed with methanol. mp. $360^O$-$370^O$C; Mass spectral analysis shows a major peak at 282 as the parent of 4 (n=1)as well as minor peaks at 399 and 517 for 4 with n=2 and 3; ir (cm$^{-1}$): 3130-2800 br m (COOH), 1685s (CO),


## 2,5-Diaminophenol dihydrochloride

To a 500 mL flask equipped with magnetic stirrer and reflux condenser was added 200 mL of 12 M (2.4 mol)hydrochloric acid, 36 mL of water, and 72 g (320 mmol) of stannous chloride dihydrate. To this reducing medium was added 12 g (78 mmol) of 2-amino-5-nitrophenol (Pfaltz and Bauer). Heating to $70^O$-$75^O$C resulted in a yellow solution. The solution was heated to $85^O$-$90^O$C for 1 h followed by cooling to $20^O$-$25^O$C. The resulting white crystalline solid was collected by filtration, washed with methanol and diethyl ether, and dried at $40^O$-$50^O$C under reduced

pressure. Two recrystallizations from dilute hydrochloric acid yielded 3.25 g (21%) of white crystalline product: mass spectrum m/e 124 (P-2HCl).

## 2-(4-(Dimethylamino)phenyl)-5-aminobenzoxazole (5)

To a 250 mL flask equipped with mechanical stirrer was added 10.7 g (54.3 mmol) of 2,4-diaminophenol dihydrochloride and 100 g of 115% phosphoric acid. The mixture was heated to $60^\circ$-$100^\circ$C for 36 h to effect loss of the hydrogen chloride. To the solution was added 9.0 g (54.5 mmol) of 4-(dimethylamino)benzoic acid and the mixture was stirred at $180^\circ$-$185^\circ$C for 6 h. The reaction mixture was quenched in water yielding a yellow solid on neutralization with sodium hydroxide. The mixture was filtered and the residue was recrystallized from toluene giving a light yellow solid (5.3 g, 38.5%): mp $197^\circ$-$200^\circ$C; mass spectrum m/e 253 (M+); ir $(cm^{-1})$: 3455m, 3335m, 2900 br w, 1610s, 1570m, 1510s, 1490s, 1185s; Anal. Calcd for $C_{15}H_{15}N_3O$: C, 71.13; H, 6.00; N, 16.59. Found: C, 71.99; H, 5.86; N, 16.60.

## 2-(4-(Dimethylamino)phenyl)-6-aminobenzoxazole (6)

To a 250 mL flask equipped with mechanical stirrer was added 3.25 g (16.5 mmol) of 2,5-diaminophenol dihydrochloride and 75 g of 115% phosphoric acid. The mixture was heated to $50^\circ$-$100^\circ$C to effect loss of hydrogen chloride. To the solution was then added 2.85 g (17.3 mmol) of 4-(dimethylamino)benzoic acid and the mixture was heated at $180^\circ$-$185^\circ$C for 20 h. The solution was cooled to $100^\circ$C, poured into water, and the solid collected by filtration. The solid was washed with sodium hydroxide to give 4.08 g of a yellow-brown solid. Recrystallization from toluene gave 2.78 g (67%) of light orange solid: mp $215^\circ$-$217^\circ$C; mass spectrum m/e 253 $(M^+)$; ir $(cm^{-1})$: 3430m, 3320m, 3200w, 2900 br w, 2800w, 1615s, 1510s, 1490s, 1450m; Anal. Calcd for $C_{15}H_{15}N_3O$: C, 71.13; H, 6.00; N, 16.59. Found: C, 71.72; H, 5.95; N, 16.15.

## Attempted Synthesis of 2-(4-(Dimethylamino)phenyl)-5-nitrobenzoxazole (7)

To a 200 mL round bottom flask equipped with reflux condenser and magnetic stirrer was added 1.0 g (3.9 mmol) of 5 and 60 mL of chloroform. To the yellow solution was added 12 mL of a solution that was prepared by dissolving 10 ml of 40% peracetic acid in acetic acid in 50 ml of chloroform. The solution became reddish-brown then yellow-green yielding a precipitate. The mixture was refluxed for 1 h, cooled to $25^\circ$-$30^\circ$C and then filtered. The yellow solid was washed with chloroform and dried (yield = 0.62 g): mp $289^\circ$-$293^\circ$C. Mass spectral analysis showed a major peak at 254 for starting compound 5, with minor peaks at 227, 240, 268, 282, 296, 476, 489, 503, 519, 533; ir $(cm^{-1})$: 3550-3350 br m, 3120-3020 br w, 1700m, 1620m, 1560w.

1. A. F. Garito, K. Y. Wong, Y. M. Cai, H. T. Man and O.Zamani-Khamiri, in <u>Molecular and Polymeric Optoelectronic Materials: Fundamentals and Applications</u>, edited by G. Khanarian, (Proceedings SPIE, <u>682</u>, August 1986) pp. 2-11; D. N. Rao, J. Swiatkiecz, P. Chopra, S.K. Ghoshal, and P.N. Prasad, Appl. Phys. Lett. <u>48</u>, 1187 (1986).

2. L. R. Dalton, J. Thomson, and H. S. Nalwa, Polymer <u>28</u>, 543 (1987).

3. A. W. Chow, P. E. Penwell, S. P. Bitler, and J. F. Wolfe, Am. Chem. Soc., Div. Polym. Chem., <u>28</u> (1), 50 (1987).

4. J. F. Wolfe, P. D. Sybert, and J. R. Sybert, U. S. Patent No. 4 533 693 (6 August 1985).

5. G. D. Green, H. K. Hall, Jr., J. E. Mulvaney, J. Noonan, and D. J. Williams, Macromolecules <u>20</u>, 716 (1987); C. Ye, T. J. Marks, J. Yang, and G. K. Wong, Macromolecules <u>20</u>,.2322 (1987); A. C. Griffin, A. M. Bhatti, and R. S. L. Hung, in <u>Molecular and Polymeric Optoelectronic Materials: Fundamentals and Applications</u>, edited by G. Khanarian (Proceedings SPIE, <u>682</u>, August 1986) pp. 65-69; J. B. Stamatoff, et al., in <u>Molecular and Polymeric Optoelectronic Materials: Fundamentals and Applications</u>, edited by G. Khanarian (Proceedings SPIE, <u>682</u>, August 1986) pp.85-92.

6. J. F. Wolfe, B. H. Loo, and F. E. Arnold, Macromolecules <u>14</u> (4), 915 (1981).

Appendix D

SYNTHESIS AND SOLUTION PROPERTIES OF EXTENDED CHAIN
POLY(2,6-BENZOTHIAZOLE) AND POLY(2,5-BENZOXAZOLE)

# SYNTHESIS AND SOLUTION PROPERTIES OF EXTENDED CHAIN POLY(2,6-BENZOTHIAZOLE) AND POLY(2,5-BENZOXAZOLE)

Andrea W. Chow,* Steven P. Bitler, Paul E. Penwell, Dyan J. Osborne, and James F. Wolfe*†

SRI International, Chemistry Laboratory,

333 Ravenswood Ave., Menlo Park, CA   94025

*To whom correspondence should be addressed.

†Current address: Lockheed Missiles & Space Co., 3251 Hanover Street, Palo Alto, CA  94304.

(Revised, February 1989)

# Abstract

The $P_2O_5$ adjustment method allows polymerization of poly(2,6-benzothiazole) (ABPBT) and poly(2,5-benzoxazole) (ABPBO) in poly(phosphoric acid) at high concentrations up to 21 wt%. ABPBO can also be prepared in methanesulfonic acid by adding up to 45 wt% of $P_2O_5$. When polymerized at concentrations above ~14 wt%, the reacting mixture became liquid crystalline and the molecular weight of the resulting polymer was significantly higher than that of mixtures polymerized in the isotropic phase (below ~14 wt%). Addition of monofunctional end-capping agents to the starting mixture depressed the final molecular weight of the polymeric products, and Flory's theory for condensation polymerization appeared to predict the degree of molecular weight depression. Dilute solution characterization of these poly(benzazole) polymers indicated stiff-chain conformations, and comparison with the Yamakawa-Fujii wormlike chain model suggested that they have persistence lengths of 90 to 130 Å. The Mark-Houwink-Sakurada constants for these semirigid polymers were also determined.

# Introduction

Our studies of aromatic heterocyclic polymers of the poly(benzazole) family are motivated by the need for lightweight, high strength, high modulus, environmentally resistant materials for use in structural applications. Within the Air Force's Ordered Polymers Research Program, our original approach focused on the rigid-rod polymer structures poly(p-phenylenebenzo-[1,2-d:4,5-d']bisthiazole) (PBT)[1] and poly(p-phenylenebenzo[1,2-d:5,4-d']bisoxazole) (PBO),[2] which formed liquid crystalline phases during polymerization at concentrations above 5 wt% [3].
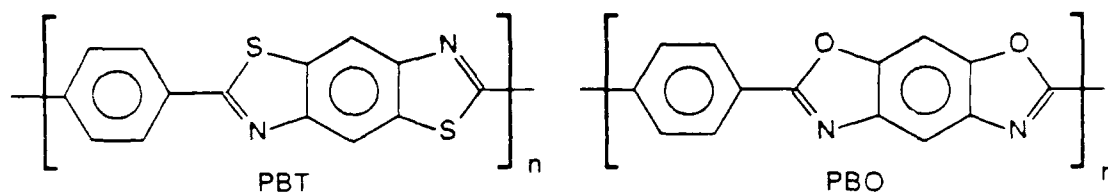


PBT

PBO

The catenation angle, which is the angle between exocyclic bonds of the rigid backbone units, is 180° for both PBT and PBO. These structures thereby provide some of the most rodlike configurations in the poly(benzazole) family.

While developing the synthesis methods for preparing PBT in poly(phosphoric acid) (PPA), we discovered that polymerization proceeded at polymer concentrations as high as 21 wt% if the $P_2O_5$ content of PPA was increased to account for the greater relative amount of water of condensation.[4] The ability to polymerize at such high concentrations led to the discovery that polymers with catenation angles much less than 180°, such as poly(2,6-benzothiazole) (ABPBT) and poly(2,5-benzoxazole) (ABPBO), also formed the liquid crystalline phase during polymerization.



ABPBT

ABPBO

2
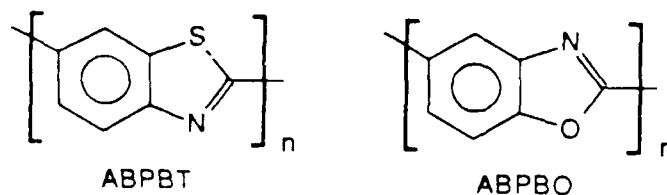
ABPBT and ABPBO are characterized by catenation angles of 162° and 150°, respectively. Because of the unrestricted rotation between repeat units,[5] these backbone diads can assume either an extended chain conformation (trans) or a coil-like conformation (cis), as illustrated in Figure 1. In dilute solution, these polymers are likely to assume a random distribution of cis- and trans-conformations if neither conformation is statistically favored. At high concentrations, the liquid crystalline phase is favored energetically, and the trans-conformation is believed to dominate to allow this phase change.

We report the synthesis method for polymerizing these poly(benzazoles) with controlled molecular weights, and the determination of their dilute solution properties by low angle light scattering and viscometry measurements. We also compare the experimental data with a wormlike chain model.

## Experimental Section

**ABPBO Monomer Synthesis.** 3-Amino-4-hydroxybenzoic acid hydrochloride (AHBAH) was prepared in two steps from p-hydroxybenzoic acid,[6] by nitration with one equivalent of nitric acid in glacial acetic acid at low temperature followed by reduction with stannous chloride and hydrochloric acid, as illustrated in Scheme I. Typical yields for the two steps were 40% and 90-95%, respectively. AHBAH was heated in water containing 1 wt% stannous chloride and obtained as small, colorless needles by adding an equal volume of concentrated hydrochloric acid. After washing with concentrated hydrochloric acid and diethyl ether, AHBAH was obtained without water of hydration by drying for 16 h at about 65°C under reduced pressure. Anal. calcd for $C_7H_8NO_3Cl$: C, 44.34; H, 4.25; N, 7.39; Cl, 18.70. Found: C, 44.41; H, 4.32; N, 7.33; Cl, 18.87.

**ABPBT Monomer Synthesis.** 3-Mercapto-4-aminobenzoic acid hydrochloride (MABAH) was prepared in two steps from p-aminobenzoic acid (PABA), as illustrated in Scheme

3

II, by dissolving PABA (6.0 mol) and sodium thiocyanate (12.7 mol) in 6 L of methanol and adding bromine (6.35 mol) over a 3.5-h period while maintaining the pot temperature at -5° to -10°C. After stirring for an additional 2 h at about 5°C, the resulting yellow precipitate was collected by filtration, washed with water, and recrystallized twice from 6 L of 1 N hydrochloric acid by heating to about 70°C, filtering, and then adding 3 L of concentrated hydrochloric acid to the filtrate. Upon cooling, the 2-amino-6-carboxybenzothiazole hydrochloride (ACBTH) was obtained as colorless needles in 50% yield: mp 288°-290°C (dec). ACBTH was hydrolyzed by heating 100 g in 800 g of 50% aqueous potassium hydroxide at the reflux temperature for 4 h. The reaction mixture was filtered and the filtrate was added to 575 mL of cold concentrated hydrochloric acid. The precipitate was collected and recrystallized twice from 1.5 L of water by adding hydrochloric acid until the product dissolved, adding 5 g of stannous chloride, heating to 7?°C, adding an additional liter of concentrated hydrochloric acid, and cooling. The yield was 29 g (33%) of MABAH: mp 192°-194°C; ir 3380 cm$^{-1}$ (O-H), 3000 cm$^{-1}$ (N-H), 2520 cm$^{-1}$ (S-H), 1700 cm$^{-1}$ (C=O), 1605 cm$^{-1}$ (C=C). Anal. calcd for $C_7H_8NO_2SCl$: C, 40.88; H, 3.92; N, 6.81; S, 15.59; Cl, 17.24. Found: C, 40.67; H, 3.91; N, 6.85; S, 15.78; Cl, 17.10.

**Polymer Synthesis.** The general method for preparing benzazole polymers in PPA in the nematic phase at polymer concentration greater than 10 wt% has been reviewed.[7] The key polymerization variables employed in this technique, which we call the $P_2O_5$ adjustment method, relate to the proper control of PPA composition at various stages of polymerization based on the concentration of the condensing species.

The variables relating to the $P_2O_5$ adjustment of PPA are

(1) Initial $P_2O_5$ content of the PPA, $P_1$, which is operative during the initial step of hydrogen chloride removal, or dehydrochlorination.

(2) Intermediate $P_2O_5$ content of the PPA, $P_2$, obtained by adding B grams of powdered $P_2O_5$ to the initial PPA/monomer mixture after hydrogen chloride removal.

(3) Final $P_2O_5$ content of the PPA, $P_3$, achieved by hydrolysis of the intermediate PPA,

having a $P_2O_5$ content of $P_2$, by the water of polycondensation.

(4) Polymer concentration, C, the weight fraction of polymer in the total weight of the solution.

(5) Polymer yield, Y.

(6) Weight of initial PPA used for the dehydrochlorination, A.

A is given by $\dfrac{Y\,\{[1\text{-}P_3]\,[(1/C) - 1] - 36.03/M\}}{(1\text{-}P_1)}$

where M is the weight of the polymer that produces 2 mol of water of condensation.

(7) Weight of $P_2O_5$ required to achieve a chosen $P_3$, B.

B is given by $Y[(1/C) - 1 - 36.03/M] - A$

(8) Amount of monofunctional reagent, or end-capper, EC%, given in moles per hundred moles of monomer.

(9) Polymerization time, PT, defined as the time that the polymerization mixture was heated above 100°C.

Typical ABPBT and ABPBO polymerizations are outlined in Tables I and II by giving these nine variables and the intrinsic viscosities of the resulting polymers.

In another experiment, ABPBO was prepared in methanesulfonic acid (MSA) instead of PPA using the $P_2O_5$ adjustment method to demonstrate the general utility of the method. The results of this experiment are discussed in the following section.

After polymerization, all polymer samples were precipitated in water, washed with water in a Soxhlet extractor to remove residual PPA, and dried under reduced pressure at 130°-140°C for 24 h to ensure complete removal of moisture. The dried samples were stored in a desiccator until use. MSA was used as solvent for dilute solution measurements, and it was distilled under reduced pressure and stored under dry nitrogen. The polymer solutions were analyzed within 3 days of preparation.

**Light Scattering from Semirigid Polymers.** Light scattering measurements were

made using a Chromatix KMX-6 (LCDC Milton Roy) low angle light scattering (LALS) photometer equipped with a polarizing filter to allow measurements of the vertical and horizontal components of the scattered light. The incident wavelength is 632.8 nm. Annulus of 6-7° and field stop of 0.2 mm were used. A narrow band interference filter was inserted between the sample and the detector to remove fluorescence radiation from the sample. All solvents and polymer solutions for light scattering were filtered through 0.2-μm (Millipore) membrane filters. The differential refractive index increments, dn/dc, were measured for each polymer sample in MSA using a 632.8-nm laser. Values for dn/dc range from 0.42 to 0.54 dL/g for ABPBT and from 0.31 to 0.43 dL/g for ABPBO. All measurements were performed at ambient temperatures of $23\pm2°C$.

Light scattering from an anisotropic element of a polymer chain involves the intrinsic anisotropy factor $\delta_0$ defined as[8]

$$\delta_0^2 = \frac{(\alpha_1 - \alpha_2)^2 + (\alpha_1 - \alpha_3)^2 + (\alpha_2 - \alpha_3)^2}{2(\alpha_1 + \alpha_2 + \alpha_3)^2} \tag{1}$$

where $\alpha_1$, $\alpha_2$, and $\alpha_3$ are the principal polarizabilities of the scattering element. The overall anisotropy of the chain, $\delta$, is dependent on the chain conformation in addition to $\delta_0$. $\delta$ can be defined as an average of $\delta_0$ for each chain segment over the conformation space. For a wormlike chain with contour length L and persistence length ρ, $\delta$ derived from theory[9] is

$$\delta^2 = \delta_0^2 \left(\frac{2}{3Z}\right) \{1 - \exp(-3Z)\} \tag{2}$$

where $Z = L/\rho$.

For LALS, the equations describing the Rayleigh ratios $R_{Vv}$ and $R_{Hv}$ for the vertical and horizontal components of light scattered in the transverse plane with vertically polarized incident light can be written as[10]

$$\lim_{\theta \to o} [R_V/KMc] = 1 + \frac{4}{5}\delta^2 - 2A_2Mc + O(c^2) \tag{3}$$

$$\lim_{\theta \to o} [R_{HV}/KMc] = \frac{3}{5}\delta^2 + O(c^2) \tag{4}$$

$A_2$ is the second virial coefficient, M is the molecular weight, and c is the solution concentration.
K is an optical constant equal to $4\pi^2 n^2 (dn/dc)^2/\lambda^4 N_A$, where n is the refractive index of the
solvent, $\lambda$ is the wavelength of the laser light, and $N_A$ is Avogadro's number. For a polydisperse
polymer, M obtained from light scattering measurements is the weight-average molecular weight
$(M_w)$.

**Intrinsic Viscosity.** Intrinsic viscosity measurements were determined in MSA at 30.0 ±
0.2°C using a Ubbelohde viscometer. For all dilutions, the flow times were above 110 s and the
kinetic energy correction was considered negligible. Solution concentrations were chosen such
that the flow time ratio of solution to solvent is between 1.1 and 1.5. The Huggins and Kraemer
equations were used to calculate $[\eta]$:

$$\eta_{sp}/c = [\eta] + k'[\eta]^2 c \tag{5}$$

$$\ln \eta_r/c = [\eta] + (k' - 1/2)[\eta]^2 c \tag{6}$$

$\eta_r$ is the flow time ratio between the solution and the solvent, $\eta_{sp} = \eta_r - 1$, and k' is an empirical
constant. Extrapolation of $\ln \eta_r/c$ and $\eta_{sp}/c$ to infinite dilution should result in the same intercept,
which is $[\eta]$.

7

## Results and Discussion

**Polymer Synthesis.** Polymerization of AHBAH at concentrations below 14.5 wt% resulted in solutions that remained optically isotropic in contrast to those of slightly higher concentration that became optically anisotropic at early stages. The effect on the intrinsic viscosity of the resulting polymer by reacting in the nematic phase was pronounced. Comparing ABPBO-2f with ABPBO-5 (see Table II) shows that polymerizing in the isotropic phase results in a substantially lower degree of polymerization (700 vs. 350). When ABPBO was polymerized at a polymer concentration of 13.6 wt%, which is below the critical concentration for formation of the nematic phase (even at a degree of polymerization of 350), the intrinsic viscosity was limited to 9.2 dL/g. On the other hand, an intrinsic viscosity of 18.0 dL/g was obtained when ABPBO was polymerized at 2.9 wt% higher, a concentration at which the nematic phase forms when the polymer reaches an average degree of polymerization of approximately 40. The onset of the nematic phase was determined by the appearance of stir-opalescence in the reaction mixture.

The effect of polymerization temperature can be seen in Figure 2, in which the apparent degree of polymerization as a function of time is plotted for three polymerizations conducted at 200°C, 185°C, and 175°C. Samples of the polymerization mixture were removed at various times and the intrinsic viscosities were measured. In the polymerization conducted at 200°C, the apparent decrease in the degree of polymerization with time may be explained by samples having extensive crystallization that does not fully dissolve during the viscosity measurement. This aggregation phenomenon was observed by Berry[10,11] for the more rigid benzazole polymer PBO and heterocyclic polymer BBL. We saw no evidence of aggregation in the samples analyzed by light scattering techniques, which were all polymerized at 185°C. Even though the polymerization rate is significantly enhanced by heating at 200°C, such an aggregation or crystallization would be expected to be detrimental to subsequent processing, and the optimal temperature for polymerizatio was therefore chosen to be 185°C.

In contrast with a typical polymerization of PBT at 185°C, polymerization of AHBAH occurs

8

over a much longer period (see Figure 2). This observation could be explained by a greater decrease in reactivity with increasing molecular weight because of the difference in molecular rigidity, or by a lower stability of the PBT monomer compared to the carboxyl-stabilized AB monomer. The apparent extent of reaction of the end-capped ABPBZ systems, as discussed below, also appears to be greater than for PBT.

The effect of PPA composition at the end of the polymerization, or final $P_2O_5$ content (P3), on the attainable molecular weight can be seen by comparing those polymerizations having P3 of 82.2% with those having $P_3$ of 83% or higher. Polymerizations with higher $P_2O_5$ contents in general have considerably higher molecular weights. We believe this effect is due to the need to maintain an effective concentration of species that perform functions such as hydrolysis of the water of condensation and activation of the functional groups. An upper limit of about 84% final $P_2O_5$ content was imposed to control solution viscosity and allow for efficient mixing of reactants.

**Effect of End-Capping on Molecular Weight.** Flory's theory[12] for the depression of molecular weight by nonequivalence of functional groups and presence of monofunctional reagents can be used to analyze the results of polycondensation reactions of ABPBT and ABPBO with end-capping agents. The number average degree of polycondensation, $x_n$, is given by

$$x_n = (1 + r)/\{2r\,(1-p) + 1 - r\} \tag{7}$$

where p is the extent of reaction (p = moles of monomer condensed /total moles of monomer), and r = moles of monomer/(moles of monomer + 2 x moles of end-capper). Degree of polymerization can then be calculated for known values of p using eq 7.

By assuming a polydispersity ($M_w/M_n$) of 2 for these ABPBZ polymers, we can calculate the experimental values of $x_n$ from $M_w$ as tabulated in Table III. The data are also plotted in Figure 3. The solid lines in Figure 3 are the theory predictions of $x_n$ as a function of percent end-capping when p = 1.0, 0.998, and 0.990. Comparison between the theoretical and

experimental values of $x_n$ demonstrates that the effect of end-capping can be modeled by Flory's theory for condensation polymerization in spite of the stiff polymer backbone structure by assuming various extents of reaction.

**Polymerization in Mixtures of Methanesulfonic Acid (MSA) and $P_2O_5$.** Three polymerizations of AHBAH were conducted by adding various amounts of $P_2O_5$ to methane-sulfonic acid (MSA) that contained 10 wt% $P_2O_5$. MSA containing 10 wt% $P_2O_5$ has been described as a convenient alternative to PPA.[13] However, we found that greater than 40 wt% $P_2O_5$ was required during the polycondensation if concentrations in the 17-19 wt% region were employed. MSA was heated with 10 wt% $P_2O_5$ for 2 h according to the published procedure. This homogeneous solvent was then used for the dehydrochlorination. The additional $P_2O_5$ was added in a manner analogous to the $P_2O_5$ adjustment of PPA. The results of these polymerizations are summarized in Table IV. Polymerization temperature was limited to 150°C because of decomposition of the solvent at higher temperatures. Attempts to polymerize the more oxidatively sensitive mercapto analog MABAH gave black, nonpolymeric products presumably owing to extensive side reactions.

**Solution Characterization.** The LALS and viscometry data are tabulated in Tables V and VI for ABPBT and ABPBO, respectively. The Mark-Houwink-Sakurada (MHS) constants, K and a, of the empirical relation

$$[\eta] = K M_w^a \tag{8}$$

can be determined by a double-logarithmic plot of $[\eta]$ as a function of weight-average molecular weight ($M_w$) as shown in Figure 4. A least-squares analysis of the experimental results indicates that the MHS relation may be written as:

$$[\eta] = 1.26 \times 10^{-4} M_w{}^{1.00} \qquad \text{for ABPBT} \qquad (9)$$

$$[\eta] = 1.09 \times 10^{-4} M_w{}^{1.02} \qquad \text{for ABPBO} \qquad (10)$$

within the molecular weight range of 2000 to 200,000 daltons.

The MHS exponents are found to be about unity experimentally for both polymers. Their values are between 1.8 for rodlike polymers (such as PBT) and 0.5 for random coil polymers (such as polyethylene) in theta solvent, indicating that this class of poly(benzazoles) is characterized by an intrinsically semirigid structure.

The second virial coefficient, $A_2$, was found to be about 0.01 to 0.02 $cm^3$ $mol/g^2$ for both ABPBZ polymers. Compared with many hydrocarbon polymers in organic solvents,[14] $A_2$ for these protonated, heterocyclic aromatic polymers is one to two orders of magnitude higher, indicating strong polymer/solvent interactions.

We found no evidence of the formation of intermolecular aggregation in these solutions under our experimental conditions, although such an effect appears to be commonly observed in other protonated chains in strong acids.[10,11]


**Model Comparison with Solution Properties.** A wormlike cylinder model has been proposed by Yamakawa and Fujii[15] to evaluate the intrinsic viscosity of stiff chains. The model requires three molecular parameters--contour length L, persistence length $\rho$, and molecular diameter d--to evaluate the intrinsic viscosity $[\eta]$:

$$[\eta] = \Phi (L/\rho)^{3/2} \rho^3/M \qquad (11)$$

$\Phi$ is a function of $(L/\rho)$ and $(d/\rho)$, and M is the molecular weight.

A comparison of the experimental results to the Yamakawa-Fujii model can be made using an iterative scheme by assuming values of $\rho$ and d until the agreement of the theoretical calculations to

the data is acceptable. Alternatively, we estimated $\rho$ and d for these ABPBZ polymers using the independent theoretical guidance described below.

Flory and coworkers have proposed a virtual bond model[16] to evaluate persistence vectors of polymers having catenation angles less than $180°$. If $\gamma$ is the acute angle between consecutive ring axes, $\zeta$ is the angle between the virtual bond and the exocyclic bond, and b is the virtual bond length as shown in Figure 5, then $\rho$ can be estimated as

$$\rho = b \left[ (u + \beta v)/(1 - \alpha) \right] \tag{12}$$

where $\alpha = \cos \gamma$, $\beta = \sin \gamma$, $u = \cos \zeta$, and $v = \sin \zeta$. The values of persistence length estimated by this model should be regarded as upper bound values and have compared favorably with experimental results on p-phenylene polyamides and polyesters.[16]

We estimated $\rho$ for ABPBT and ABPBO based on their molecular geometry such as bond lengths and bond angles taken from x-ray crystallographic results on oriented fibers.[17] For ABPBT, $\gamma = 18°$, $\zeta = 16.2°$, b = 6.08 Å, and $\rho$ is 130 Å. For ABPBO, $\gamma = 30°$, $\zeta = 17°$, b = 5.90 Å, and $\rho$ is 50 Å. ABPBO has a lower value of $\rho$ because of its higher value of $\gamma$.

In addition to $\rho$, d is required to calculate $[\eta]$ from the Yamakawa and Fujii model. We estimated d for the ABPBZ polymers using the orthogonal distance from the extended chain axis to the atom farthest from the axis as illustrated in Figure 5. This estimate yields d = 5.5 Å for ABPBT and 7.5 Å for ABPBO. Table VII summarizes the theoretical estimates of $\rho$ and d. These values can then be used to calculate $[\eta]$ as a function of M according to eq 11 and the numerical values of $\Phi$ given in Ref. 15. The contour length L is determined from $L = M/M_L$, where $M_L$ is a shift factor equal to 21.88 daltons/Å (133 daltons/6.08 Å) for ABPBT and 19.83 daltons/Å (117 daltons/5.90 Å) for ABPBO.

Both the experimental results and theoretical model calculations of $[\eta]$ versus $M_w$ for ABPBT and ABPBO are plotted in Figure 6. The solid line is the wormlike cylinder model prediction using d = 5.5 Å and $\rho$ = 130 Å for ABPBT. Model comparison with the ABPBT

12

experimental data (open diamonds) is very good. The broken line represents the model calculation obtained for ABPBO based on the value of d = 7.5 Å and ρ = 50 Å. In this case, the model fits poorly with the ABPBO results (filled diamonds). This discrepancy can be greatly reduced by increasing ρ from 50 Å to 90 Å for ABPBO as indicated by the dash-dot line.

A number of factors may account for the discrepancy in the value of persistence length estimated by Flory's virtual bond treatment and that determined by fitting the Yamakawa-Fujii model to our experimental results. ABPBZ chains, when dissolved in strong protic acid such as MSA, are protonated and therefore should be described as macroions. Electrostatic interactions among chain elements can affect the dilute solution conformation of the polyelectrolyte molecule to assume a more extended one in equilibrium, thereby increasing the persistence length of the chain.[18-20] In such case ρ may be written as:

$$\rho = \rho_e + \rho_c \tag{13}$$

where $\rho_e$ is the electrostatic contribution and $\rho_c$ is other conformational and steric contribution to the persistence length.

Polydispersity in the molecular weight of our polymer samples may also be a factor to the qualitative difference between theory and experiments. Finally, the excluded volume effect, not accounted for in the Yamakawa-Fujii model, may be another reason for the disagreement.

In Figure 6, the theory predictions show a gradual increase in slope (hence an increase in the value of the HMS exponent) with decreasing $M_w$ for semirigid chains. In contrast, flexible chains have been reported to exhibit a constant HMS exponent over many decades of $M_w$.[21] Because the accuracy of our experimental results does not permit clear differentiation of such slight change in slope, more accurate viscometry and molecular weight measurements over a wider range of molecular weights are needed to confirm this prediction by the wormlike chain model.

Figure 7 plots the LALS results of $\delta^2/\delta_0^2$ versus $L/\rho$. The solid line represents the model calculations using eq 2. The anisotropy factor $\delta^2$ has been normalized by the intrinsic anisotropy

$\delta_o^2$, which was estimated after model comparisons with experimental data were made. Experimentally determined $\delta_o^2$ is 0.84 for ABPBT and 1.10 for ABPBO. The measured molecular weight was first reduced to the contour length L then normalized by the persistence lengths with $\rho = 130$ Å for ABPBT and $\rho = 90$ Å for ABPBO. Comparison of the experimental data with the model prediction is satisfactory. The scatter in the data points is most likely due to the difficulty in obtaining good measurements of $R_{Hv}$.

## Concluding Remarks

Our study indicates that ABPBT and ABPBO are characterized by persistence lengths of 90 to 130 Å, which are in fair agreement with the virtual bond model predictions. This comparison suggests that these extended-chain polymers assume a near random distribution of cis- and trans-conformation, with a slight preference for the trans-conformation due to intramolecular electrostatic interactions, in dilute solution. At concentrations above ~14 wt%, ordered phases form during polymerization, and the trans-conformation is believed to dominate to allow this phase change.

# References

(1)   Wolfe, J. F.; Loo, B. H.; Arnold, F. E.; <u>Macromolecules</u> 1981, <u>14</u>, 915.

(2)   Wolfe, J. F.; Arnold, F. E.; <u>Macromolecules</u> 1981, <u>14</u>, 909.

(3)   Chow, A. W.; Hamlin, R. D.; Sandell, J. F.; Wolfe, J. F.; "Mesophase-Enhanced Polymerization and Chemo-Rheology of Poly(p-phenylenebenzobisthiazole)", <u>Proceedings of the Materials Research Society Meeting</u>, November 1988, in press.

(4)   Wolfe, J. F.; Sybert, P. D.; Sybert, J. R.; US Patent No. 4,533,693, August 1985 (to SRI International).

(5)   Hwang, W.-F.; Wiff, D. R.; Benner, C. L.; Helminiak, T. E.; <u>J. Macromol. Sci., Phys.</u> 1983, <u>B22</u>, 231.

(6)   Jannelli, L.; Giordano-Orsini, P.; <u>Gazz. Chim. Ital.</u> 1958, <u>88</u>, 331.

(7)   Wolfe, J. F.; in <u>Encyclopedia of Polymer Science and Engineering</u>, H. F. Mark; et. al.; Eds., 2nd ed., John Wiley & Sons, New York, Vol. 11, 1988, p. 601.

(8)   Horn, P.; <u>Ann. Phys.</u> 1966, <u>10</u>, 386.

(9)   Nagai, K.; <u>Polym. J.</u> (Tokyo) 1972, <u>3</u>, 67.

(10)  Berry, G. C.; <u>J. Polym. Sci.; Polym. Symp.</u> 1978, <u>65</u>, 143.

(11)  Wong, C.-P.; Ohnuma, H.; Berry, G. C.; <u>J. Polym. Sci.; Polym. Symp.</u> 1978, <u>65</u>, 173.

(12)  Eaton, P. E.; Carlson, G. R.; Lee, J. T.; <u>J. Org. Chem.</u> 1973, <u>38</u>, 4071.

(13)  Flory, P. J.; <u>Principles of Polymer Chemistry</u>, Cornell Universtiy Press, Ithaca, New York. 1953, pp. 92-93.

(14)  Brandrup, J.; Immergut, E. H.; Eds., <u>Polymer Handbook</u>, 2nd ed., John Wiley & Sons, New York, 1975, pp. IV-91.

(15)  Yamakawa, H; Fujii, M.; <u>Macromolecules</u> 1974, <u>7</u>, 128.

(16)  Erman; B.; Flory, P. J.; Hummel, J. P.; <u>Macromolecules</u> 1980, <u>13</u>, 484.

(17) Fratini, A. V.; Cross, E. M.; O'Brien, J. F.; Adams, W. W.; J. Macromol. Sci., Phys. **1985-86**, B24, 159.

(18) Berry, G. C.; "Properties of Solutions of Rodlike Chains from Dilute Solutions to the Nematic State"; Proceedings of the Materials Research Society Meeting, November 1988, in press.

(19) Fixman, M; J. Chem. Phys. **1982**, 76, 6364.

(20) Davis, R. M.; Russel, W. B.; J. Polym. Sci.; Polym. Phys. **1986**, 24, 511.

(21) Fujita, H.; Macromolecules **1988**, 21, 179.

## Figure Captions

**Figure 1.**   Schematic illustration of the coil-like and extended-chain conformations of ABPBO.

**Figure 2.**   Plot of the apparent degree of polymerization as a function of reaction time for ABPBO polycondensation at various reaction temperatures. The polymerization progress of PBT is included for comparison.

**Figure 3.**   Effects of end-capping on the degree of polymerization of ABPBT ($\Diamond$) and ABPBO ($\square$). Solid lines represent predictions of Flory's theory at various extents of reaction, p.

**Figure 4.**   Double logarithmic plots of intrinsic viscosity and molecular weight to determine the Mark-Houwink-Sakurada constants for (a) ABPBT and (b) ABPBO.

**Figure 5.**   Schematic diagram illustrating the determination of molecular parameters needed for the wormlike model calculations.

**Figure 6.**   Comparison of experimental results and model predictions of the Mark-Houwink-Sakurada relationships for ABPBO and ABPBT.

**Figure 7.**   Comparison of experimental results and model predictions of normalized anisotropy factor ($\delta^2/\delta_0^2$) as a function of normalized length ($L/\rho$).
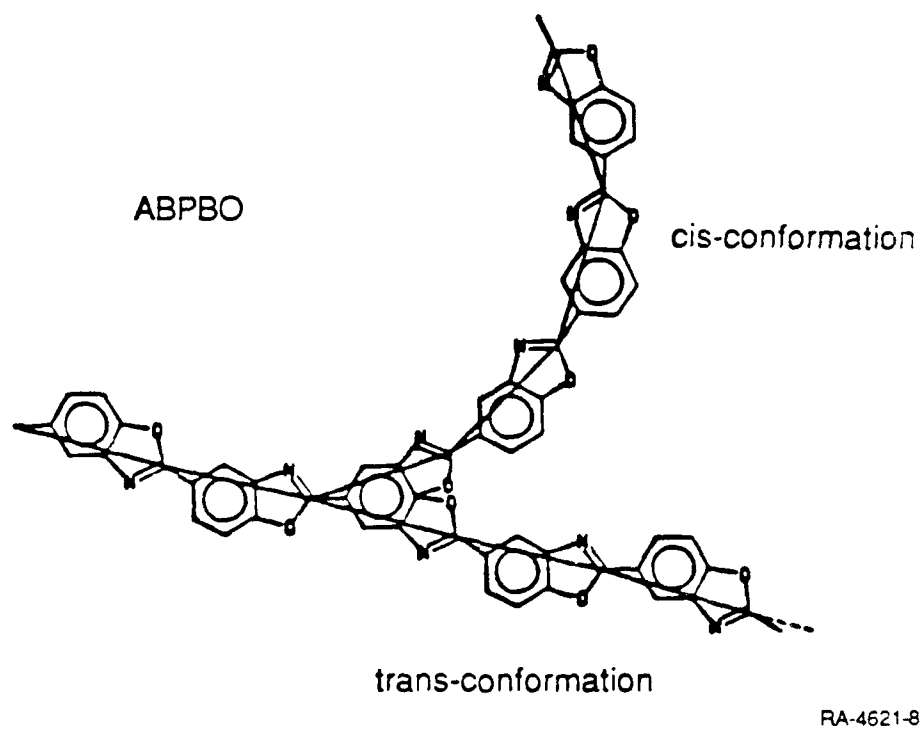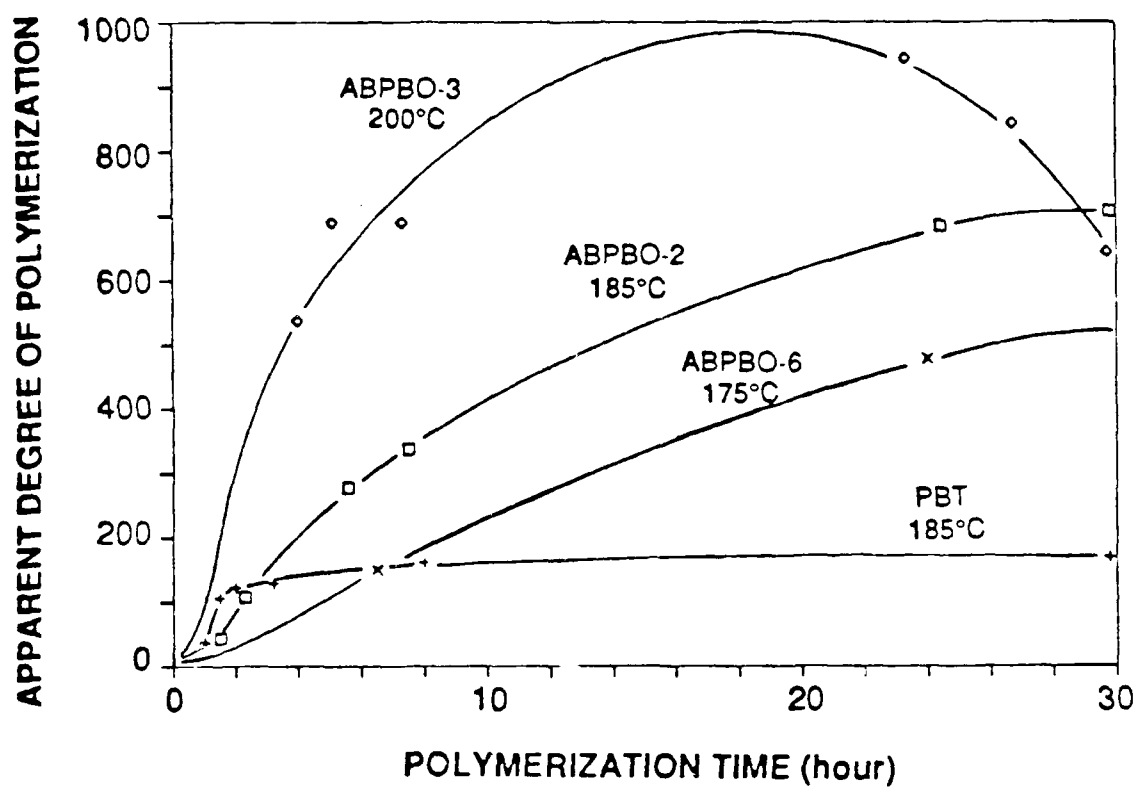
ABPBO
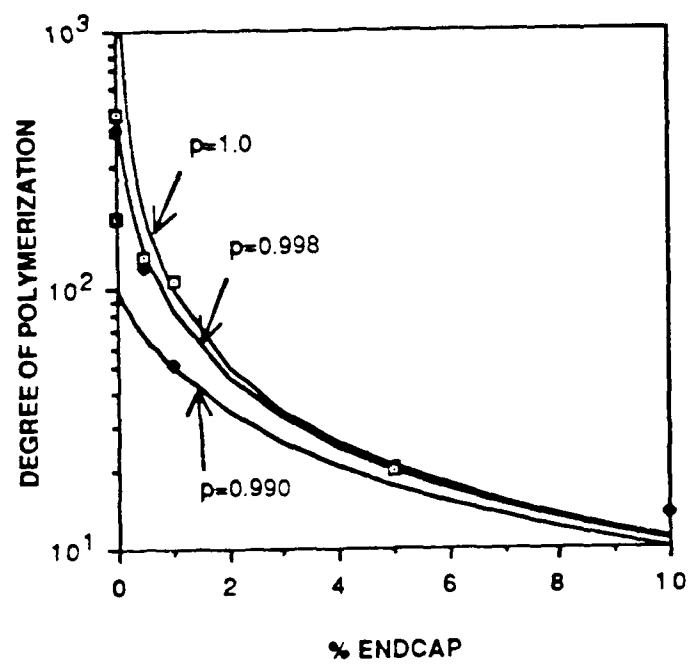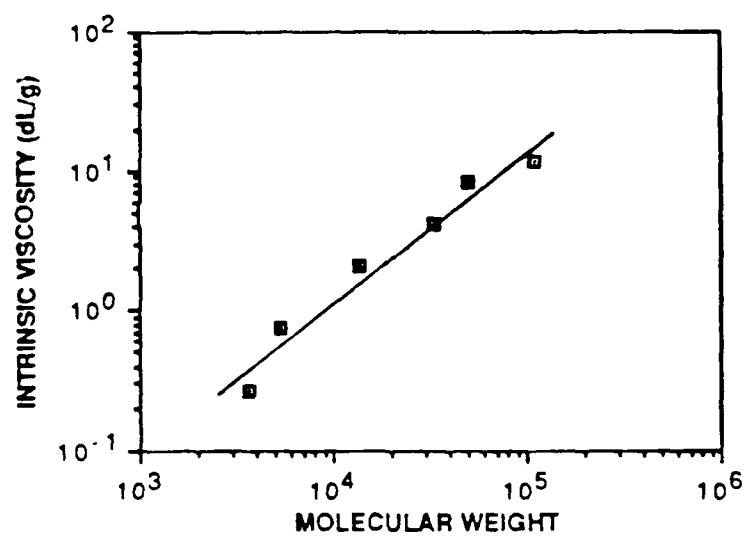
cis-conformation

trans-conformation
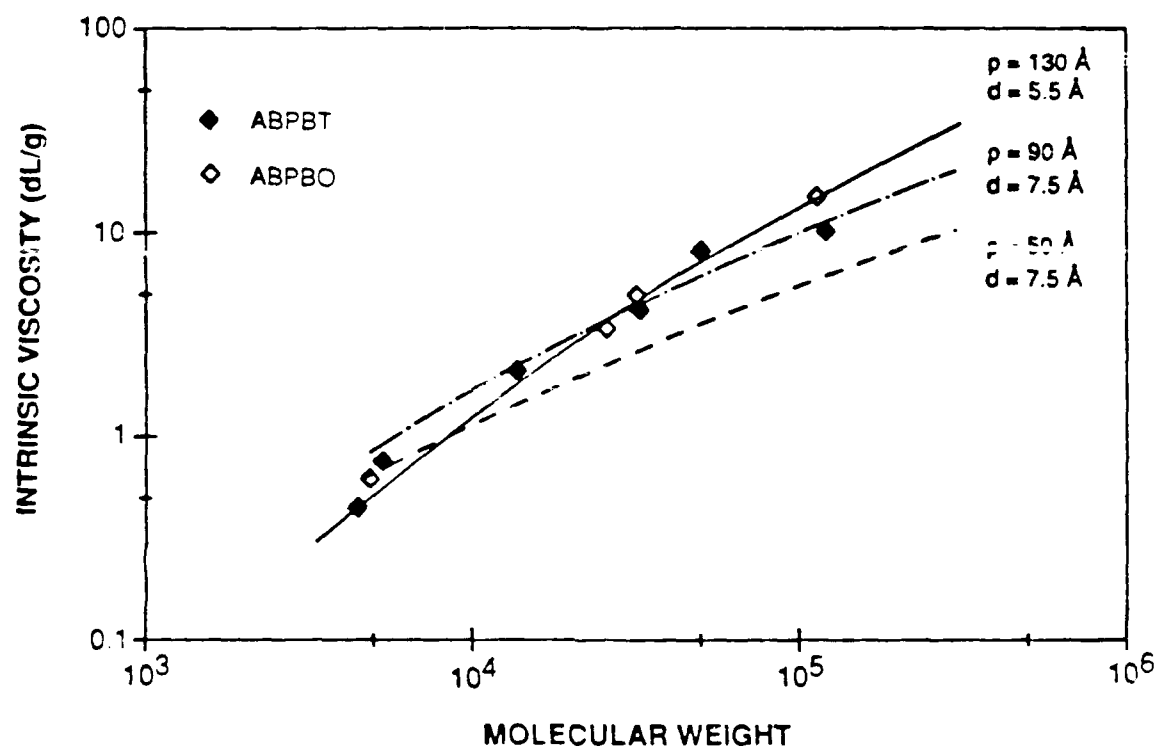
RA-4621-8

Figure 1.

RA-4621-9

Figure 2

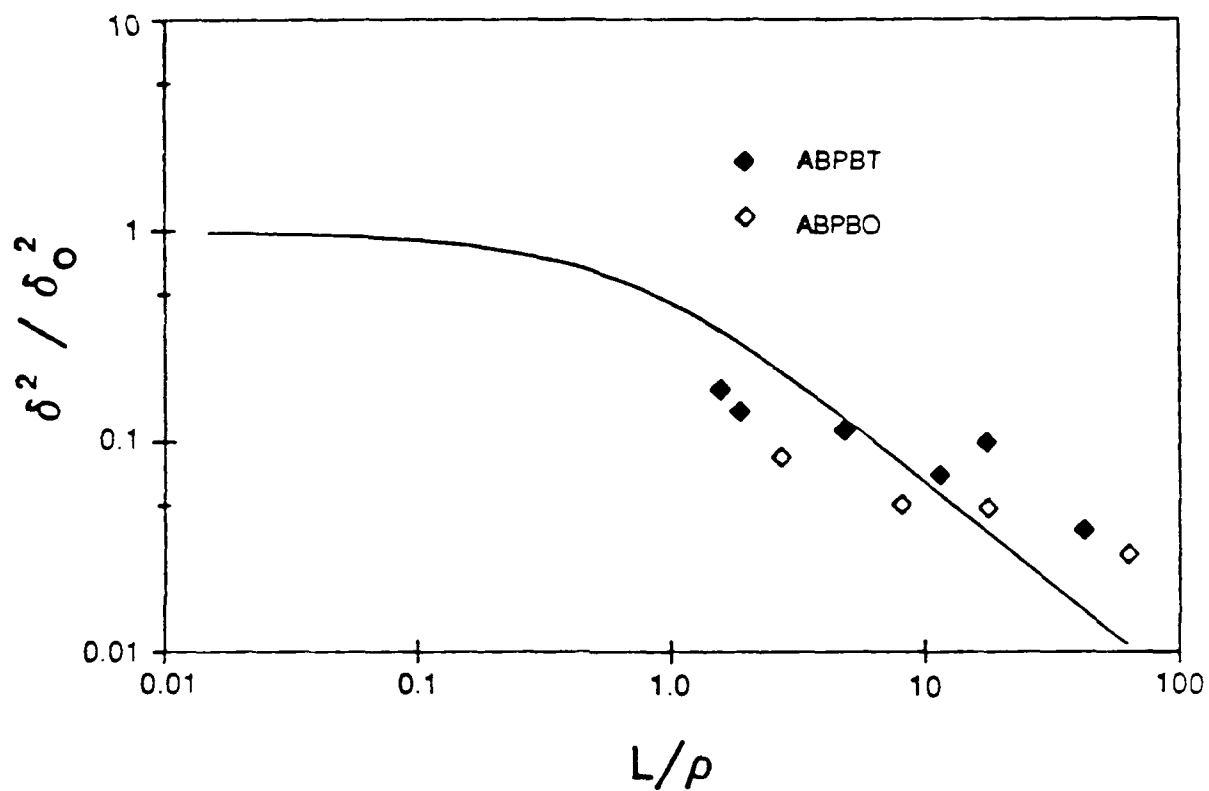RA-4621-10

Figure 3.
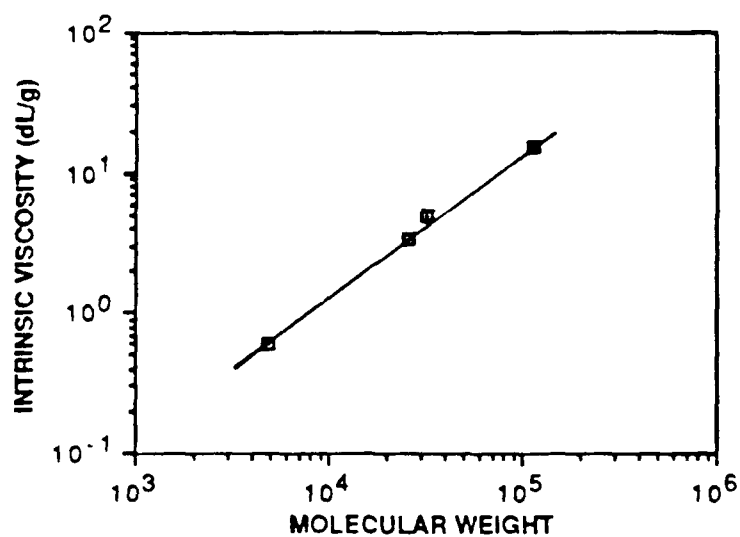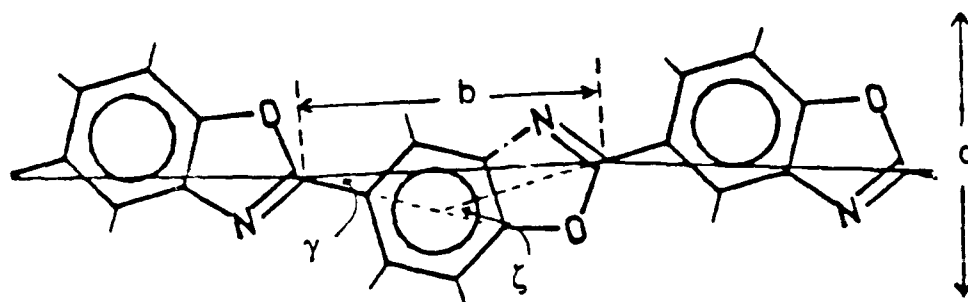
Figure 4.
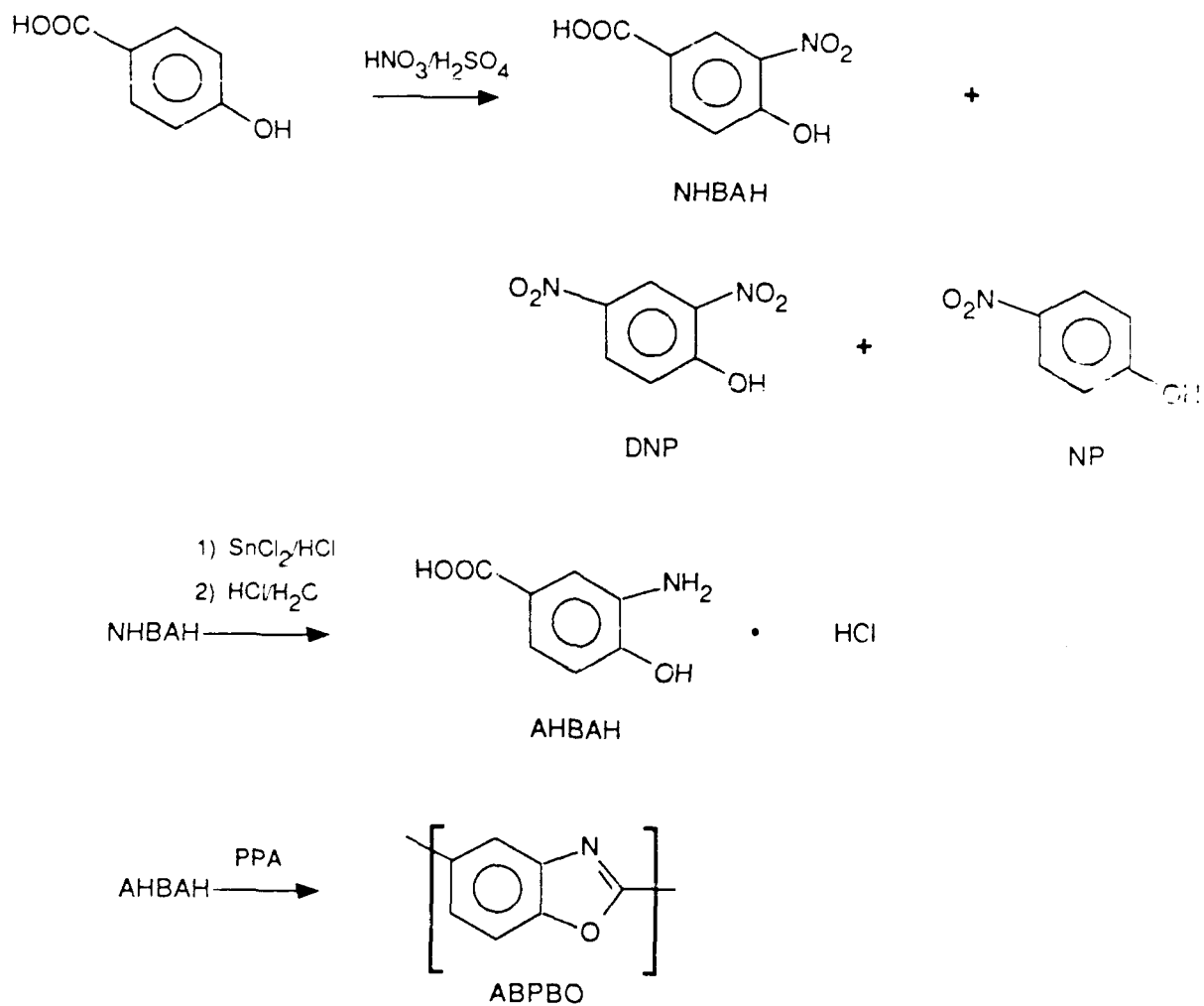
RA-4621-12

Figure 5.

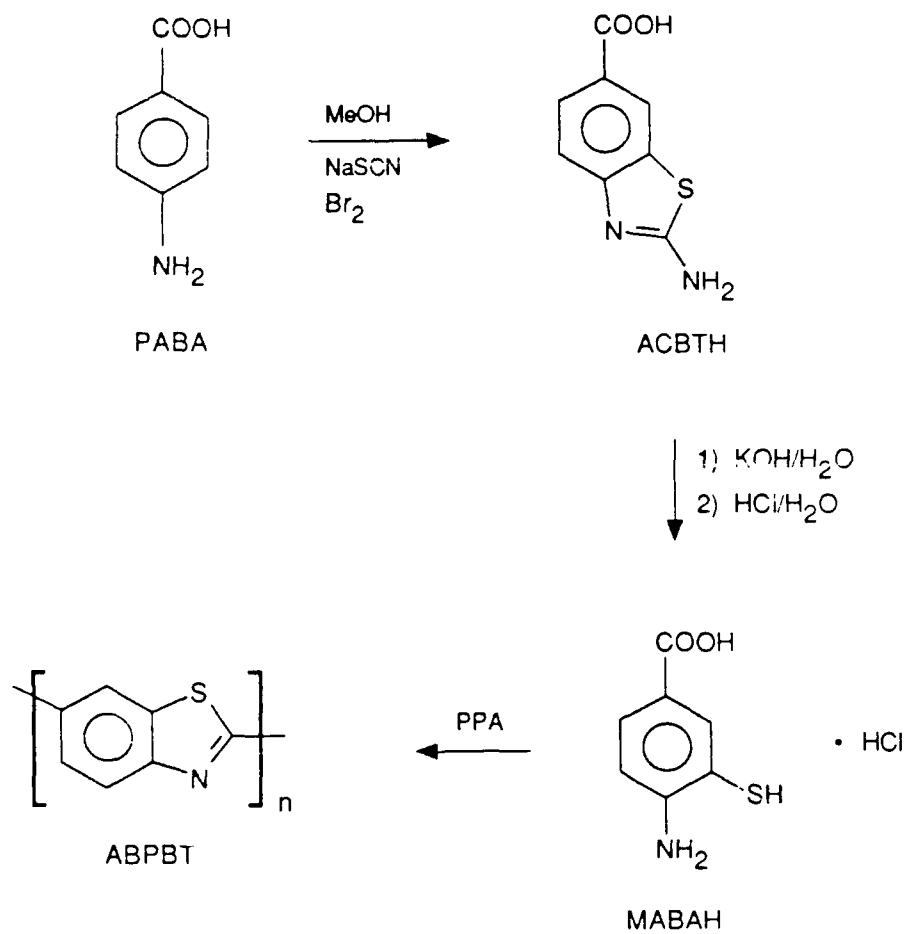Figure 6.

RA-4621-13

Figure 7.

RA-4621-14

RA-4621-17

**SCHEME I ABPBO SYNTHESIS**

RA-M-4621-18

**SCHEME II ABPBT SYNTHESIS**

## Table I

### Polymerizations of MABAH with EC% of Monofunctional Reagent (M = 133.17)

| ABPBT[a] | P1 (%) | P2 (%) | P3 (%) | C (%) | Y (g) | A (g) | B (g) | EC% (%) | PT[e] (h) | [η] (dL/g) |
|---|---|---|---|---|---|---|---|---|---|---|
| -1 | 77.3 | 89.5 | 83.4 | 20.1 | 30.0 | 51.65 | 59.72 | 0 | 48 | 11.5 |
| -2 | 77.3 | 87.5 | 82.3 | 17.9 | 26.55 | 63.32 | 51.34 | 0 | 36 | 8.14 |
| -3 | 77.2 | 86.5 | 82.7 | 13.9 | 10.0 | 35.00 | 24.06 | 0 | 24[f] | 7.55 |
| -4 | 77.0 | 87.9 | 83.0 | 17.0 | 10.0 | 24.3 | 22.0 | 0.5[c] | 21 | 4.18 |
| -5 | 77.0 | 87.9 | 83.0 | 17.0 | 10.0 | 24.3 | 22.0 | 1.0[c] | 21 | 2.11 |
| -6[b] | 77.0 | 87.9 | 83.0 | 17.0 | 10.0 | 24.3 | 22.0 | 5.0[d] | 21 | 0.76 |
| -7[b] | 77.0 | 87.9 | 83.0 | 17.0 | 10.0 | 24.3 | 22.0 | 10.0[d] | 21 | 0.27 |

[a] All polymerization mixtures, which are characterized by PPA having a $P_2O_5$ content between $P_2$ and $P_3$ (depending on the extent of reaction) and polymer concentration and intrinsic viscosity as indicated, were liquid crystalline except those indicated by footnote b (isotropic).

[b] Isotropic.

[c] Benzoic acid was the monofunctional reagent.

[d] Nicotinic acid was the monofunctional reagent.

[e] After removal of hydrogen chloride and addition of B grams of $P_2O_5$ at temperatures below 100°C, all PPA/monomer mixtures were heated within 1 h to 185°C and maintained at that temperature unless otherwise noted.

[f] Heated at 175°C for the time indicated in column PT.

## Table II

### Polymerizations of AHBAH with EC% Benzoic Acid (M = 117.11)

| ABPBO[a] | P1 (%) | P2 (%) | P3 (%) | C (%) | Y (g) | A (g) | B (g) | EC%[d] (%) | PT[e] (h) | [η] (dL/g) |
|---|---|---|---|---|---|---|---|---|---|---|
| -1 | 77.3 | 87.85 | 82.2 | 17.3 | 10.2 | 24.4 | 21.28 | 0 | 28 | 15.0 |
| -2a[b] | 77.2 | 88.4 | 83.0 | 16.5 | 10.0 | 26.65 | 25.55 | 0 | 1.5 | 1.1 |
| -2b[b] | | | | | | | | | 2.3 | 2.8 |
| -2c[b] | | | | | | | | | 5.6 | 7.1 |
| -2d[b] | | | | | | | | | 7.5 | 8.6 |
| -2e[b] | | | | | | | | | 24.5 | 17.4 |
| -2f[b] | | | | | | | | | 29.8 | 18.0 |
| -3a[b] | 77.2 | 88.4 | 83.0 | 16.5 | 8.0 | 19.37 | 18.74 | 0 | 4.0[f] | 13.7 |
| -3b[b] | | | | | | | | | 5.1[f] | 17.6 |
| -3c[b] | | | | | | | | | 7.3[f] | 17.6 |
| -3d[b] | | | | | | | | | 23.3[f] | 24.1 |
| -3e[b] | | | | | | | | | 26.7[f] | 21.5 |
| -3f[b] | | | | | | | | | 29.7[f] | 16.4 |
| -4 | 77.6 | 87.5 | 82.2 | 16.7 | 17.8 | 28.65 | 22.82 | 0 | 40 | 13.8 |
| -5[c,d] | 77.2 | 86.6 | 83.0 | 13.6 | 10.0 | 41.24 | 29.23 | 0 | 29.5 | 9.2 |
| -6a | 77.3 | 87.4 | 83.02 | 13.9 | 10.0 | 32.59 | 25.96 | 0 | 6.5[g] | 3.85 |
| -6b | | | | | | | | | 24.0[g] | 12.7 |
| -7 | 73.9 | 89.7 | 83.6 | 17.0 | 10.0 | 17.56 | 27.1 | 0.5 | 20.0 | 4.95 |
| -8 | 73.9 | 89.7 | 83.6 | 17.0 | 10.0 | 17.56 | 27.2 | 1.0 | 18.0 | 3.39 |
| -9[c] | 78.0 | 91.0 | 85.0 | 16.0 | 11.49 | 22.45 | 31.1 | 5.0 | 25.0 | 0.62 |

[a] All polymerization mixtures, which are characterized by PPA having a $P_2O_5$ content between P2 and P3 (depending on the extent of reaction) and polymer concentration and intrinsic viscosity as indicated, were liquid crystalline except those indicated by footnote c (isotropic).

[b] The same monomer sample was used for these polymerizations.

[c] Isotropic.

[d] Benzoic acid was the monofunctional reagent.

[e] After removal of hydrogen chloride and addition of B grams of $P_2O_5$ at temperatures below 100°C, all PPA/monomer mixtures were heated within 1 h to 185°C and maintained at that temperature unless otherwise noted.

[f] ABPBO-3a-f were heated at 200°C for the time indicated in column PT.

[g] ABPBO-6a and -6b were heated at 175°C for the time indicated in column PT. Both samples were optically isotropic at 175°C but were birefringent at room temperature.

## Table III

**Experimental Results and Theoretical Calculations
of the Effects of End-Capping on Molecular Weight**

| | Experimental | | | Theoretical $x_n$ | | |
| | % End-cap | $M_w$ | $x_n$ | p = 1.00 | p = 0.998 | p = 0.990 |
|---|---|---|---|---|---|---|
| ABPBΓ | | | | | | |
| 5350-24 | 0.0 | 111,000 | 415.4 | ∞ | 500.0 | 100 |
| 5350-43 | 0.0 | 50,000 | 188.0 | ∞ | 500.0 | 100 |
| 7266-8 | 0.5 | 33,100 | 123.1 | 201 | 143.6 | 67.0 |
| 7266-7 | 1.0 | 13,700 | 51.7 | 101 | 84.2 | 50.5 |
| 7266-12 | 5.0 | 5,300 | 20.1 | 21 | 20.2 | 17.5 |
| 7266-11 | 10.0 | 3,600 | 13.4 | 11 | 10.8 | 10.0 |
| ABP30 | | | | | | |
| 27 | 0.0 | 113,000 | 474.4 | ∞ | 500.0 | 100 |
| 7266-5 | 0.5 | 32,000 | 133.6 | 201 | 143.6 | 67.0 |
| 7266-3 | 1.0 | 26,000 | 108.4 | 101 | 84.2 | 50.5 |
| 7615-22 | 5.0 | 4,900 | 20.5 | 11 | 20.2 | 17.5 |

## Table IV

### Polymerizations of AHBAH in MSA/P$_2$O$_5$ Mixtures

| ABPBO | C (%) | Y (g) | MSA-P$_2$O$_5$[a] (g) | P$_2$O$_5$ (g) | Total P$_2$O$_5$ (%) | PT[b] (h) | $[\eta]$ (dL/g) |
|---|---|---|---|---|---|---|---|
| -10 | 17.5 | 15.0 | 38.36 | 27.65 | 44.6 | 49 | 16.0 |
| -11 | 17.6 | 15.0 | 44.60 | 20.89 | 35.7 | 46 | 4.75 |
| -12 | 19.0 | 18.0 | 47.36 | 16.60 | 30.2 | 24 | <1 |

[a] 10 wt% P$_2$O$_5$ dissolved in MSA by stirring for 2 h.

[b] Length of time that the monomer/MSA/P$_2$O$_5$ mixture was heated at 150°C.

## Table V

### Light Scattering and Intrinsic Viscosity
### Measurements for ABPBT Solutions

| Sample | % End-cap | $M_w$ (daltons) | $\langle \rangle^2$ | $A_2$ | $[\eta]$ (dL/g) |
|--------|-----------|-----------------|----------|-------|-----------------|
| 5350-24 | 0.0 | 111,000 | 0.028 | 0.0101 | 11.5 |
| 5350-43 | 0.0 | 50,000 | 0.083 | 0.0231 | 8.14 |
| 7266-8 | 0.5 | 33,000 | 0.058 | 0.0099 | 4.18 |
| 7266-7 | 1.0 | 13,700 | 0.095 | 0.0107 | 2.11 |
| 7266-12 | 5.0 | 5,300 | 0.117 | 0.0212 | 0.758 |
| 7266-11 | 10.0 | 3,600 | 0.124 | 0.0251 | 0.272 |

## Table VI

### Light Scattering and Intrinsic Viscosity
### Measurements for AEPBO Solutions

| Sample | % End-cap | Mw (daltons) | $\delta^2$ | $A_2$ | $[\eta]$ (dL/g) |
|--------|-----------|--------------|------------|-------|------------------|
| -27 | 0.0 | 113,000 | 0.032 | 0.0078 | 15.0 |
| 7266-5 | 0.5 | 32,000 | 0.052 | 0.0094 | 4.95 |
| 7266-3 | 1.0 | 26,000 | 0.067 | 0.0125 | 3.39 |
| 7615-22 | 5.0 | 4,900 | 0.092 | 0.0247 | 0.618 |

## Table VII

### Molecular Parameters for ABPBT and ABPBO Molecules

| Molecular Paramater | ABPBT | ABPBO |
|---|---|---|
| $\Gamma$ | 18° | 30° |
| $\gamma$ | 16.2° | 17.0° |
| b | 6.08Å | 5.90 Å |
| $\rho$ | 130 Å | 50 Å |
| d | 5.5 Å | 7.5 Å |

Appendix E

MESOPHASE-ENHANCED POLYMERIZATION AND CHEMO-RHEOLOGY
OF POLY(p-PHENYLENEBENZOBISTHIAZOLE)

# MESOPHASE-ENHANCED POLYMERIZATION AND CHEMO-RHEOLOGY OF POLY(p-PHENYLENEBENZOBISTHIAZOLE)

ANDREA W. CHOW, RICHARD D. HAMLIN, JANET F. SANDELL,
AND JAMES F. WOLFE*
SRI International, 333 Ravenswood Avenue, Menlo Park, CA 94025
*Present Address: Lockheed Missiles & Space Co., 3251 Hanover St., Palo Alto, CA 94304

## ABSTRACT

The phenomenon of mesophase-enhanced polymerization of the rodlike polymer poly(p-phenylenebenzobisthiazole) in polyphosphoric acid was investigated. When the polymer concentration was greater than 5 wt%, the reacting mixture became anisotropic at an early stage of the polymerization. The reaction rate increased significantly at the isotropic-nematic phase transition as the rods were aligned in positions more favorable for the condensation reaction to occur. At 4.5 wt% of polymer, the reacting mixture remained isotropic for up to 1500 min of reaction time. The chemo-rheological properties of the 15 wt% reaction mixture indicate the occurrence of the phase change in either the shear viscosity or the first normal stress difference measurements.

## INTRODUCTION

Initial research on the synthesis of rigid rod polymer poly(p-phenylenebenzo-[1,2-d:4,5-d']bisthiazole) (PBT) was conducted in polyphosphoric acid (PPA) at concentrations below 3 wt% of polymers to avoid the extremely high shear viscosity of the reacting mixtures. Such reaction mixtures remained isotropic throughout the polymerization. The maximum attainable molecular weight was low, and the polymer had to be isolated and redissolved at a higher concentration for fiber processing. The practical need for higher efficiency motivated attempts to polymerize at higher concentrations. At greater than 5 wt%, liquid crystalline domains were formed during the polymerization of PBT, and the reacting mixture remained tractable. The reaction kinetics and final attainable molecular weight were greatly enhanced when the reaction medium became anisotropic. We call this phenomenon mesophase-enhanced polymerization (MEP).

In this paper, we describe a quantitative study of MEP of PBT polycondensation at concentrations near and above 5 wt%. The chemo-rheological properties of the reacting mixtures, under conditions that cause the liquid crystalline phase transition to occur during polymerization, are also reported. The effects of phase change and shear rate are discussed.

## SYNTHESIS OF PBT

The synthesis of PBT, reported in detail previously [1], is typically performed by the condensation of 2,5-diamino-1,4-benzenedithiol dihydrochloride (DABDT) and terephthalic acid (TA) in PPA following the removal of hydrogen chloride:
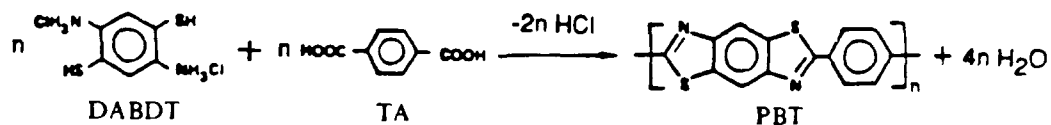


In this reaction, PPA serves as a solvent, catalyst, and dehydrating agent. Hydrogen chloride is first completely removed from the reaction mixture of DABDT in PPA before the addition of 10μm TA particles. Solid $P_2O_5$ is then added according to the $P_2O_5$ adjustment method [2] to ensure adequate reaction conditions for a high degree of polymerization. After being stirred at 90°C for sufficient time to dissolve the solids, the mixture of monomers, PPA, and $P_2O_5$ is ready for polymerization at temperatures above 150°C.

# REACTION KINETICS

The polymerization temperature profile used for this study was as follows: the monomer mixture was first heated from 90° to 180°C at a rate of 0.75°C/min, and the temperature was maintained at 180°C throughout the polymerization. During polymerization, small aliquots of the reation mixture were removed periodically from the reactor to analyze the progress of polymerization. The removed aliquot was precipitated in deionized water and the residual PPA was thoroughly removed by extraction with water in a Soxhlet apparatus. The polymer was completely dried under reduced pressure at >130°C overnight.

The weight-average molecular weight, $M_w$, of PBT was determined by measuring the intrinsic viscosity of the polymer and using the Mark-Houwink-Sakurada relationship [3]. The solutions for intrinsic viscosity measurements were prepared by dissolving dried PBT in freshly distilled methanesulfonic acid (MSA), and they were analyzed at 30.0°C using an automated Cannon-Ubbelohde microdilution viscometer.

We examined the reaction kinetics at three polymer concentrations: 15 wt%, 5.0 wt%, and 4.5 wt%. Figure 1 shows the change in the intrinsic viscosity as a function of reaction time of 15 Wt% PBT in PPA. The broken line shows the temperature profile throughout the reaction starting from 150°C. The intrinsic viscosity can be converted to the degree of polymerization $(x_n)$ through $M_w$. Figure 2 plots $x_n$ as a function of reaction time.
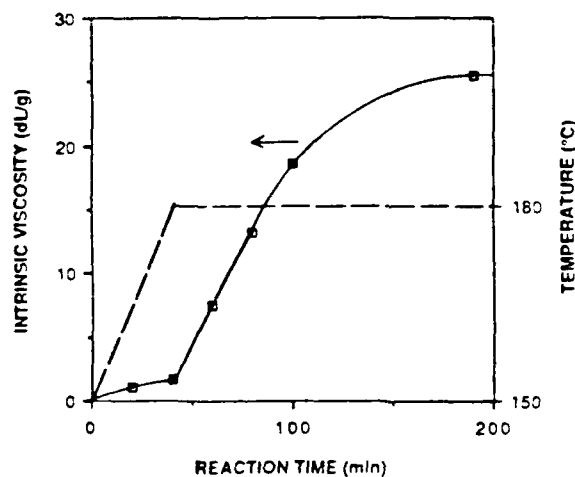


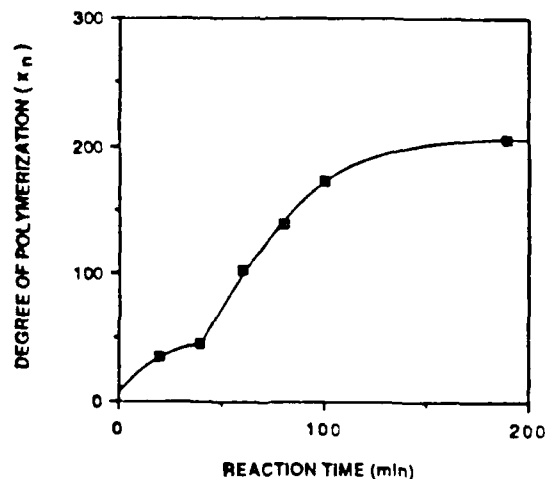Figure 1 Increase in polymer intrinsic viscosity during polycondensation of 15 wt% PBT in PPA.



Figure 2 Degree of polymerization as a function of reaction time for polycondensation of 15 wt% PBT in PPA.

The salient feature of Figures 1 and 2 is the sharp increase in the intrinsic viscosity and $x_n$ at about 40 min ($t_1$) after time t = 0 at 150°C. The slope of the curve immediately following $t_1$ increases significantly. Figure 3 shows the rate of polymerization, $d(x_n)/dt$, which is calculated from the slope of the curve in Figure 2 at the midpoint between data points. More than a five-fold increase in the polymerization rate is observed at the transition. In contrast, polycondensation of poly(p-phenylenebenzobisoxazole) (PBO) at low concentrations (below 2 wt%) exhibits a decreasing rate of polymerization throughout the entire reaction [4]
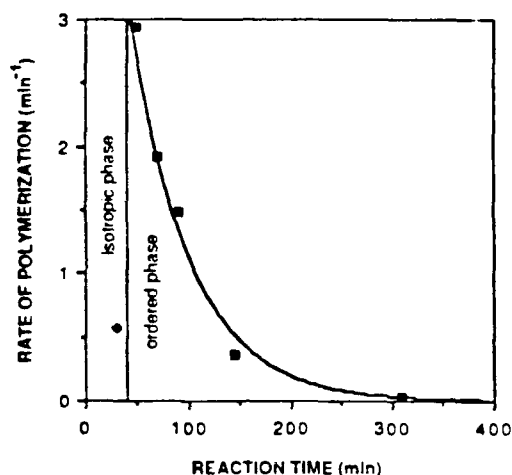


**Figure 3** Rate of polymerization as a function of reaction time for polycondensation of 15 wt% PBT in PPA.

Direct observation indicates that, at the same time that the kinetic rate increases abruptly, the reacting dope becomes stir-opalescent, indicating the onset of anisotopy in the dope. The abrupt increase in the reaction rate is therefore interpreted as a quantitative description of MEP by which the enhancement in kinetics is due to the alignment of rigid rods in the ordered phase.

It is coincidental that $t_1$ appears very close to the point at which the temperature reaches 180°C. The observed change in the reaction kinetics at $t_1$, however, is unlikely to be due to the increase in temperature because previous study on polycondensation of PBO in the isotropic phase does not indicate any discontinuous change in the polymerization rate with temperature from 150 to 185°C.

The polymer molecular weight at which the phase transition occurs can be compared with theoretical predictions using Flory's statistical mechanical model for athermal systems [5]. The model predicts that $\phi_c$, the critical volume fraction of rodlike solute at which phase separation first occurs, is related to the axial ratio (y) of monodisperse rods by:

$$\phi_c = (8/y)\,(1 - 2/y) \tag{1}$$

For 15 wt% PBT, the specific gravity of PBT is about 1.5 and that of PPA is 2.0, $\phi_c$ is therefore 0.19 and y is 40 according to Eq. (1). Experimentally, we observed a phase change when $x_n$ = 45 or y = 40, which compares favorably with the theoretical value.

From previous studies, we observed that the transition from isotropic to anisotropic polymerization occurs at ~5 wt% for PBT. To further investigate the phenomenon of MEP, we examined the reaction kinetics of PBT polymerization near 5 wt% Figure 4 plots the increase in intrinsic viscosity of PBT with reaction time for 5.0 and 4.5 wt% PBT polycondensation. We found that the 5.0-wt% dope became anisotropic whereas the 4.5-wt% dope was isotropic up to 1500 min of reaction time. An increase in the kinetics was measured for the 5.0 wt% solution at the same time the solution became stir-opalescent. We performed duplicate measurements for the intrinsic viscosity of the polymer samples removed near the phase transition to ensure the accuracy of the kinetic curve. The axial ratio (y) of PBT at the phase transition is calculated to
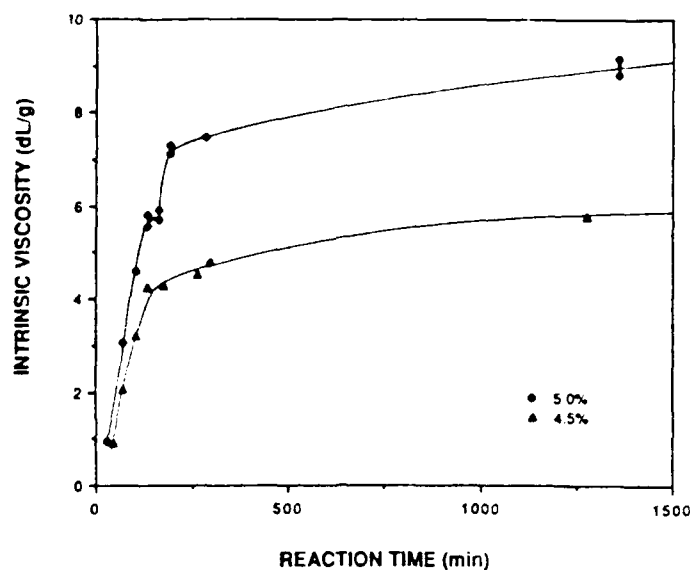
Figure 4  Increase in polymer intrinsic viscosity during polycondensation of 5.0 and 4.5 wt% PBT in PPA.
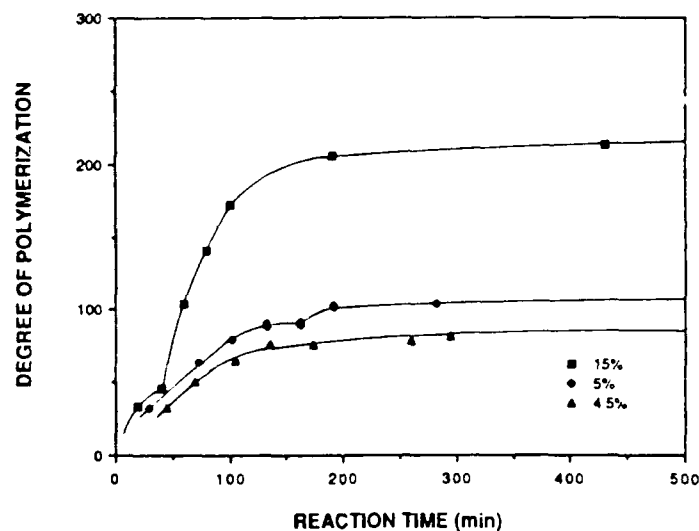


Figure 5  Degree of polymerization as a function of reaction time for polycondensation of 15, 5.0 and 4.5 wt% PBT in PPA.

be 81 based on the intrinsic viscosity results. On the other hand, the Flory model predicts that the transition occurs when y = 120 at 5 wt% (6.56 vol%). The agreement between experimental and theoretical values is only fair. Figure 5, a plot of $x_n$ versus reaction time, summarizes the reaction kinetics for all three concentrations.

CHEMO-RHEOLOGICAL PROPERTIES

The rheological behavior of lyotropic, rigid rod polymers near the isotropic-nematic phase transition has been a subject for numerous theoretical as well as experimental investigations [6]. In many studies, the shear viscosity is measured as a function of concentration at a fixed molecular weight and temperature. The viscosity shows the characteristic shape of first increasing with concentration, reaching a maximum near the phase transition, and decreasing in the nematic phase region at higher concentrations.

In the PBT polymerization, the volume fraction of rods stays constant while the molecular weight and the temperature vary with time. The shear viscosity of the 15 wt% reacting media, monitored by a Rheometrics mechanical spectrometer in cone-and-plate geometry, is shown in Figure 6 for shear rates of 1, 5, 10, and 10 s$^{-1}$. Figure 7 shows the corresponding plots of the first normal stress difference at these shear rates during polymerization. The temperature profile in these experiments follows that in the kinetic study described in the previous section: an increase of 0.75°C/min from 90 to 180°C, followed by a hold at 180°C throughout the remaining time of the reaction.

The resulting reaction mixtures polymerized at these four shear rates were liquid crystalline after 300 min. To our surprise, the viscosity data at low shear rates (1 and 5 s$^{-1}$) provide little indication of the isotropic-nematic phase transition. At higher shear rates (10 and 50 s$^{-1}$), a slight break in slope of the viscosity function near 40 to 50 min is observed. This break is very close to, and therefore suspected to be related to, the phase transition observed in the kinetic study. On the other hand, the normal stress shows a discontinuity near the phase transition at low shear but not at high shear rates.

At high shear rates, we observe an onset of flow instability in the liquid crystalline phase. Both the viscosity and normal stress functions show nonperiodic fluctuations. Such behavior does not occur at lower shear rates or in the isotropic phase at high shear rates.

## CONCLUSIONS

This study demonstrates quantitatively the enhancement in the polymerization kinetics of PBT when ordered domains form in the polymerizing solution. In polycondensation of rigid rod polymers, the two reactive chains have to be adjacent and colinear axially before the condensation reaction can take place. In the ordered phase, the molecules are already aligned in positions favorable for condensation, the polymerization rate therefore increases over that in the isotropic phase. The degree of enhancement in the reaction kinetics and final polymer molecular weight is dependent on the polymer concentration.

## ACKNOWLEDGEMENT

## REFERENCES

1.    J. F. Wolfe, B. H. Loo, and F. E. Arnold, Macromolecules, 4, 915 (1981).

2.    J. F. Wolfe, in Encyclopedia of Polymer Science and Engineering, edited by H. F. Mark, et al., 2nd ed., Vol. 11, (John Wiley & Sons, New York, 1988), pp. 601.

3.    G. C. Berry, P. C. Metzger, S. Venkatraman, and D. B. Cotts, Am. Chem. Soc., Div. Polym. Chem., 20, 42 (1979).

4.    D. B. Cotts and G. C. Berry, Macromolecules, 4, 930 (1981).

5.    P. J. Flory, Proc. R. Soc., London (A), 234, 73 (1956).
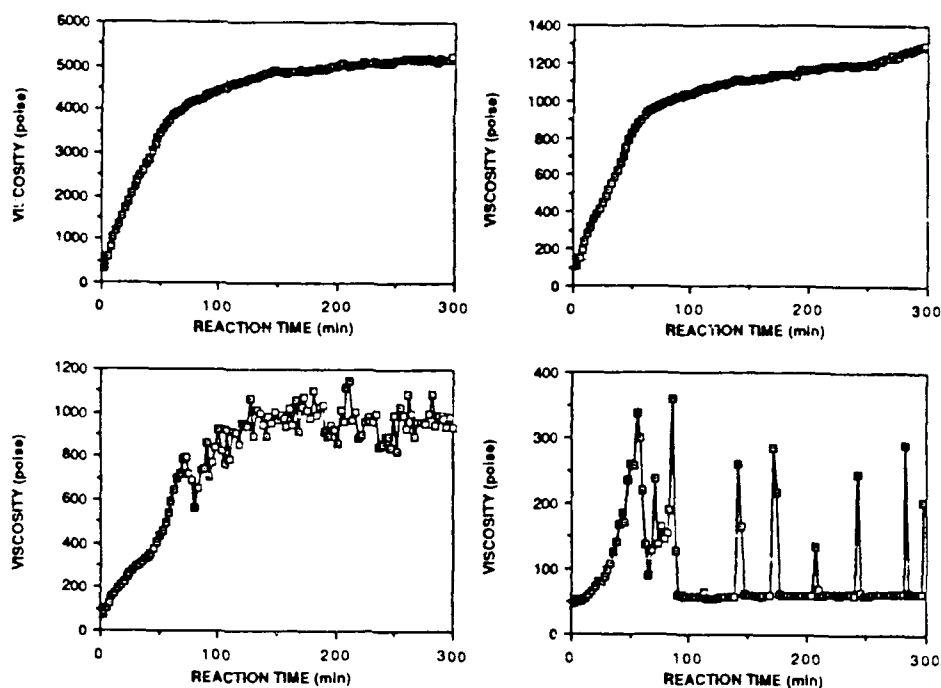
6.    K. F. Wissbrun, J. Rheol., 25, 619 (1981).

Figure 6  Shear viscosity versus reaction time during polymerization of 15 wt% PBT in PPA at shear rates of 1.0, 5.0, 10 and 50 s$^{-1}$.
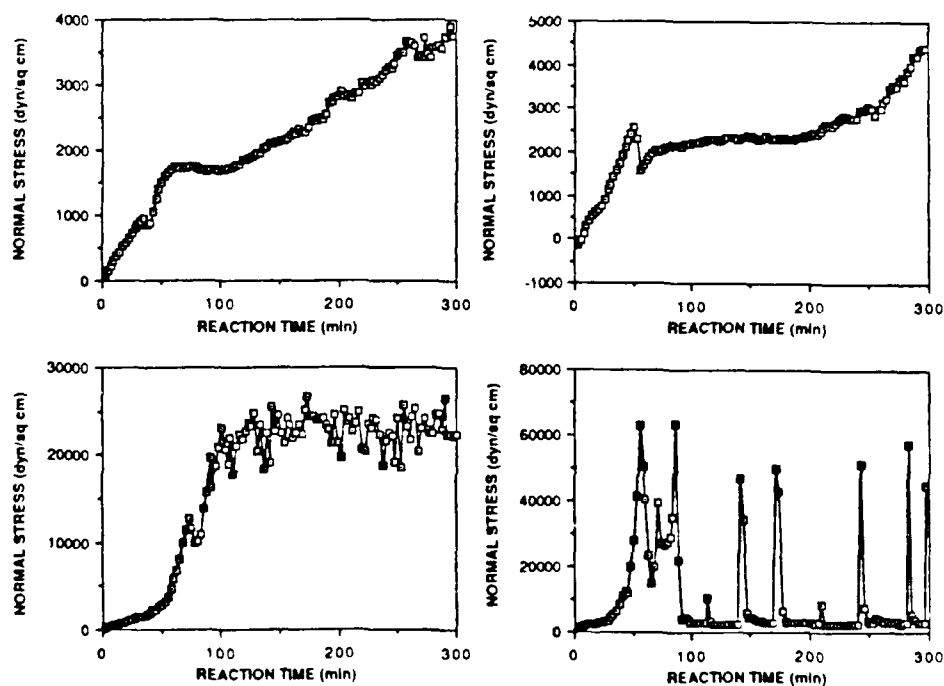


Figure 7  First normal stress difference versus reaction time during polymerization of 15 wt% PBT in PPA at shear rates of 1.0, 5.0, 10 and 50 s$^{-1}$.

Appendix F

SYNTHESIS AND DILUTE SOLUTION CHARACTERIZATION OF
EXTENDED-CHAIN POLY(BENZAZOLES)

# SYNTHESIS AND DILUTE SOLUTION CHARACTERIZATION OF EXTENDED CHAIN POLY(BENZAZOLES)

ANDREA W. CHOW, STEVEN P. BITLER, PAUL E. PENWELL,
AND JAMES F. WOLFE*
SRI International, 333 Ravenswood Avenue, Menlo Park, CA 94025
*Present Address: Lockheed Missiles & Space Co., 3251 Hanover St., Palo Alto, CA 94304

## ABSTRACT

This paper reports the synthesis method for polymerizaing poly(2,6-benzothiazole) (ABPBT) and poly(2,5-benzoxazole) (ABPBO), and their dilute solution porperties using low angle light scattering and viscometry. Our data indicate that the Mark-Houwink-Sakurada exponents for these extended-chain polymers are near unity, suggesting a semi-rigid conformation in dilute solutions. The solution properties agree well with the Yamakawa-Fujii worm-like chain model when persistence lengths of 130 Å and 90 Å are assumed for ABPBT and ABPBO, respectively. These values of persistence length are also in good agreement with those predicted by Flory's virtual bond model using information on the molecular geometries taken from x-ray crystallographic data on oriented fibers of ABPBT and ABPBO.

## INTRODUCTION

Poly(2,6-benzothiazole) (ABPBT) and poly(2,5-benzoxazole) (ABPBO) belong to a class of rigid, aromatic, heterocyclic polymers characterized by high thermal stability and solubility only in strong acids. The catenation angle, which is the angle between exocyclic bonds of the rigid backbone units, is 162° for ABPBT and 150° for ABPBO.



ABPBT          ABPBO
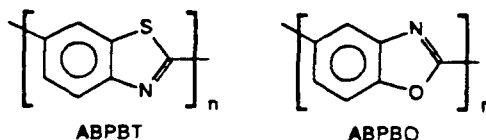
Because of the unrestricted rotation between repeat units [1], these backbone diads can assume either an extended chain conformation (trans) or a coil-like conformation (cis) as illustrated in Figure 1.
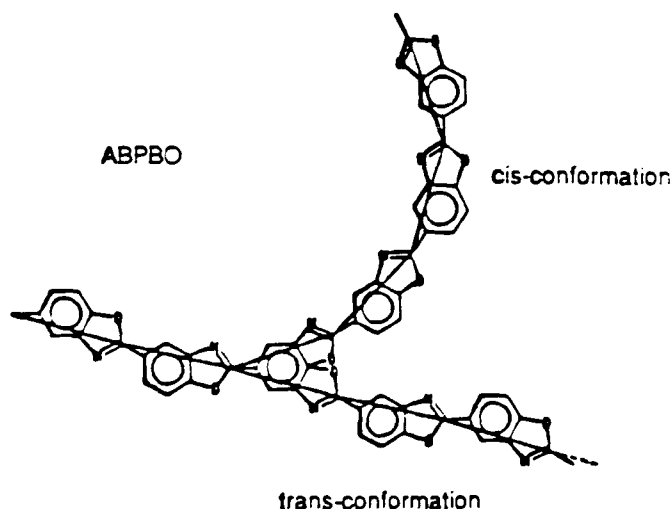


Figure 1  Schematic illustration of the coil-like and extended chain conformations of ABPBO.

# POLYMER SYNTHESIS

While developing the synthesis methods for preparing rigid rod poly(benzazoles) in poly(phosphoric acid) (PPA), we discovered that polymerization proceeded at polymer concentrations as high as 21 % by weight if the $P_2O_5$ content of PPA was increased sufficiently to acccount for the water of condensation.[2] The ability to polymerize at such high concentrations led to the discovery that less than rigid ABPBT and ABPBO also form ordered phases during polymerization. Anisotropic solutions can be obtained from the polymerization when the polymer concentration is greater than ~14 wt%. This critical concentration is about 3 times higher than that required for polymerizing anisotopic solutions of rigid rod poly(benzazoles) such as poly(p-phenylenebenzobisthiazole) (PBT). When polymerized in the ordered phases, we found that both the reaction kinetics and the molecular weight of the final polymers could be enhanced significantly.[3]

## Monomer Synthesis

The monomer for ABPBO, 3-amino-4-hydroxybenzoic acid hydrochloride (AHBAH) was prepared in two steps from p-hydroxybenzoic acid [4], by nitration with one equivalent of nitric acid in sulfuric acid at low temperature followed by reduction with stannous chloride and hydrochloric acid, as illustrated in Scheme I. The monomer for ABPBT, 3-mercapto-4-aminobenzoic acid hydrochloride (MABAH) was prepared in two steps from p-aminobenzoic acid (PABA), as illustrated in Scheme II. Detailed experimental conditions for preparing these monomers can be found in Reference 5.
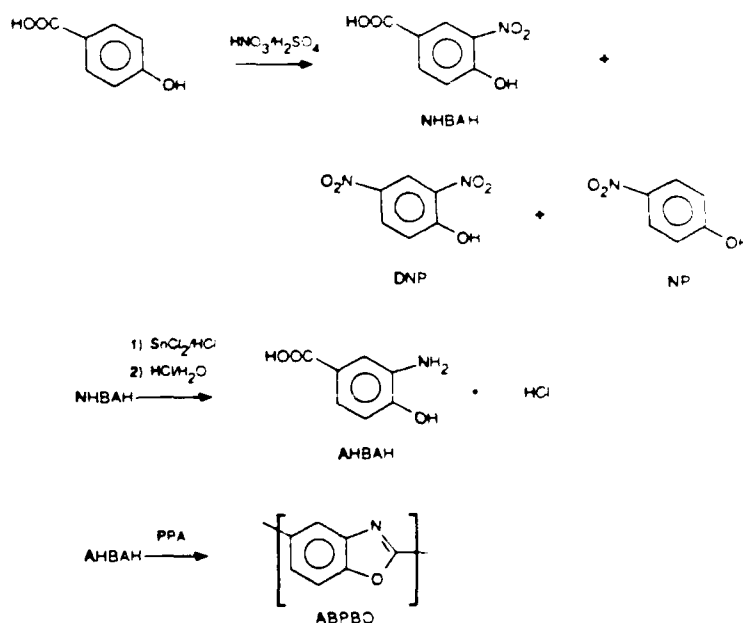


**SCHEME I ABPBO SYNTHESIS**
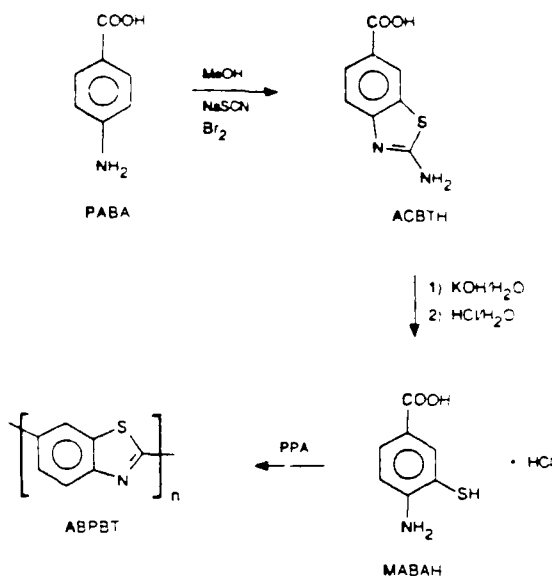
**SCHEME II ABPBT SYNTHESIS**

## $P_2O_5$ Adjustment Method

The general method for preparing benzazole polymers in PPA in the nematic phase at polymer concentration greater than 10 wt % involves the addition $P_2O_5$ powders to control the PPA composition at various stages of polymerization based on the concentration of the condensing species. The effect of PPA composition at the end of the polymerization, or final $P_2O_5$ content ($P_3$), on the attainable molecular weight can be deduced by comparing polymerization having $P_3$ of 82.2% with those having $P_3$ of 83% or higher.[5] Polymerizations with higher $P_2O_5$ contents in general have considerably higher molecular weights. We believe this effect is due to the need to maintain an effective concentration and activation of the functional groups. An upper limit of about 84% final $P_2O_5$ content was imposed to control solution viscosity and allow for efficient mixing of reactants.

## DILUTE SOLUTION CHARACTERIZATION

### Mark-Houwink-Sakurada Constants

Low angle light scattering (LALS) and intrinsic viscosity measurements ($[\eta]$) were used to characterize the dilute solution properties of ABPBO and ABPBT. Methanesulfonic acid (MSA) was used as the solvent. The Mark-Houwink-Sakurada (MHS) constants, K and a, of the empirical relation $[\eta] = K\, M_w{}^a$ can be determined by a double-logarithmic plot of $[\eta]$ as a function of weight-average molecular weight ($M_w$) as shown in Figure 2.

A least-squares analysis of the experimental results indicates that the MHS relation may be written as:

$$[\eta] = 1.26 \times 10^{-4}\, M_w{}^{1.00} \qquad \text{for ABPBT} \tag{1}$$

$$[\eta] = 1.09 \times 10^{-4}\, M_w{}^{1.02} \qquad \text{for ABPBO} \tag{2}$$

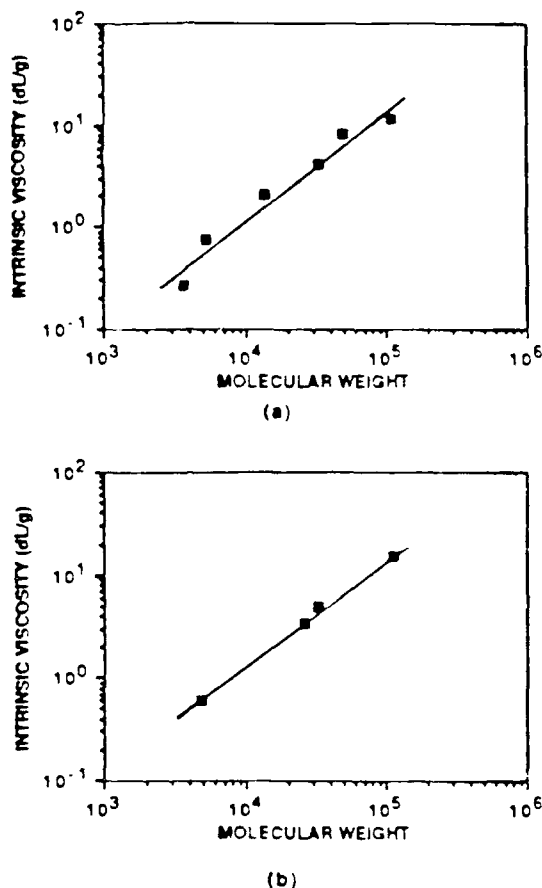within the molecular weight range of 2,000 to 200,000 daltons.

Figure 2  Double logarithmic plots of intrinsic viscosity and molecular weight to determine the Mark-Houwink-Sakurada constants for (a) ABPBT and (b) ABPBO.

The MHS exponents are found experimentally to be about unity for both polymers. The values are between 1.8 for rodlike polymers (such as PBT) and 0.5 for random coil polymers (such as polyethylene) in theta solvent, indicating that this class of poly(benzazoles) is characterized by an intrinsically semirigid structure.

Persistence Length

A wormlike cylinder model has been proposed by Yamakawa and Fujii [6] to evaluate the intrinsic viscosity of stiff chains. The model requires three molecular parameters--contour length L, persistence length $\rho$, and molecular diameter d--to evaluate the intrinsic viscosity [$\eta$]. To obtain these molecular parameters for ABPBT and ABPBO polymers, we estimated $\rho$ and d using x-ray crystallographic information on oriented fibers [7] and Flory's virtual bond model [8] to evaluate chain flexibility of polymers having catenation angles less than 180°. Values of L were calculated using the molecular weight measurements from LALS.

Both the experimental results and theoretical model calculations of [$\eta$] versus $M_w$ for ABPBT and ABPBO are plotted in Figure 3. The solid line is the wormlike cylinder model prediction using d = 5.5 Å and $\rho$ = 130 Å for ABPBT. Model comparison with the ABPBT experimental data (open diamonds) is very good. The broken line represents the model calculation obtained for ABPBO based on the value of d = 7.5 Å and $\rho$ = 50 Å. In this case, the model fits poorly with the ABPBO results (filled diamonds). This discrepancy can be greatly reduced by increasing $\rho$ from 50 Å to 90 Å for ABPBO as indicated by the dash-dot line.

In Figure 3, the theory predicts a gradual increase in slope (hence an increase in the value of the HMS exponent) with decreasing $M_w$ for semirigid chains. In contrast, flexible chains have been reported to exhibit a constant HMS exponent over many decades of $M_w$ [9]
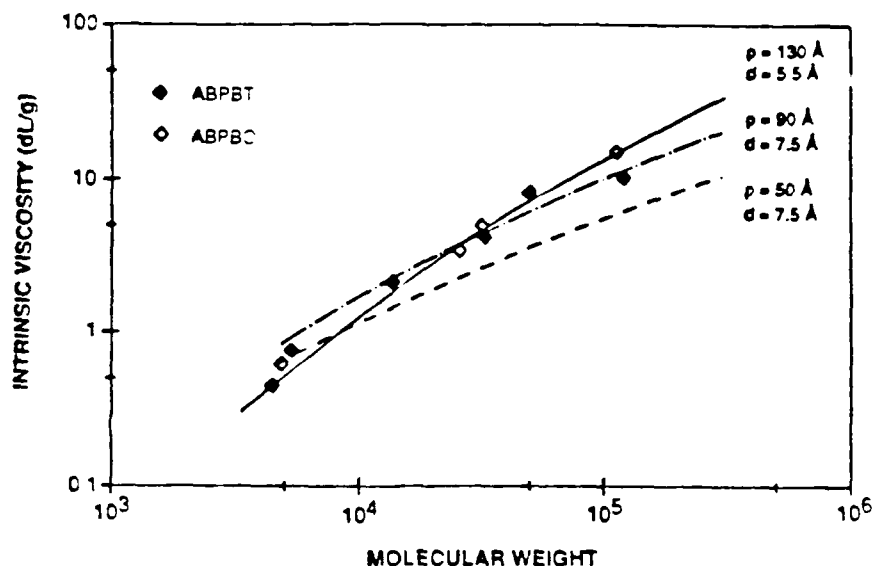
Figure 3 Comparison of experimental results and model predictions of the MHS relationships for ABPBO and ABPBT.

## CONCLUSIONS

Our study indicates that ABPBT and ABPBO are characterized by persistence lengths of 90 to 130 Å, which are in good agreement with the virtual bond model predictions. This comparison suggests that these extended chain polymers assume a random distribution of cis- and trans-conformations in dilute solutions. At concentrations above ~14 wt%, ordered phases form, and the trans-conformation is believed to dominate to allow this phase change.

## ACKNOWLEDGEMENT

## REFERENCES

1.    W.-F. Hwang, D. R. Wiff, C. L. Benner, and T. E. Helminiak, J. Macromol. Sci., Phys., B22, 231 (1983).

2.    J. F. Wolfe, in Encyclopedia of Polymer Science and Engineering, edited by H. F. Mark, et. al. 2nd ed., Vol. 11, (John Wiley & Sons, New York, 1988) pp. 601.

3.    A. W. Chow, J. F. Sandell, and J. F. Wolfe, Polymer, 29, 1307 (1988).

4.    L. Jannelli and P. Giordano-Orsini, Gazz. Chim. Ital., 88, 331 (1958).

5.    A. W. Chow, S. P. Bitler, P. E. Penwell, D. J Osborne, and J. F. Wolfe, submitted to Macromolecules.

6.    H. Yamakawa and M. Fujii, Macromolecules, 7, 128 (1974).

7.    A. V. Fratini, E. M. Cross, J. F. O'Brien, and W. W. Adams, J. Macromol. Sci., Phys., B24, 159 (1985-86).

8.    B. Erman, P. J. Flory, and J. P. Hummel, Macromolecules, 13, 484 (1980).

9.    H. Fujita, Macromolecules, 21, 179 (1988).